Upregulating PHD2 activity to downregulate HIF-1 alpha and subsequently FASN in mammary gland carcinoma

THESIS

Submitted to

Babasaheb Bhimrao Ambedkar University

(A Central University)

Lucknow

For the Degree of

Doctor of Philosophy

In

PHARMACEUTICAL SCIENCES

By:

Lakhveer

Enrollment No. - 1232/15

Supervisor:

Dr. Gaurav Kaithwas

Associate Professor

DEPARTMENT OF PHARMACEUTICAL SCIENCES

SCHOOL FOR BIOSCIENCES AND BIOTECHNOLOGY

BABASAHEB BHIMRAO AMBEDKAR UNIVERSITY

(A CENTRAL UNIVERSITY)

VIDYA VIHAR, RAE BARELI ROAD, LUCKNOW-226025 (U.P.), INDIA

2020

DECLARATION

I hereby declare that the thesis entitled **"Upregulating PHD2 activity to downregulate HIF-1alpha and subsequently FASN in mammary gland carcinoma"** has been prepared by me, under the supervision **Dr. Gaurav Kaithwas** at Department of Pharmaceutical Sciences, School for Biosciences and Biotechnology, Babasaheb Bhimrao Ambedkar University, Lucknow (U.P.).

No part of this thesis has formed the basis for the award of my degree, diploma or fellowship previously. I further declare that the material embodied in the present work is based on original research work and indebtedness to others has been duly acknowledged at relevant places. I hereby also declare that the thesis is essentially free from all kind of plagiarism.

Date:
Place:

Lakhveer
Enrolment No:1232/15

CERTIFICATE

This is to certify that the thesis titled **"Upregulating PHD2 activity to downregulate HIF-1alpha and subsequently FASN in mammary gland carcinoma''** submitted by **Mr. Lakhveer (Enrollment no. 1232/15)** is an original work and has not been previously submitted in part or full for the award of any other degree or diploma to this or any other university.

The thesis submitted to Babasaheb Bhimrao Ambedkar University Lucknow satisfies all the requirements as stipulated in the Doctor of Philosophy (Ph.D.) regulations as amended time to time and it is fit for submission and evaluation for the award of the degree of Doctor of Philosophy of the University.

08/09/2020

Supervisor

Date:

Place:

Head of the Department

ACKNOWLEDGEMENT

I consider myself most lucky to work under the guidance of ***Dr. Gaurav Kaithwas, Associate Professor****, Babasaheb Bhimrao Ambedkar University, Lucknow (U.P) for his valuable support. His discipline, principles, simplicity, caring attitude and provision of fearless work environment will be cherished in all walks of my life. I am very much grateful for his invaluable guidance and everlasting encouragement throughout my course.*

I express my heartly and humble thanks to ***Prof. Shubhini A.Saraf****, Professor and Head of the Department, Babasaheb Bhimrao Ambedkar University, Lucknow (U.P) for making all facilities available, her timely help, encouragement, boosting my confidence in the progress of my dissertation work.*

I wish to offer my sincere thanks to ***Prof. Sanjay Singh****, Honourable Vice Chancellor of Babasaheb Bhimrao Ambedkar University, Lucknow for providing infrastructure facilities for carrying the project advices throughout my academic carrier.*

Besides my advisor, I would like to thank the rest of DRC committee members: ***Dr. V.Elangovan****,* ***Dr. N.K.S.More*** *and* ***Dr. Sudipta Saha, Dr. P.S. Rajanikant, Dr. Vikas Mishra, Dr. Sapana*** *for their encouragement, insightful comments and meaningful quires.*

My sincere thanks also go out to Controller of examination and supportive staff for their guidance. I also want to acknowledge the ***University Grant Commission****,* ***Government of India*** *for providing me fellowship to pursue the research work.*

I would like to express my sincere thanks to ***Dr. Sunil Goria*** *(Librarian),* ***Mr. O.P.Saini*** *(Assistant Librarian) BBAU*

for their kind support. I must place on record very special thanks to my seniors, juniors,batchments and friends, ***Dr. Subhadeep Roy, Dr. Manjari Singh, Dr. Swetlana, Dr. Rajnish kumar Yadav, Dr. Jitendra Kumar Rawat, Shubham Rustogi, Anurag Choudhary, Amit Kumar, Sonia, Ravinder*** *for their charming company, kind co-operation and encouragement throughout my doctoral study.*

I wish to thank the staff members, ***Mr. Anand Pandey, Mr. Amar, Miss Seema*** *and* ***Mr. Bhandari*** *for providing all the needful official accessories.*

Finally, I acknowledge the people who mean a lot to me, my parents, my wife and my friends for showing faith in me and giving me liberty to choose what I desired. I wish to thank almighty God who keep his blessings on me every second and giving me the strength and patience to work through all these years so that today I can stand proudly with completion of my research work.

Lakhveer

TABLE OF CONTENT

List of tables

List of Figures

List of Abbreviations

PHD2: Prolyl hydroxylase-2

HIF-1α: Hypoxia inducible factor-1α

FASN: Fatty acid synthase

ER+: Estrogen receptor positive

VOA: Voacamine

VIN: Vincristine

TMX:Tamoxifene

NCI: National Cancer Institute, USA

DMSO: Dimethyl sulfoxide

APS: Ammonium per sulfate

TEMED: Tetramethylenediamine

SLS: Sodium lauryl sulfate

BSA: Bovine serum albumin

CDRI: Central Drug Research Institute

CPCSEA: Committee for the Purpose of Control and Supervision of Experiments on Animals

DMBA: 7, 12-Dimethyl benzanthracene

ECG: Electrocardiogram

ABs: Albeolar buds

TED: Terminal end duct

TEB: Terminal end bud

Los: Lobules

H&E: Hamatoxyline and Eosin

TBARS: Thiobarbituric acid reactive substances

SOD: Superoxide dismutase

PC: Protein carbonyl

GSH: Glutathione

FAME: Fatty acid methyl ester

NMR: Nuclear magnetic resonance

TSP: 3-trimethylsilysily-(2,2,3,3-d4)-propionic acid

CPMG: Carr-Purcell-Meiboom-Gill

PCA: Principle Component Analysis

PLS-DA: Partial Least Squares Discriminant Analysis

RIPA lysis buffer: Radioimmunoprecipitation assay buffer

PMSF: Phenylmethylsulfonyl fluoride

SDS-PAGE: Sodium dodecyl sulfate-polyacrylamide gel electrophoresis

PVDF: Polyvinylidene difluoride

SREBP-1c: Sterol regulatory element binding protein-1c

TC: Toxic control

NC: Normal control

BC: Bowmans capsule

G: Glomerulus

PCT: Proximal convoluted tubule

DCT: Distal convoluted tubule

PUFA: Poly unsaturated fatty acids

LDL: Low density lipoprotein

VLDL: Very low density lipoproteins

GC-FID: Gas chromatography-Flame ionization detector

LD: Lactiferous duct

AD: Adipocytes

DE: Ductal epithelium

He: Hepatocytes

dSn: Distorted sinusoids

Lo: Lobules

ROS: Reactive oxygen species

GLUT-1: Glucose transporter one

VEGF: Vascular endothelial growth factor

CHAPTER 1

INTRODUCTION

1. Introduction

Cancer, medically known as malignant neoplasm occurs when cellular proliferation in normal cells is no longer under normal control due to genetic mutations primarily caused by environmental factors [1].This uncontrolled growth and division of cells eventually forms a mass of cells termed as tumor which interferes with the normal functioning of the organs; either at the site of origin or through spreading to other parts of the body [2]. Tumors can be further differentiated into benign and malignant tumors. A benign tumor remains localized to their organ of origin, does not grow uncontrollably but malignant tumors are metastatic in nature, invade the nearby organs, blood vessels and transmit to the distant organs. They are fatal and difficult to manage.

Treatment strategies for malignant tumors include surgery, radiotherapy, chemotherapy, hormone therapy, immunotherapy and targeted drug therapy (drugs that interfere with tumor cell growth by targeting specific molecules) [3]. Most of the early tumors respond well to radiotherapy and chemotherapy. However, failure of radiotherapy and chemotherapy in most of the solid tumors has been observed due to hypoxia, a condition characterized by low oxygen concentration in solid tumors as a consequence of cellular proliferation and angiogenesis (abnormal blood vessels formation)[4,5].Tumor cells in this situation extract energy mainly from glycolysis (anaerobic mode of energy production) which makes the tumor microenvironment more acidic, further enhancing the resistance to radiotherapy and chemotherapy.

Tumor hypoxia is not only the biggest prohibition in the path of tumor therapy but it also helps the tumor cell in attaining the most hostile environment for proper growth and development [6]. In a hypoxic environment, tumor cells cause activation of a cytoplasmic protein known hypoxia inducible factor-1α (HIF-1α). HIF-1α once

activated, enhances the expression of numerous genes assisting the endurance of cancer cells in anoxic condition. HIF-1α up-regulates the genes for angiogenesis, metastasis, invasiveness, metabolic reprogramming, changes in extracellular pH (pHe) and intracellular pH (pHi), downstream regulation of immune response and resistance to chemotherapy (**Figure1**) [7].

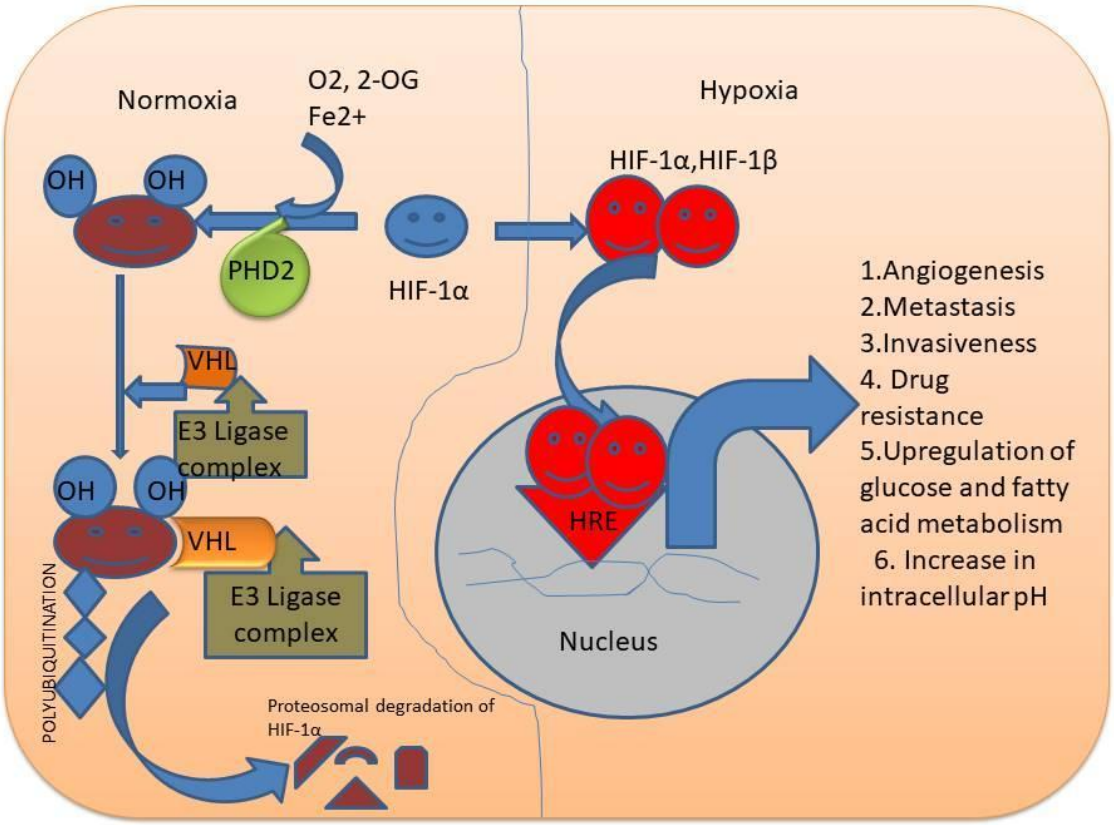

Figure 1: Effect of normoxic and hypoxic condition on HIF-1α

In normoxic condition HIF-1α is hydroxylated by PHD2 in presence of O_2, Fe2+, and 2-OG. This hydroxylated complex is recognized by the pVHL -a tumor suppressor gene which causes polyubiquitination and finally proteasomal degradation of HIF-1α. On the other hand, hypoxia causes stabilization of HIF-1α, which after dimerization with HIF-1β subunit translocates to the nucleus. Translocation of dimerized complex causes activation of numerous genes, which enhances the metabolism glucose, fatty acids, angiogenesis, metastasis and invasiveness. **HIF-1α**: hypoxia-inducible factor-1α, **HRE**-: hypoxia response element**, PHD2**: Prolyl hydroxylase 2, **2-OG**-2-oxoglutarate, **pVHL**-von Hippel-Lindau tumor suppressor protein.

For instance, under the influence of HIF-1α, cancer cells express more glycolytic enzymes, which peculiarly decrease the pH in the extracellular region. Thereby over-

expression of fatty acid synthase (FASN) and other enzymes involved in fatty acid biosynthesis is essentially needed to meet the lipid requirement of the rapidly proliferating cells [8].

This pH-induced over-expression of FASN in rapidly dividing cancer cells can be reverted through the modulation of prolyl hydroxylase 2 (PHD2) activities. PHD belongs to the family of iron and 2-oxoglutarate (2-OG) dependent dioxygenases causing hydroxylation and eventually proteasomal degradation of HIF-1α. A down-regulation or up-regulation of PHD2 activity can modify the activity of HIF-1α downstream and upstream. Inhibition of PHD2 activity increases the HIF-1α stability and this mechanism can be beneficial in disease conditions like myocardial infarction and anemia. Some compounds like 1-(6-(2,6-dimethylphenoxy)-7-fluoro-4oxo-3,4-dihydroquinazolin-2-yl)-H-pyrazole-4-carboxylic acid (JNJ-42905343) have already been developed and tested pre-clinically for management of myocardial infarction and anemia [9]. On the other side, up-regulation of PHD2 activity could curtail HIF-1α expression and therefore PHD2 could be exploited therapeutically to combat cancer progression.

The present review summarizes the role of HIF-1α cumulated pHe on up-regulation of enzymes involved in glucose and lipid metabolism. The review also attempts to summarize the role of PHD2 in the modulation of HIF-1α and explore the possibilities of PHD2 being a target for cancer research.

1.2. HIF-1α-oxygen sensing mechanism

Rapid growth and division is generally observed in tumor cells and those near to the blood vessel can easily take up oxygen and nutrients from there [10]. As the tumor size increases, the cells located at the periphery become deficient in oxygen and nutrients [11].This condition is termed as hypoxia. Generally, normal cells undergo

apoptosis, so-called programmed cell death, however during hypoxia, tumor cells fail to do so. Development of tumor hypoxia is recognized as the main cause for stabilization of cytoplasmic protein known as HIF-1α s.

HIF-1α consist of a basic helix-loop–helix Per-ARNT Sim (PAS) domain which undergoes hetero-dimerization at 2 subunits present at the amino terminal of half of each subunit and form a DNA binding complex, which is translocated to the nucleus and enhances the expression of several genes . In normoxia, PHD2 causes hydroxylation of HIF-1α at proline residue 402 or 564 and an interface is created as a result of this modification where the von Hippel-Lindau tumor suppressor (pVHL) protein can bind to carry out polyubiquitination of HIF-1α after recruiting an E3 ubiquitin ligase and eventually target it for proteasomal degradation **(Figure-2)** [12].

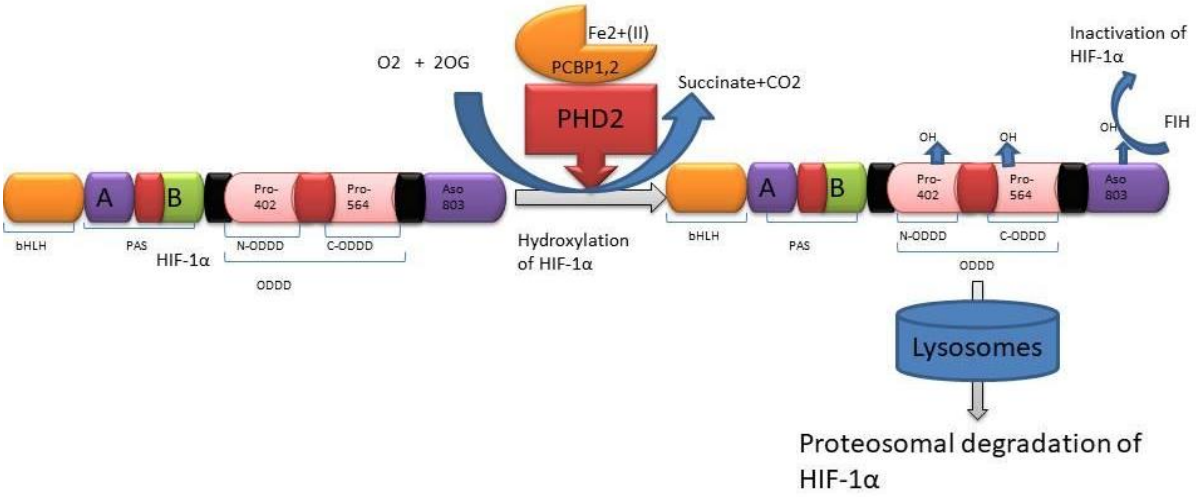

Figure 2: The relation between HIF-1α and PHDs

HIF-1α and PHDs, both are expressed equally in normal cells. The HIF-1α, being a basic helix loop helix protein possesses 402 and 564 proline residues on its oxygen dependent degradation domains. PHDs carry out hydroxylation of HIF-1α at Pro402 and Pro564 residues. Like PHD2, FIH also catalyzes hydroxylation of HIF-1α at the aspartic residue in order to reduce HIF-1α mediated transcription. The hydroxylated HIF-1α undergoes proteasomal degradation. **HIF-1α**: hypoxia inducible factor-1α, **PHDs:** Prolyl hydroxylases, FIH: factor inhibiting HIF-1α **2-OG:** 2-oxoglutarate, **PCBP**: poly (C) binding protein 1, 2.

It is very well evident from numerous studies that PHD2 plays an important role in the proteasomal degradation of HIF-1α [13]. Activation and inhibition of PHD2 can affect the stability of HIF-1α which in turn can speed up or down the proliferation of tumor cells through multiple pathways [14].

During hypoxic condition, HIF-1α becomes more stable and its binding affinity with another constitutively expressed unit, HIF-1β transiently increases, and this complex transit to the nucleus where it causes activation of several genes . HIF-1α, being a central transcription factor modulates the expression of many genes involved in cell metabolism, angiogenesis, invasiveness, and proliferation. For instance, it enhances the expression of genes encoding erythropoietin, enzymes involved in the glucose metabolism, lipid metabolism and transport thereof [15]. HIF-1α promotes metastasis of tumor cells to distant organs, transforming benign tumors to malignant tumors[16].

1.3. PHDs

PHDs are the oxygen dependent family of enzymes causing proteasomal degradation of HIF-1α in normoxic cells. Molecular oxygen is must for their hydroxylation activity on HIF-1α that is why they are regarded as oxygen sensor of cells [17]. Till date three isoforms of PHDs i.e. PHD1, PHD2, and PHD3 have been discovered which are known to have a role in oxygen sensing s. The decreasing order of *in vitro* hydroxylation potential of all the PHDs towards HIF-1α is as: PHD2>PHD3 >PHD1. PHDs add hydroxyls (OH^-) group at the proline residue of HIFs but differ in their substrate specificity and distribution. It was reported that PHD2 more efficiently hydroxylates HIF-1α as compared to HIF-2α and HIF-3α whereas HIF-2α is more efficiently hydroxylated by PHD1 and PHD3.

PHD2 is specifically expressed in the adipose tissue, PHD1 is expressed in testis cells while PHD3 is expressed in cardiac cells [18]. PHD2 remains localized to the

cytoplasmic region of the cell, PHD3 founds in the nuclear region whereas PHD3 can be present in both, cytoplasmic as well as in nuclear regions.

1.4. PHDs- A negative regulator of HIF-1α

A direct relationship between hypoxia and PHDs have been confirmed by various studies [19]. Subsidence in the expression of PHD2 has been observed in hypoxic tumor cells in numerous studies. It is inferred that PHD2 controls degradation of HIF-1α in presence of oxygen. Although oxygen is the prime factor involved in the hydroxylation of HIF-1α, other factors like Fe (II), ascorbate, 2-OG also play an important role in HIF-1α degradation.

In normoxic condition, oxygen is abundant in cells which enhances the hydroxylation activity of PHDs [20]. Activated PHDs add up hydroxyl (OH^-) group at P^{402} and P^{502} residue of C-terminal of HIF-1α. Hydroxylation reaction involves the splitting of dioxygen into two oxygen atoms transferring one oxygen to proline residue to form hydroxyl group and another to the 2-OG to generate succinate and CO_2 [21]. Fe^{2+} at the active site of the PHDs remains loosely bound by two histidine residues and one aspartic acid forming a 2-histidine-1-carboxylase coordination motif. Ascorbate helps to maintain Fe in the ferrous (Fe^{2+}) state and is important in maintaining and achieving the full activity of the PHDs [22].

Once HIF-1α is hydroxylated at proline residues by PHD2, it is further captured by the pVHL protein. X-ray crystallographic studies of the pVHL/HIF-1α complex have revealed that pVHL has a surface pocket into which the hydroxylated proline residue of HIF-1α fits accurately and the overall binding is highly specific. After this, proteins elongin (C, elonginB, cullin, and Rbx1) bind with the pVHL/HIF-1α complex to form another complex named VCB-Cul2E3 ligase. Binding of HIF-1α to this complex E3 causes polyubiquitination of HIF-1α and ultimately targeting its proteasomal

degradation [23]. Like PHD2, HIF-1α also hydroxylated by an another cytoplasmic protein known as factor inhibiting HIF-1α (FIH) at the aspartic residue of HIF-1α which further enhances degradation of HIF-1α and thereby reducing its transcriptional activation in tumor cells [24].

1.5. Effect of HIF-1α on cellular physiology

The normal cellular physiology of tumor cells is considerably affected by HIF-1α as the enzymatic machinery of glucose and fatty acid metabolism is tightly regulated at the genetic level. Alongside expression of genes for glucose and fatty acid metabolism, HIF-1 α also imparts tumor cell an invasive and metastasis character which further increases the complications.

1.6. Effect of HIF-1α on cellular respiration and energy production

Altered metabolism is the hallmark of tumor cells. The most commonly observed metabolic alteration in tumor cells is enhanced glucose uptake and oxidation of glucose through glycolysis (termed as the Warburg effect) [25].

It is well defined that, oxidation of glucose in normal cells occurs first by glycolysis in the cytoplasmic region and then by citric acid cycle in mitochondria. Glucose taken inside the cell undergoes oxidation and reduction reactions to yield two moles of pyruvate as a end product [26]. Pyruvate is further translocated to the mitochondria where it is oxidized to Acetyl CoA. Acetyl CoA thus formed, enters into the citric acid cycle and energy-rich compounds in the form of GTP, NADP, and $FADH_2$ are obtained [27]. Further oxidation of above compounds through oxidative phosphorylation yields 36 ATP which serves as fuel for various biological processes occurring in a cell (**Figure 3**).

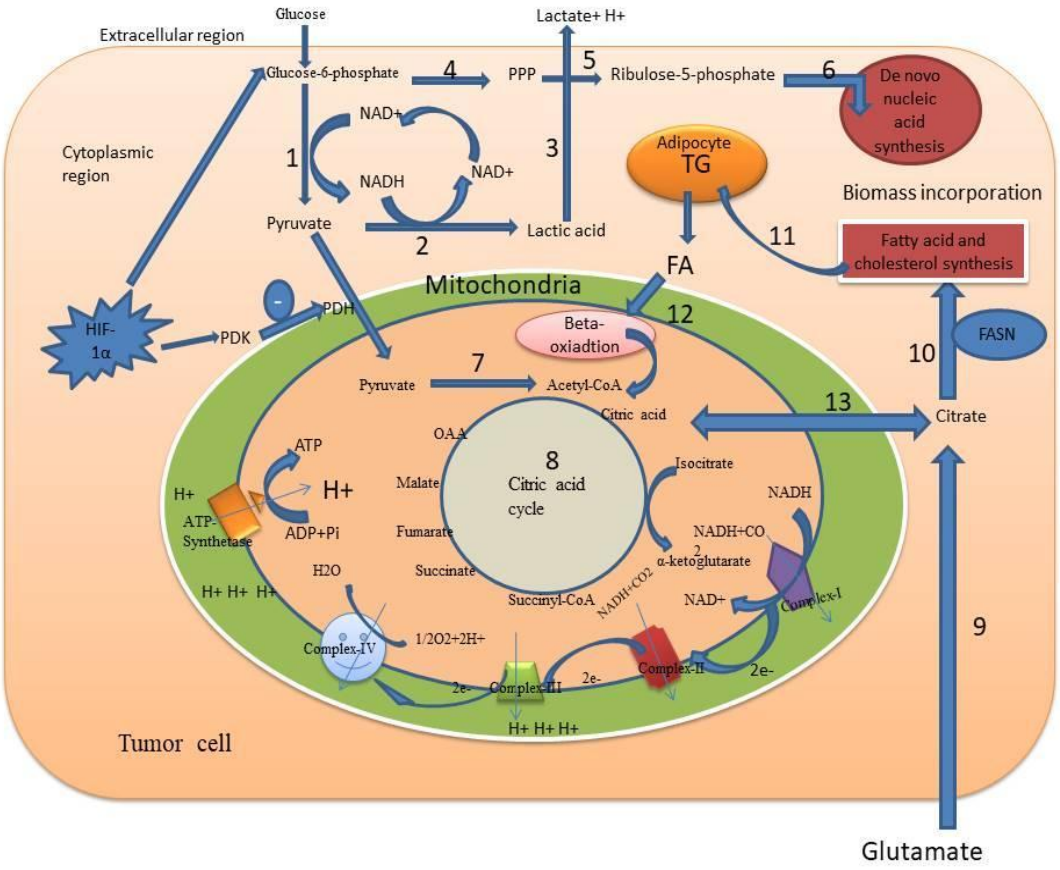

Figure 3: Effect of HIF-1α on cellular respiration and energy production

HIF-1α enhances the uptake and utilization of glucose in tumor cells. (1) Oxidation of glucose in tumor cells mainly occurs through glycolysis pathway and yields 2 moles of pyruvate as the end product (2, 3) Pyruvate is rather converted to lactic acid which is exported outside. (4, 5, 6) glucose is also metabolized through PPP to yield five carbon sugars like ribulose-5-phosphate to be used in *de novo* nucleic acid synthesis. . (7, 8) further oxidation of pyruvate in mitochondria is inhibited by PDK. (9, 10) Circulating glutamine serves as a major bio-energetic substrate and nitrogen donor for proliferating cells, provides citrate to be utilized in cholesterol and fatty acid synthesis. (13) Citrate is also provided from TCA cycle. (11, 12) excess fatty acids are stored in adipocytes and used when energy is required through β-oxidation. **HIF-1α**: hypoxia inducible factors-1α, **PDK**: pyruvate dehydrogenase kinase, **PDH:** pyruvate dehydrogenase, **PPP:** pentose phosphate pathway, **TCA**: tricarboxylic acid cycle.

To extract such a large amount of energy from a single glucose molecule, oxygen is must for normal cells as well as for tumor cells.

Both tumor and normal cells remain dependent upon glucose for all their energy requirements. The blood vessels in the nearby tissue ensures a constant supply of

oxygen and other essential nutrients required for proper growth and development [28]. As the tumor mass increases beyond limits, nourishing blood vessels becomes inefficient and in this way tumor cells at the periphery of tumor mass do not get oxygen and nutrients. Generally, normal cells stop dividing in oxygen scarcity but this is not true for tumor cells as they keep on dividing even in absence of oxygen [29].

How tumor cells manage to survive in absence of oxygen and what fuel they use? – was a long-standing question for researchers. At last, warburg and friends discovered that tumor cells have a high rate of glucose uptake and perform glucose metabolism mainly through glycolysis with the formation of lactic acid [8]. The warburg effect is crucial for rapidly dividing cells as it enables the tumor cells to generate more building blocks which are important for cell proliferation [30].

Also, under this oxygen tension tumor cells stabilize HIF-1α which plays a pivotal role in tumor progression as discussed in earlier sections [31]. In context to metabolism, enzymes for glucose and fatty acid metabolism are regulated by HIF-1α [32]. HIF-1α is the main accused who shifts the metabolism of glucose from highly efficient oxidative phosphorylation to less efficient glycolytic pathway in order to maintain energy needs in a hypoxic environment. This again raises the question: why would proliferating cells (including tumor cells) will choose a pathway that produces less ATP? Possible reply to this question is that a cell requires other molecules in addition to ATP to divide. Macromolecules such as amino acids, nucleotides, and fatty acids are needed for cellular replication. Consequently, a pathway that supports the synthesis of these biomolecules is preferentially selected [33].

Due to this reason, more and more glucose is consumed in order to meet the energy needs and other requirements. This effect is mediated by HIF-1α, which enhances the trans-activation of glucose transporters (GLUTs) and enzymes of the glycolytic

pathway which increases glucose intake and utilization by tumor cells. Glucose inside tumor cells is rapidly metabolized through glycolysis to yield pyruvate as an end product. Further oxidation of glucose in mitochondria is interrupted and lactic acid as an end product of this pathway is exported outside the tumor microenvironment [34]. In tumor cells, conversion of pyruvate to lactic acid is an adaptive mechanism in order to keep the rate of glycolysis pathway unusually high. In normal conditions, NAD+ is recycled through oxidative phosphorylation. But in anoxic conditions, NAD^+ is regenerated only when pyruvate is converted into lactic acid by lactate dehydrogenase (LDH) [35]. Under these circumstances, tumor cells oxidize glucose only through glycolytic pathway and finally through lactic acid pathway. Lactate thus formed, is transported outside the cell which is responsible for decreasing the pH in tumor microenvironment [36].

1.7. Effect of HIF-1α on cellular pH

Due to aberrant metabolism guided by HIF-1α, a tumor cell produces more lactic acid which disturbs the pHi and pHe in the tumor microenvironment. These changes affect the molecular process such as cell cycle, cell proliferation, differentiation, metastasis, cell metabolism and angiogenesis. Disturbed pHi and pHe in tumor cells accomplish following three objectives: 1) intracellular alkaline pH stimulates proliferation; 2) extracellular acidity is a necessary feature for the activation of degrading enzymes like cathepsin, heparanase, and metalloprotease. This matrix degradation is necessary for migration, invasion, and eventually metastasis. 3) Extracellular acidity blocks immunogenic attacks against malignant cells and decreases tumor access of certain chemotherapeutics [37]. All in all, hypoxia and acidic pHe contributes tumor progression in the manner of Darwinian selection of resistant cells that may survive in this harsh environment.

Increase in pHe with decrease in pHi, is accompanied by production and venting of metabolic acid resulted from aerobic glycolysis, fatty acid oxidation and oxidative phosphorylation [38]. The resultant amendment in the aforesaid metabolic pathway is essential to attain a glycolytic phenotype [39]. Tumor cells have two main objectives behind the adoption of glycolytic pathway, as the main source of energy in-spite of low energy efficacy of this pathway. Firstly, it decreases reactive oxygen species (ROS) production that is much higher under oxidative phosphorylation and secondly, it is essential for the production of biological building blocks that are being used in other anabolic processes occurring elsewhere in tumor cells. Despite the number of beneficial effects of glycolytic phenotype, it has some disadvantages too. The main disadvantage of glycolytic phenotype is the production of excess protons responsible for decreasing pHi. Lactic acid produced as a result of enhanced glycolysis, ATPs generated through oxidative phosphorylation and carbonic acid produced as a result of hydration of carbon dioxide is the responsible factor for reduction of pHi.

Tumor cells also develop special regulatory proteins like vacuolar H+-ATPases (V-ATPases), Na+/H+ exchanger (NHE), bicarbonate transporter, monocarboxylate transporters (MCTs) and carbonic anhydrase on their membrane to get rid of this excessive intracellular acidity [37,40]. These pH regulatory proteins tightly control the disturbed pH homeostasis in tumor cells.

V-ATPases are ATP driven proton pumps that function in a wide array of normal physiological processes coupled with energy released from ATP-hydrolysis to transport protons out of the cytosol [41]. The V-ATPase is highly expressed in tumor cell membranes to promote invasions and migration, which is essential for activation of extracellular proteases like cathepsins that facilitate invasion. The activity of cathepsins depends on pH. Lower pHe facilitates activation and lower pHi facilitates

inactivation of cathepsins [42]. So, V-ATPases enhances extracellular acidity by extruding metabolically generated protons on glucose metabolism.

Although, tumor cells have developed numerous cellular mechanisms to get rid of excessive pHi but activated NHE-1 plays pivotal role in cumulation of extracellular acidity and present a direct benefit to the tumor cells by regulating their motility, and invasion via activation of epidermal growth factor receptor **(**EGFR). The NHE-1, being an integral membrane protein regulates the pHi by interchanging the cytosolic proton (H+)with extracellular sodium ion (Na+) [43]. Role and over activation of NHE-1 in tumor cells have been documented in various studies [44].

Lactate is transported through MCTs. MCTs are generally found in the plasma membrane of erythrocytes, neutrophils including tumor cells. Till date, MCTs of 1-4 isoforms have been isolated and identified. Generally, most of the tissue cells express MCT-1 on their surface but at very low level. The occurrence of MCT-2 and MCT-3 is limited only to certain tissues only: liver, kidney, and neurons express MCT-2, whereas retinal pigmented epithelium and the choroid plexus express MCT-3 transporter. MCT-4 is mainly expressed by testicular, lungs and placental tissue [45]. HIF-1α also enhances the expression of MCTs on the plasma membrane of tumor cells in order to pump out protons generated from lactic acid hydrolysis **(Figure-4)** [46].

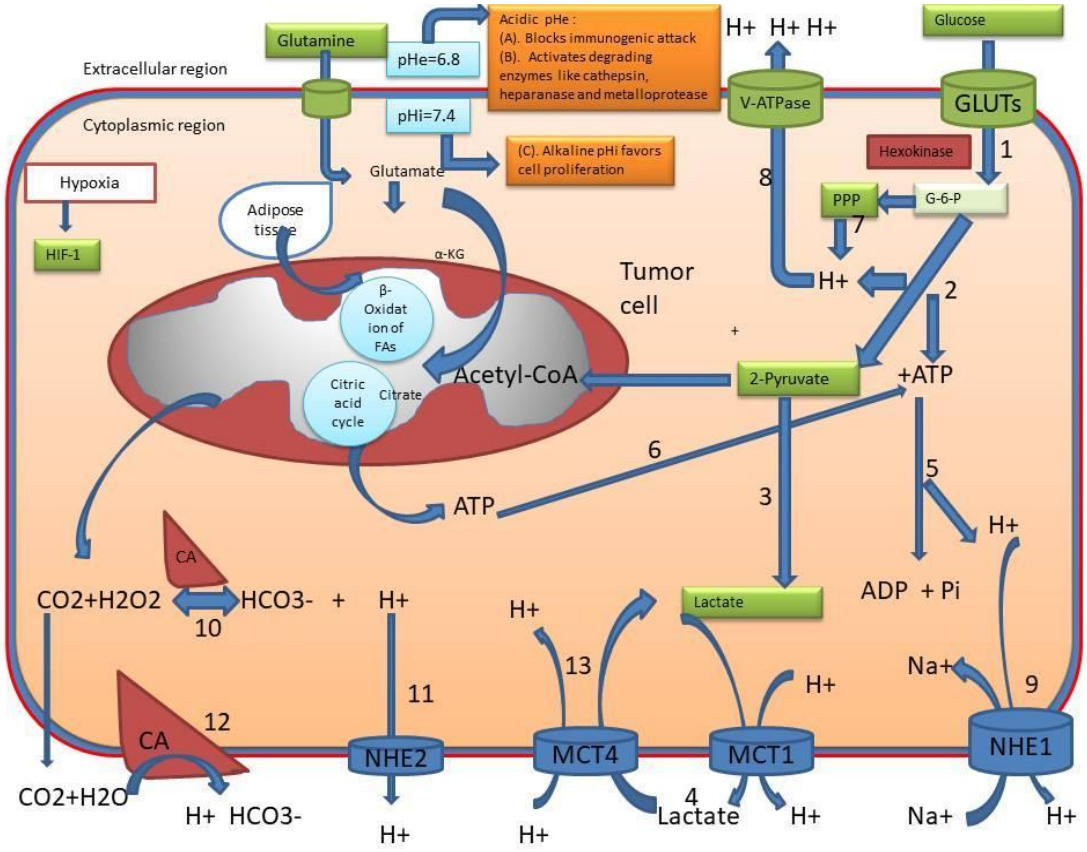

Figure 4: HIF-1α role in regulation of pHi and pHe in tumor cells

HIF-1α enhances the expression of various proton transporters to regulate the pHi and pHe in tumor cells. Proton generated from glycolysis and PPP extruded by V-ATPase (1, 2, 7, 8). NHE1 transport protons generated from hydrolysis of ATP (2, 5, 6, and 9). Lactic acid accumulated as a consequence of inhibition TCA cycle is first hydrolyzed to lactate and H+ ion which is transported outside through MCT1(2,3,4). Acidity raised by carbonic acid formed by the activity C.A is reduced by extruding protons through NHE2 (10, 11). Due to its high partition coefficient, CO2 is passively diffused out through the plasma membrane and extracellularly again converted to carbonic acid (12). Lactate from the extracellular side is also pumped back in tumor cells through MCT4. Due to continuous production and venting of protons through these transporters, tumor microenvironments become acidic (pHe=6.8). Reduced pHe and increased pHi in tumor cell is essential to fulfill the objectives A, B, and C. **HIF-1α**: hypoxia inducible factor-1α, **V-ATPase**: vacuolar-ATPase, NHE1-2: sodium hydrogen exchanger 1-2, C.A: carbonic anhydrase, **MCT1-4:** monocarboxylate transporters 1-4, **PPP:** pentose phosphate pathway.

Tumor cells use above all mechanisms to keep pHi at normal or slightly alkaline, while pHe in tumor microenvironment becomes slightly acidic and hence a pH gradient is quickly established [47].

1.8. Effect of HIF-1α on fatty acid metabolism

Lipids, like cholesterols, isoprenoids, acylglycerols, and phospholipids constitute a major part of the biological membranes of every cell. They are used for energy metabolism and storage, and have an important role in cell signaling [48]. For instance, lipids like diacylglycerol (DAG) and phosphatidylinositol-3,4,5-triphosphate (PIP_3), are two important cell signaling molecules which are formed in response to extracellular stimuli [49]. Similarly, stored lipids in the liver and adipocytes are broken down by β-oxidation to release energy during requirement. In fact, lipids are the most essential nutrients for normal as well as for tumor cells, as they are being constantly used for generating the membrane constituents necessary for proliferating cells, but also for biophysical, and signaling pathways that drive diverse aspects of tumorigenesis [50].

Although, earlier it was presumed that altered metabolism of only glucose is the characteristic feature of the tumor cells. But recent work has delineated that aberrant lipid metabolism is another metabolic perturbation [51].

Previously, it has been published that fatty acids are required in the much larger amount in the rapidly proliferating cells [52] and tumor cells must adopt an alternative pathway to uptake and synthesize fatty acids for their membrane synthesis and energy needs. Hypoxia plays a crucial role in adopting this alternative pathway. A study on breast cancer cells reported that genes induced by hypoxia are involved in lipid synthesis, storage, and uptake **(Figure-5)**. In hypoxic tumor cells, HIF-1α enhances the expression and translocation of fatty acid binding proteins (FABP-3 and FABP-7) which significantly increases the

accumulation of lipid droplets (LD). The study also suggested that during hypoxia-reoxygenation, β-oxidation of fatty acid or glycogen degradation can increase ROS

toxicity which in turn strongly impairs tumorigenesis [53]. Another study conducted by Roy and colleagues confirmed a relationship between HIF-1α and FASN. In fact, exogenous lipid supplementation curtailed the HIF-1α induced fatty acid synthesis in experimental animals [54]. Further, a direct relationship between the FASN gene and hypoxia was established by Menedez and colleagues. They observed that endogenous fatty acid synthesis was blocked by inhibition of FASN gene and silencing of FASN gene resulted in overexpression of vascular

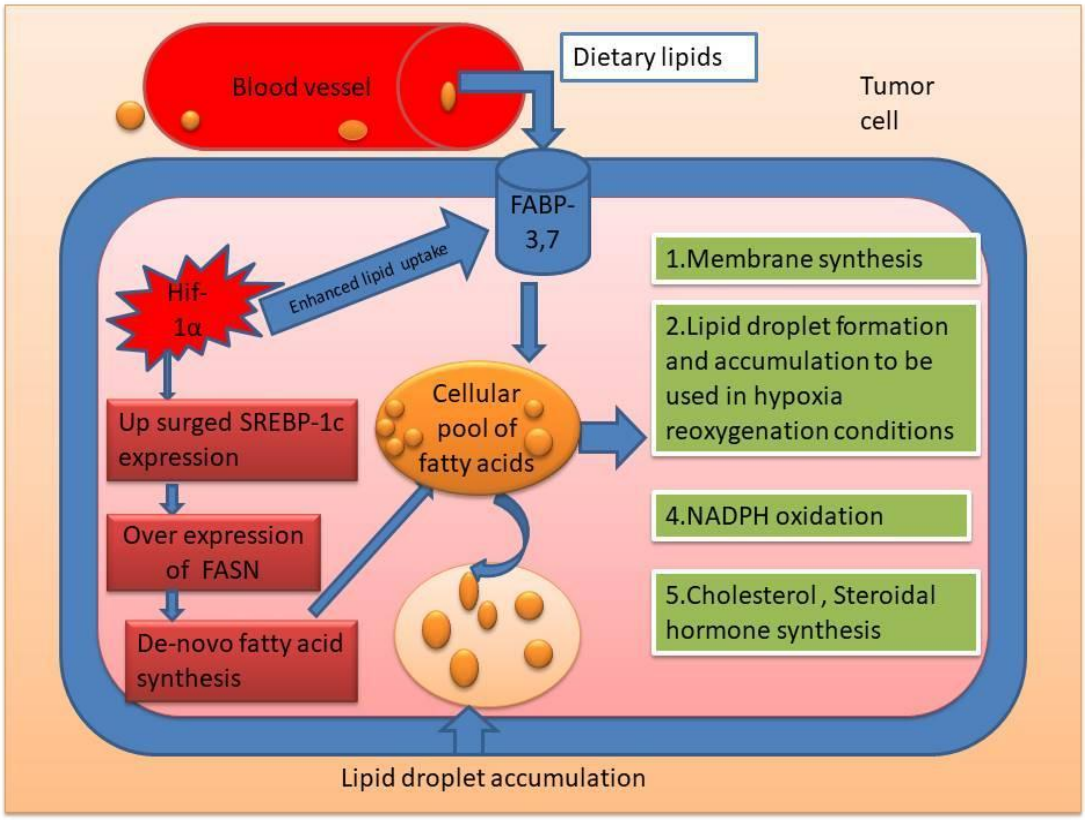

Figure 5: Effect of HIF-1α on fatty acid metabolism

HIF-1α increases the both fatty acid synthesis and uptake. The FABPs are over expressed and translocated to the cell membrane where it enhances the uptake of dietary fatty acids. The SREBP-1c causes over expression of FASN that further enhances the lipid biosynthesis. Excess lipids are accumulated as lipid droplets. **FASN**: fatty acid synthase; **SREBP-1c**: sterol regulatory element binding protein-1c; **FABP 3-7**: fatty acid binding proteins 3-7; **HIF-1α:** hypoxia inducible factor-1α.

endothelial growth factor (VEGF) in response to activation of HIF-1α.

Although hypoxia and HIF-1α regulate glycolysis, glutaminolysis and lipid synthesis in tumor cells, suppression of β-oxidation of long-chain polyunsaturated fatty acid (PUFAs) has been reported as well, as PUFAs are critical for cell membrane synthesis [55]. Hypoxia enhances the expression of long-chain acyl-CoA dehydrogenase (LCAD) and medium-chain acyl-CoA dehydrogenase (MCAD) enzymes which inhibit the first step of β-oxidation in mitochondria. This results in accumulation of PUFAs and decrease in expression of a tumor suppressor phosphatase and tensin homolog gene (PTEN gene) which promotes cell proliferation [56]. Another study confirmed that expression of sterol regulatory element binding protein-1c (SREBP-1c), a major transcriptional regulator of the FASN is significantly up-regulated in response to hypoxia. To examine the effect of hypoxia on the expression of the FASN gene, the breast tumor cell lines MX1, MCF-7, and MDA-MB157 were cultured in hypoxic and normoxic conditions. SREBP is a membrane bound basic helix-loop-helix leucine zipper (bHLHZ) transcription factor that plays a crucial role in fatty acid metabolism by controlling the synthesis of fatty acids, triglycerides and cholesterol [57]. Since its discovery, three isoforms of mammalian SREBPs (SREBP-1a, SREBP-1c and SREBP-2) have been identified and characterized with distinct but overlapping transcriptional roles in lipogenic programs. SREBP-1a activates fatty acid and cholesterol synthesis, SREBP-1c regulates fatty acid synthesis, and SREBP-2 guides the cholesterol synthesis and uptake. Previous studies have established the role of SREBPs in lipid homeostasis and regulation of cholesterol and its oxysterol derivatives .

These findings, altogether suggest that hypoxia itself and hypoxia induced pH in tumor microenvironment plays pivotal roles in fatty acid synthesis and uptake in tumor cells.

1.9. The interplay between HIF-1α, pH, SREBP-1c and FASN

HIF-1α induced aberrant metabolism of glucose in tumor cells results in formation of lactic acid, which when transported to the tumor microenvironment causes reduction in pHe. Protons generated from hydrolysis of ATPs, formation of carbonic acid and pentose phosphate pathway (PPP), further augment the pHe in tumor microenvironment. As a result of continuous production and venting of protons in hypoxic tumor cells, pHe in tumor microenvironment become acidic (pHe-6.8) whereas pHi becomes alkaline (pHi-7.8). Reduced pHe rewards the tumor cells in several ways [58]. It has been proved by Ayano et al

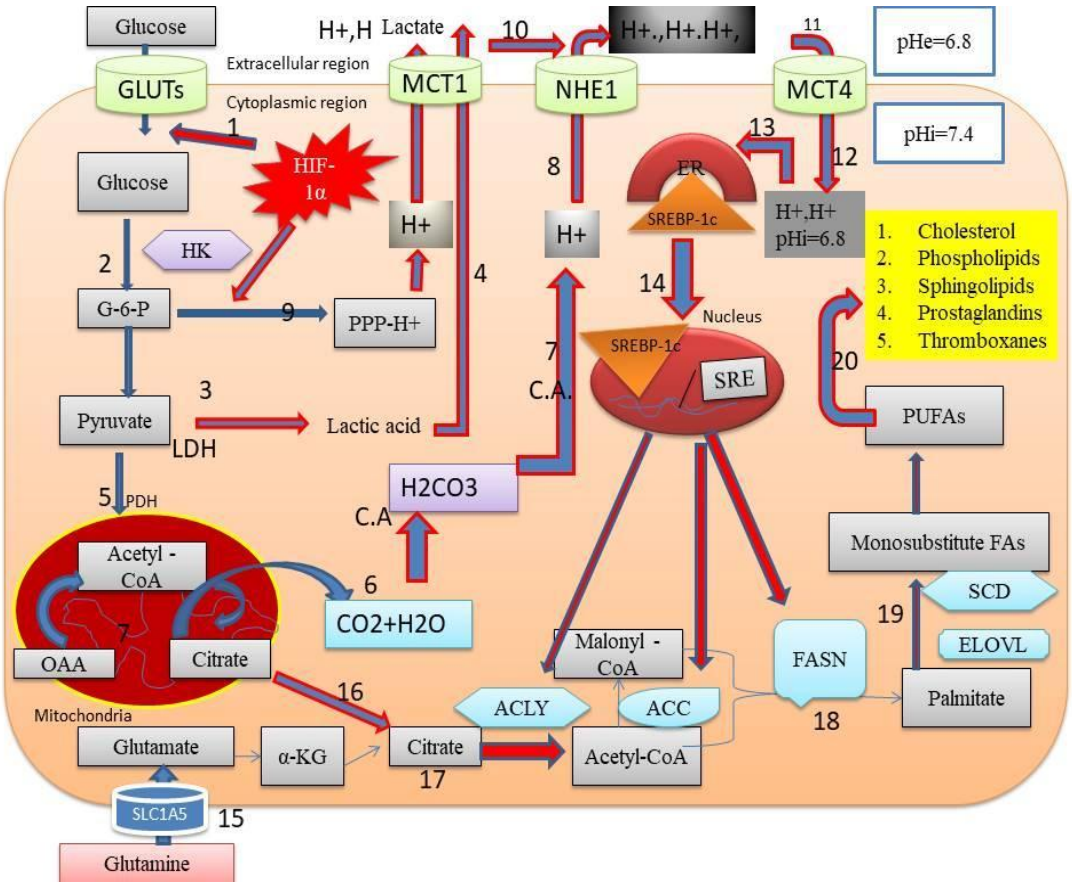

Figure 6: The interplay between HIF-1α, pH, SREBP-1c and FASN

HIF-1α is a master regulator of interplay between pH, SREBP-1c and FASN. Glucose metabolism through glycolytic pathway results in accumulation of lactic acid which is pumped out through the MCT1 (1, 2, 3, 4). Carbonic acid produced through metabolic conversion of CO_2 and H_2O by C.A is transported out through NHE1 (6, 7, 8).

Protons are also generated through glycolysis and PPP which are exerted out (9). pHe in tumor microenvironment becomes acidic and thus a proton gradient develops across the plasma membrane (10). Due to proton gradient protons from the extracellular region move back through MCT4 transporter and pHi again become acidic (11, 12). Acidic pHi activates SREBP-1c located in ER which is translocated in the nucleus where it causes activation of genes of enzymes involved in fatty acid synthesis like FASN, ACC and ACALY (13, 14). Deamination of circulating glutamine to glutamate provides citrate which is used in fatty acid synthesis (15, 16). Citrate is also provided from the TCA cycle to be used in fatty acid synthesis (17). Finally citrate is converted to palmitate which is further utilized to form long chain PUFAs like cholesterol, sphingolipid and thromboxane (18, 19,20). **FASN**: Fatty acid synthesis, **SREBP-1c**: sterol regulatory element binding protein 1-c, **ACC**: acetyl-CoA carboxylase, **ACLY**: ATP citrate lyase, **SCD**: stearoyl-CoA desaturase-1, **ELOVL-1**-elongation of very long chain fatty acids-1, **PUFA**-polyunsaturated fatty acids, **C.A**-carbonic anhydrase, **pHe**:, **pHi**: intracellular pH, **GLUTs**: glucose transporters, **NHE-1**: Na+H+ exchanger-1, **PPP:** pentose phosphate pathway.

that a difference in pHe and pHi in tumor cells causes destabilization of an endoplasmic protein SREBP-1c which further enhances the over expression of enzyme involved in fatty acid biosynthesis, cholesterol biosynthesis after binding with a sterile responding element (SRE) **(Figure-6)** [59]. Recently, Martin et al have reported mild hypoxia, but not severe increase in adipogenesis, lipogenesis and lipolysis in 3T3-L1 cells [60]. Various studies have reported the overexpression of SREBP-1c and FASN in response to mild hypoxia.

From the above discussion, it can be stated that there is a strong interplay between HIF-1α, pH, SREBP-1c and FASN.

1.10. Hypothesis

From the above discussion, it can be hypothesized that activation of PHD2 can regulate the interplay between HIF-1α, pH, SREBP-1c and FASN. Hypoxia-activated HIF-1α is the central regulatory pathway which works in the very smart way and alters the metabolism of glucose. HIF-1α limits the metabolism of glucose through glycolysis and consequently, pHe is reduced. A pH gradient is developed across the

plasma membrane of tumor cells which activates the endoplasmic protein SREBP-1c. Activated SREBP-1c translocates to the nucleus and leads to over expression of FASN and other enzymes involved in lipid metabolism. HIF-1α is the master regulator of glycolysis, pH, SREBP-1c and FASN. Most of the solid tumors transform into malignant due to aforesaid effects of HIF-1α and then therapy becomes even more difficult. It is well understood that PHD2 is a negative regulator of HIF-1α, which (**Figure-7**) causes first, its hydroxylation, followed by polyubiquitination and eventually its proteasomal degradation. So, chemical activation of PHD2 can down regulate all effects of HIF-1α and stop the propagation of cancer to the other organs. Exogenous activation of PHD2 could be a novel strategy to control the tumor microenvironment.

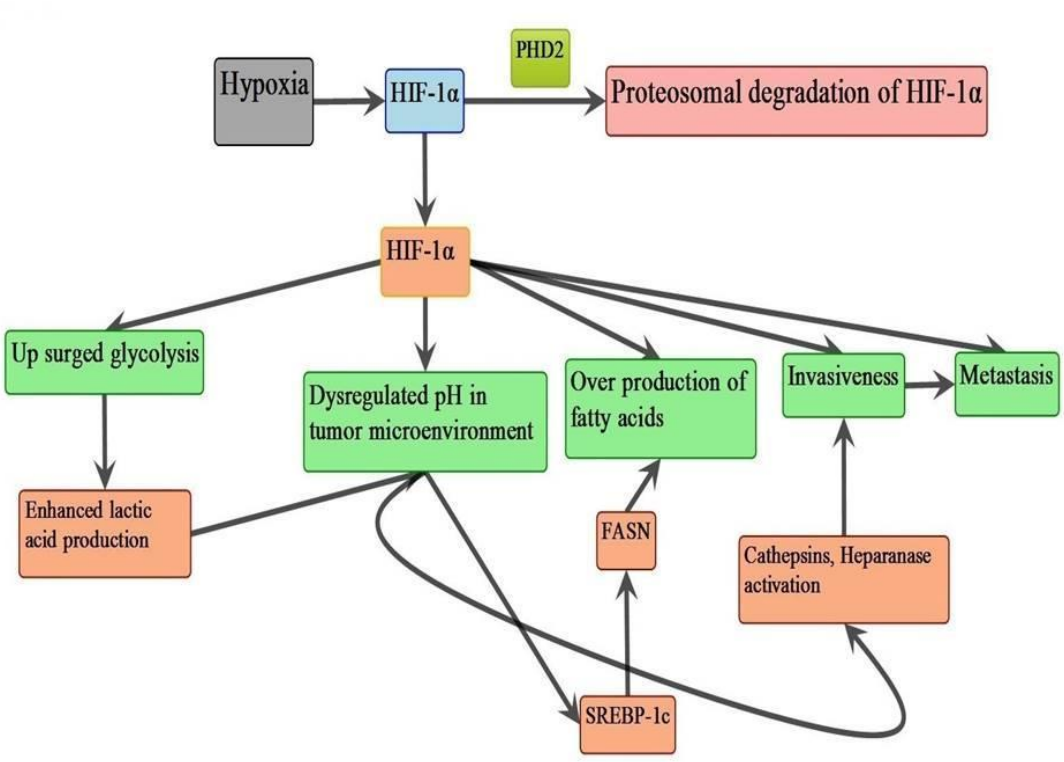

Figure 7: Hypothesis; PHD2-regulate the interplay between HIF-1α, pH, SREBP-1c and FASN

Hypoxia activated HIF-1α enhances the expression of GLUT-1 and GLUT-4 receptors in order to enhance glycolysis. Glucose is finally oxidized to the pyruvate lactate pathway and thus reduces pHe in the tumor microenvironment. Reduced pHe activates SREBP-1c protein which in turn enhances the expression of FASN and thus fatty acid synthesis. Acidic tumor microenvironment also activates the enzymes like cathepsins, Heparanase which enhances invasiveness. Lower pHe also enhances the process of angiogenesis and metastasis in tumor cells. PHD2 is a negative regular of HIF-1α, can down regulate series of its effects. **HIF-1α:** hypoxia –inducible factor-1α, **FASN:** fatty acid synthase, **SREBP-1c**: sterol regulatory element binding protein-1c.

1.11. Literature survey

Furuta et al (2016) found that FAS was significantly up-regulated by hypoxia, which was also accompanied by reactive oxygen species (ROS) generation in human breast cancer cell lines. The FAS expression was also activated by H2O2, whereas N-acetyl-L-cysteine, a ROS inhibitor, suppressed the expression. They also found that the hypoxia significantly up-regulated sterol regulatory–element binding protein (SREBP)-1, the major transcriptional regulator of the FAS gene, via phosphorylation of Akt followed by activation of hypoxia-inducible factor 1 (HIF1)[7].

Bauerschlag et al (2015) reported that cancer cells remain in high demand of fatty acids and therefore de novo fatty acid synthesis and Fatty acid synthase (FASN) enzyme is crucial for tumor cells. During a study on the ovarian cancer cell lines and primary cell culture they observed high expression of FASN. Results documented 1.8 fold higher expression in FASN protein in tumor cell lines of ovarian tissue. Based on these findings, they recognized FASN as a therapeutic and chemo sensitizing target in ovarian cancer [8].

Bensaad et al (2014) reported that hypoxia unregulated the expression Fatty acid binding protein 3 (FABP3) and 4.Both of these proteins are involved in fatty acid uptake and identified during in vivo antiangiogenic therapy with bevacizumab

treatment . They observed a significant lipid droplet accumulation and Adipophillin under the influence of hypoxia.

Gregg L. Semenza (2013) explained that hypoxia occurs frequently in human cancers and induces adaptive changes in cell metabolism that include a switch from oxidative phosphorylation to glycolysis, increased glycogen synthesis, and a switch from glucose to glutamine as the major substrate for fatty acid synthesis. This broad metabolic reprogramming is coordinated at the transcriptional level by HIF-1, which functions as a master regulator to balance oxygen supply and demand. HIF-1 is also activated in cancer cells by tumor suppressor (e.g., VHL) loss of function and oncogene gain of function (leading to PI3K/AKT/mTOR activity) and mediates metabolic alterations that drive cancer progression and resistance to therapy. Inhibitors of HIF-1 or metabolic enzymes may impair the metabolic flexibility of cancer cells and make them more sensitive to anticancer drugs [5].

Ilias Mylonas et al (2012) postulated that hypoxia induced metabolic reprogramming is essential during physiological and pathological conditions. The study reported that hypoxia leads to accumulation of triglycerides and lipid droplets in human cells which is accompanied by induction of lipin-1. Lipin-1 is a member phosphatidate phosphatase isoforms that makes the essential step in triglyceride biosynthesis. HIF-1α binds to the single distal hypoxia response element in the lipin-1 promoter gene region and leads to its up regulation in low oxygen tension. Further study reported that triglycerides accumulation can be inhibited by silencing the Lipin-1 with siRNSor by inhibiting HIF-1α with Kaempferol

Hoperton K (2012) reported that FASN is over expressed in many cancers and its activity is required for cancer cell survival. To understand this, he compared the utilization of fatty acids synthesized endogenously by FASN to those supplied

exogenously in the culture medium. He found that endogenously fatty acids are esterified to the same lipid and phospholipid classes in the same proportions as those derived exogenously and that endogenous fatty acids are excreted [9].

Francis P. Kuhajda (2006) reported that fatty acid synthase(FAS) enzyme , the most important enzyme in de novo fatty acid synthesis is extensively expressed in most of the carcinomas. The high expression of FAS enzyme is attributed to poor prognosis of breast and prostate cancer. Inhibition of FAS and fatty acid metabolism is a potential target in diagnosis and treatment of cancer [7].

JinHyen et al (2005) reported that OS-9 is an essential protein product of genes which interact both with HIF-1α as well as with prolyl hydroxylase. According to the findings, activated form of OS-9 promotes hydroxylation of HIF-1α, its binding with VHL and subsequently its proteasomal degradation and finally inhibition of HIF mediated transcription of genes. Contrary to this, opposite effects of HIF-1α were observed. When OS-9 function is lost due to RNA interferences, the level of HIF-1 protein increased along with VEGF mRNA expression increased in non-hypoxic conditions. These findings clearly depicted that OS-9 is an essential component of a complex of proteins which regulate HIF-1 level in an O2 dependent manner [12].

Elisa Temes et al (2005) reported in his study that Hypoxia inducible factor -1α is the main hero which makes various decisions to make the cells adaptive to the low oxygen environment. Futhere , he explained that in the presence of oxygen the HIF-1subunit becomes hydroxylated and finally degraded by the hydroxylases after being recognized by the von Hippel-Lindau (VHL) protein. But in absence of oxygen, HIF-1α escapes from proteolytic degradation, bonds with other subunits to form a dimer which translocates to the nucleus, enhances the transcription of numerous genes

involved in metabolism, metastasis, and angiogenesis. In their previous studies , he has already explained the efficacy of of a nobel compound R59949 to inhibit the HIF-1α and in this study they explained that HIF-1α inhibitor activity of R59949 was arised due the activation of the prolyl hydroxylase by R59949. Further they found that R59949, not only activates prolyl hydroxylase in the presence of oxygen (21% oxygen) but it can also activate prolyl hydroxylase at 1% oxygen [13].

Kizaka-Kondoh et al (2003) reported that tumor hypoxia is a potential therapeutic problem encountered in radiotherapy and as well as in chemotherapy as it makes the tumor cell resistance to ionizing radiation and chemotherapeutic agents. He also reported that tumor hypoxia helps in the malignant transformation of most of the solid tumors. For example, it enhances the metastasis, invasiveness, and angiogenesis in solid tumors. Further, he added that hypoxia does not occur in the normal tissue compared to the hypoxic tumors (severe hypoxia pO2<0.33%, 2.5 mmHg), hence can be exploited theoretically. But ,selective targeting of hypoxic tumors cell is very difficult due to following three obstacle-firstly, it it is very difficult to deliver a drug to the remote hypoxic region due to poor blood supply, secondly, it is extremely difficult to selectively damage the hypoxic cancer cell , protecting the near well oxygenated cells and thirdly, severely hypoxic cancer cells have stopped dividing [3].

Martin J brown et al (1999) first time reported that hypoxia in solid tumors only a major obstacle in radiation therapy but also leads to resistance to most of the drugs. He also added that hypoxia accelerated malignant progression and increased metastasis and therefore researchers should focus on discovery of drugs which are effective in hypoxic environments. A number of drugs that are active in hypoxic environments have already been discovered, tirapazamine is one example. The said drug is highly toxic to hypoxic cancer cells and efficacy has been proven in

potentiation of cisplatin in randomized phase-III- clinical trials. Hypoxia in cancers tumors provided an important target for selective cancer therapy [2]

Hockel M. et al (1996) first reported that tumor cells always possess a small fraction of the microregion which is deficient in availability of oxygen. It is proved experimentally that hypoxia has a considerable influence on the malignant progression. They measured the level of oxygen in the advanced cancers of the cervix using a computerized polarographic electrode system.

CHAPTER-2

AIM & OBJECTIVES

2. Research envisaged

The proposed work is based upon the hypothesis that the PHD 2 induction will enhance hydroxylation and thereby increases proteolytic degradation of HIF-1α protein leading to decreased expression of FASN and thereby decreased tumor growth. FASN is an enzyme responsible for fatty acid synthesis and is reported to be overexpressed in tumors particularly in mammary gland tumors. Clearly, over expression of FASN is attributed to the hypoxia and increased lipid requirement of tumor cells. The inhibitors of FASN have been previously reported to exhibit good anti-tumor effects. The hypoxia causes inhibition of PHD 2 and enhances stability of HIF-1 α, which further regulates the glycolytic pathway hence modulates FASN over expression.

In the present study we are planning to screen natural available biomolecules to activate PHD 2 by using computer aided drug designing modeling to evaluate their effect on tumor hypoxia and thus on FASN overexpression. The study will be further extended to enumerate the effect of PHD2 inducers on tumor growth, angiogenesis, metastasis and apoptosis.

Aim and Objectives

The proposed study is aimed to screen /identify possible bio- activators of PHD2 and to evaluate them against mammary gland carcinoma to achieve following objectives-

- To screen the possible PHD2 inducers with structural similarity to ethnobiological known anticancer agents like Vincristine, Vinblastine etc.
- To evaluate the HIF-1α inhibitory and glycolysis inhibitory activity of screened PHD2 inducers *in Vivo*.
- To investigate the effects of PHD2 inducers on glycolysis and FASN over expression in normoxic and hypoxic condition.
- To enumerate the effect of screened PHD2 inducers on tumor metastasis, angiogenesis and apoptosis *in Vivo.*

CHAPTER-3

MATERIALS

&

METHODS

3. Material & methods

3.1. *In silico* study

3.1.1. Software used

PyRx (https://pyrx.sourceforge.io/)

CDRUG server

Autodock 4.2

ADME predictor

ProTOX-II

3.1.2. Screening of compounds and docking

Virtual screening and Docking: PyRx (https://pyrx.sourceforge.io/**) software was used for virtual screening of compounds.** It is a computational screening tool, used in drug discovery to search libraries of small molecules in order to identify those structures which bind to a drug target. Computational tool Autodock was used to determine the strength of interaction between a variety of ligands and targets in combination with three dimensional visualization. Ligands structure was searched from **ZINC database** and protein structure was searched from **Protein Data Bank (pdb id-2G19).**

Our hypothesis for this study is to search chemical activators of PHD2 which could cause rapid degradation of HIF-1α leading to favourable outcomes against cancer.

With this objective, a library of 5000 natural compounds of natural origin was downloaded based on their 60% structure similarity with **Vincristine**.

All the compounds were filtered by the Lipinsky Drug Liken (http://www.niper.gov.in/pi_ dev_tools/DruLiToWeb/DruLiTo_index.html) Tool and then individual compound were docked with PHD2 protein to determine the binding energy. Compounds with their very good binding energy with PHD2 were selected and shown below in the **Table1:-**

Table 1: List of compounds docked with PHD2 along with their binding energy.

Compound ID/Name	Compound Structure	Binding energy	Amino acids	Binding interaction
Vincristine	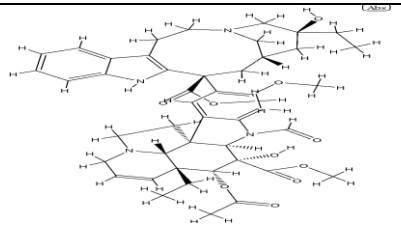	-10.46	VAL401, TYR403, LYS402	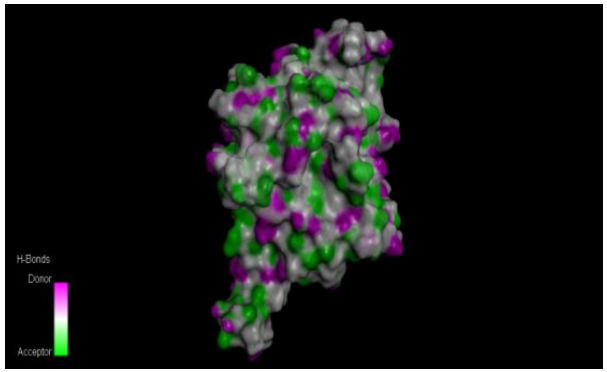
Voacamine	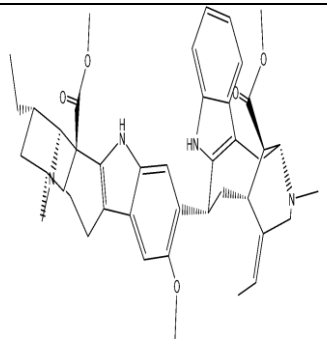	-9.46	LEU271,THR218LEU193, LEU191,HIS282,ARG282, ARG281,ALA190,LEU18 8,PHE213,GLY213,LEU2 14,GLU217,,ASP278,SER 275, SER214,	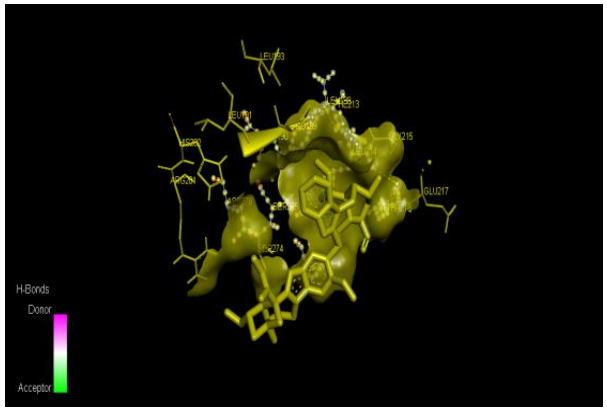

Image-9915	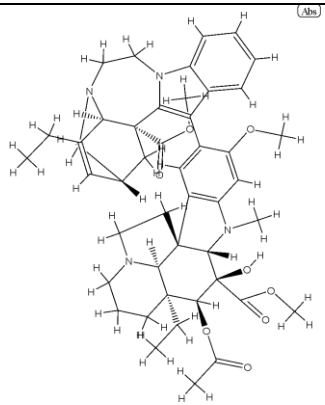	-13.04	ARG322,TRP389,TYR310 ,ASP254GLN239,THR236 ,ILE256,TRP258,MET299, TRP389	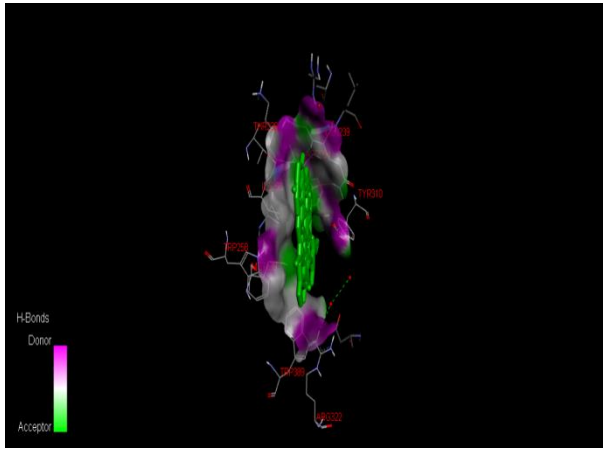
Image-8266	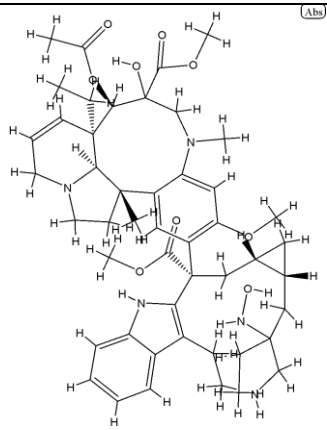	-10.00	ALA336, LYS337, SER339, GLY340, ALA381, TYR386	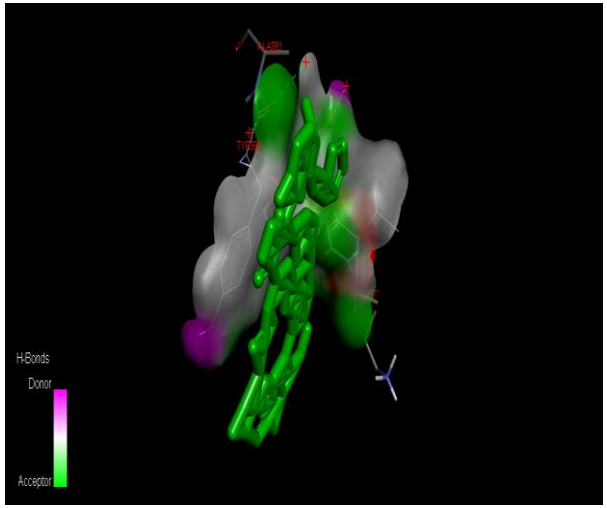

Image-7112	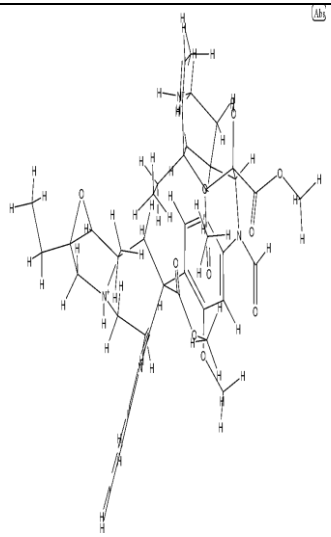	-8.46	ALA381, THR392, LYS332, ASP333	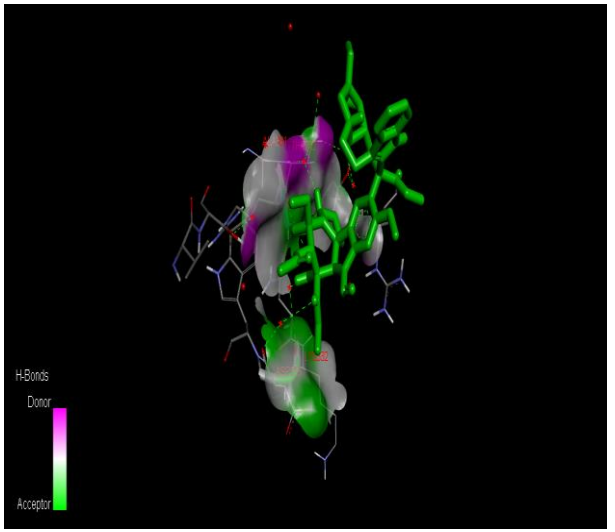
Image-7078	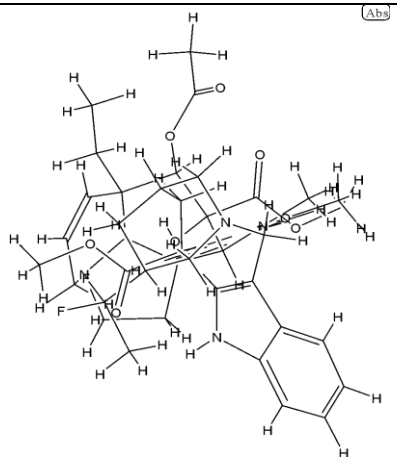	-7.52	ASP224, GLU225,ALA228, THR232, GLY265	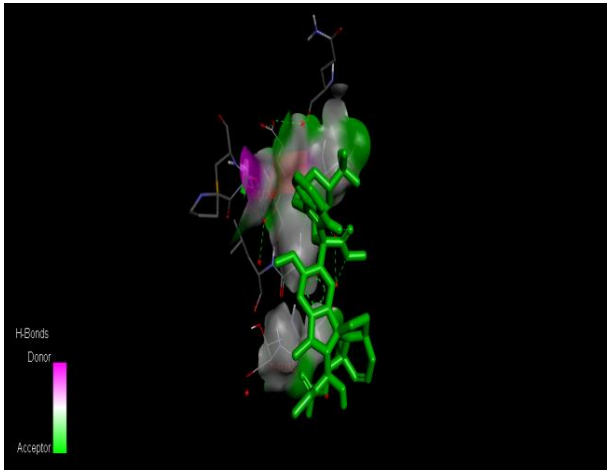

Image-7036	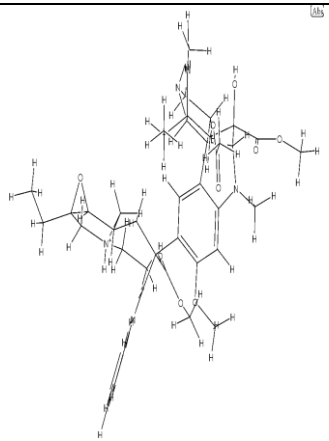	-8.12	GLN239,ILE256,TRY258, MET299,TRY389,TRY31 0,VAL311,ARG312,HIS31 3,VAL314,ASP315, PRO317,ARG322,TRY389 ,ASN318	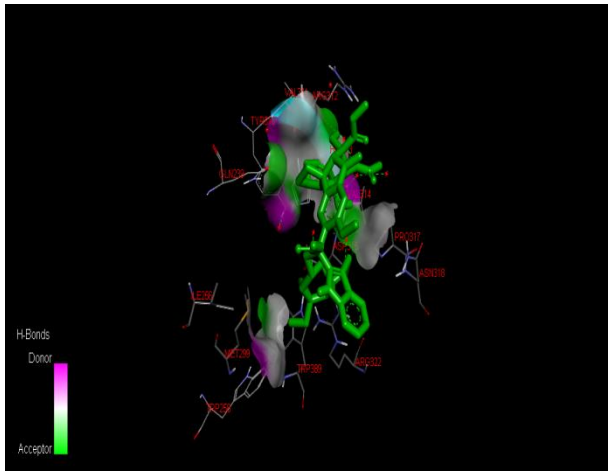
Image-7025	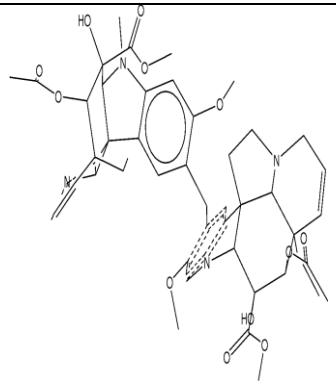	-7.07	ASP237,PHE235,THR236, ILE256,THR257,TRY258, LYS297	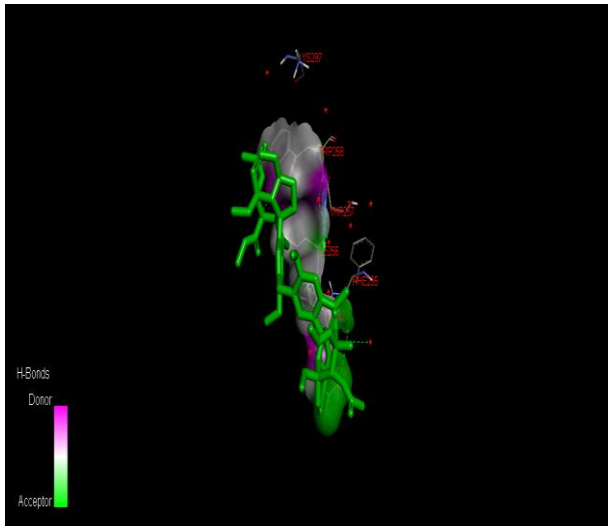

Image-7004	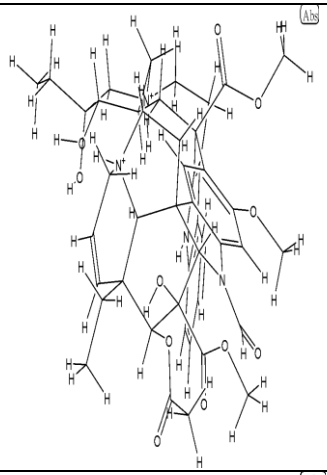	-8.93	TRP258, LYS297, GLU263	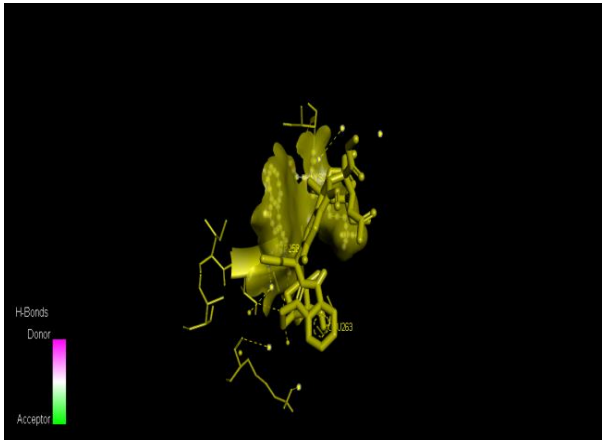
Image-6958	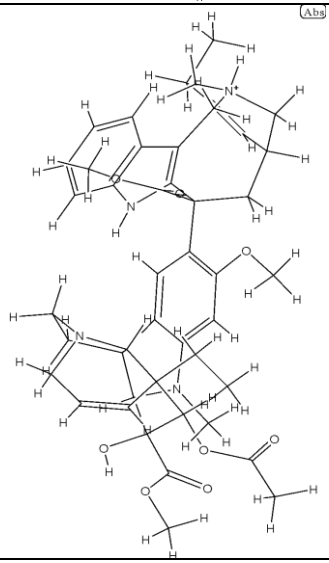	-7.92	ARG398,GLU395, GLY319,ASN318, ASN316.PRO317, ASP369, ARG370, TRP290, SER289ARG371,	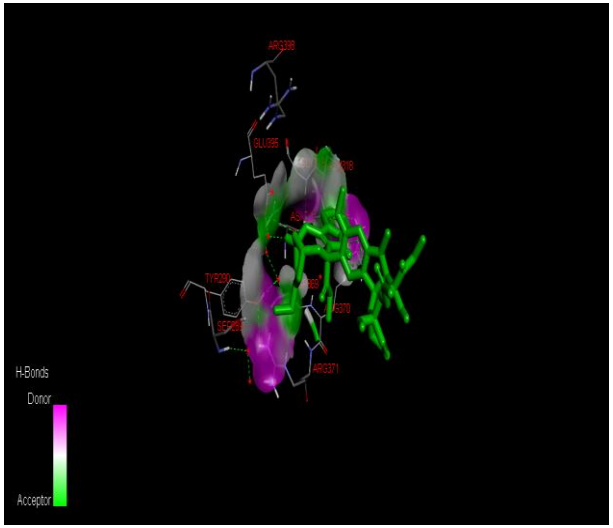

Image-6401	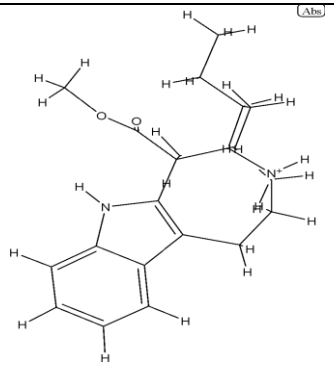	-7.37	LYS297,TRP258, THR257 THR236,ILE259, LYS234,GLU263	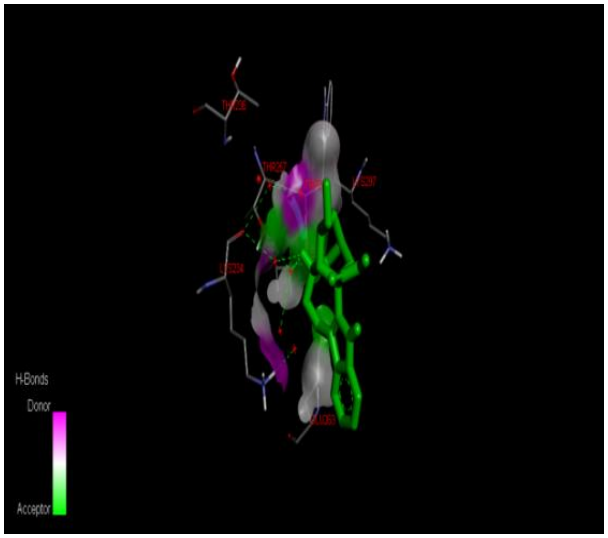
Image-5914	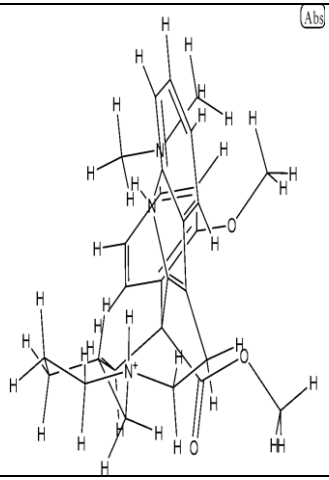	-6.12	LYS234, GLU263, THR257, TRP258, LYS297	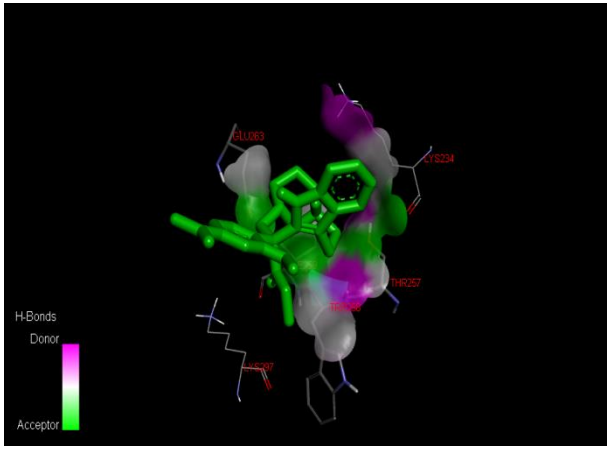

Image-3255	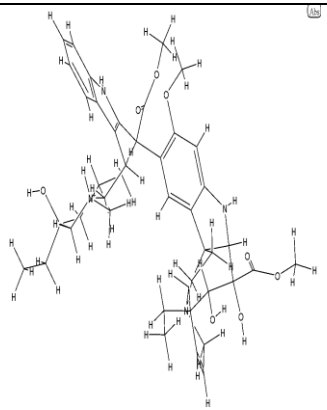	-10.60	TRP258, LYS297, THR296	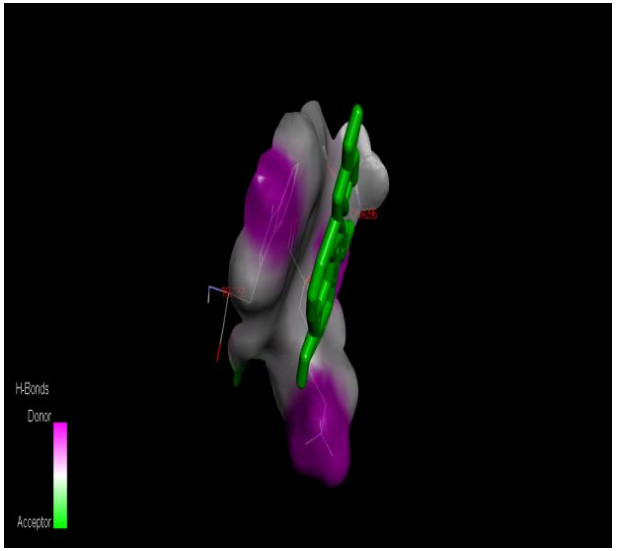
Image-3241	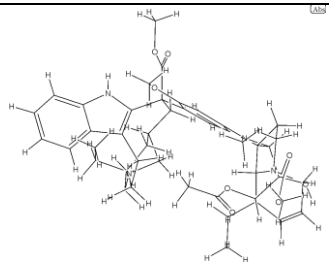	-9.06	ASP333, TRP334, SER339	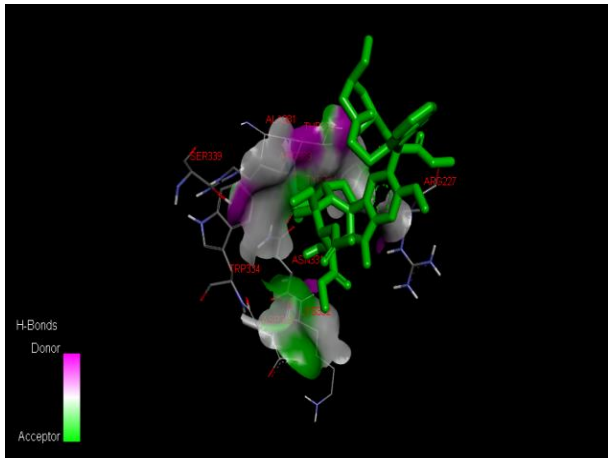

3.1.3. ADME and toxicity of VOA

Rodent oral toxicity of screened compounds

Toxic doses are often given as LD 50 mg/kg body weight. The LD50 can be defined as the median lethal dose at which 50% of test subjects like mice die with exposure to the compound. Oral rodent toxicity and LD 50 of VOA was determined with ProTox-II software which acts as a virtual lab for the prediction of toxicities of small molecules. ProTox-II has been designed based on the molecular similarity, fragments propensities, and machine learning to predict acute toxicity, hepatotoxicity, immunotoxicity and adverse outcome pathways. Toxicity class is defined according to the globally harmonized system of classification of chemicals (GHS). LD_{50} values are given in [mg/kg]:

1. Class I: fatal if swallowed ($LD_{50} \leq 5$ mg/kg
2. Class II:fatal if swallowed ($5 < LD_{50} \leq 50$)
3. Class III: toxic if swallowed ($50 < LD_{50} \leq 300$)
4. Class IV:harmful if swallowed ($300 < LD_{50} \leq 2000$)
5. Class V: may be harmful if swallowed ($2000 < LD_{50} \leq 5000$)
6. Class VI: nontoxic ($LD_{50} > 5000$)

VOA and VIN and TMX were subjected to predict oral toxicity and the calculated LD50 and class of toxicity is shown in the table 2.

In Silico ADME studies

ADME involves absorption, distribution, metabolism and excretion of drugs which is described as pharmacokinetics in pharmacology means movement of drug in the body. Absorption of the drug depends upon the ionization and unionization of the drug in the solution. Ionized form of drugs is slowly absorbed but unionized form of drugs can easily pass through the plasma membrane transporter. Secondly, highly, lipophilic drugs can easily pass through the biological membrane. Bioavailability, another factor which affects the absorption of drugs and depends upon the type of dosage form a drug. It can be defined as a rate and extent at which a drug reaches to the systemic circulation. Distribution of drugs depends upon the lipid solubility, pH, extent of plasma protein binding, presence of tissue specific receptors and differences in regional flow. Metabolism of drugs means biotransformation of drugs which render the hydrophobic drugs to more water soluble form that can be excreted out from the body. Liver is the major site of drug metabolism, but lungs, kidney and intestines also metabolize a fraction of drugs. In the liver, different isoforms of the cytochrome P450 are present which carry out biotransformation of drugs. Excretion of metabolized drugs is mainly carried out through filtration by the kidney. Predicted ADME and LD_{50} of docked compounds is shown below in Table **2**.

Table 2: Predicted ADME and LD_{50} of screened compounds

Compound Name	Predicted LD_{50}	Predicted toxicity class.	Pgp inhibitor	Solubility	Liver enzymes inhibited	Plasma protein binding	BBB
Vincristine	305mg/kg	Class:2	Non	**Pure_water_solubility_mg_L** =0.146855 **Buffer_solubility_mg_L** = 0.00993934	**CYP_2C19_inhibition** - Non **CYP_2C9_inhibition** - Inhibitor **CYP_2D6_inhibition** - Non **CYP_2D6_substrate** - Weakly **CYP_3A4_inhibition** - Inhibitor **CYP_3A4_substrate** – Substrate	**Plasma_Protein_ Binding** =19.721138	**BBB** - 0.0649079
Voacamine	68mg/kg	Class: 3	Inhibitor	**Pure_water_solubility_mg_**L=0.00868525 **Buffer_solubility_mg_L** =0.201054	**CYP_2C19_inhibition** - Non **CYP_2C9_inhibition** Inhibitor **CYP_2D6_inhibition** Non **CYP_2D6_substrate** Weakly **CYP_3A4_inhibition** Inhibitor **CYP_3A4_substrate** Substrate	**Plasma_Protein_ Binding**=84.588839	**BBB**- 6.73675
3241	305mg	Class: 4	Inhibitor	**Pure_water_solubility_mg/L-**	**CYP_2C19_inhibition** Non	**Plasma_Protein_ Binding**	**BBB** - 0.613435

				0.0254425 **Buffer_solubility_mg/L** - 0.181635	**CYP_2C9_inhibition** Inhibitor **CYP_2D6_inhibition**Non **CYP_2D6_substrate** Weakly **CYP_3A4_inhibition** Inhibitor **CYP_3A4_substrate**Substrate	=39.711298	
3255	210mg/kg	Class: 3	Inhibitor	**Pure_water_solubility_mg/L** 17.786 **Buffer_solubility_mg/L** 328.706	**CYP_2C19_inhibition** - Non **CYP_2D6_inhibition** - Inhibitor **CYP_2D6_substrate**- Substrate **CYP_3A4_inhibition** - Non **CYP_3A4_substrate** Substrate	**Plasma_Protein_Binding** =78.419353	**BBB** - 5.22932
5914	210mg/kg	Class: 3	Inhibitor	**Pure_water_solubility_mg/L** 9.32987 **Buffer_solubility_mg/L**- 10.4384	**CYP_2C19_inhibition** Non **CYP_2C9_inhibition** Inhibitor **CYP_2D6_inhibition** Inhibitor **CYP_2D6_substrate** Weakly **CYP_3A4_inhibition** Inhibitor **CYP_3A4_substrate** – Substrate		**BBB** 4.44206

6401	130mg/kg	Class: 3	Inhibitor	**Pure_water_solubility_mgL** - 36.8709 **Buffer_solubility_mg/L** - 964.704	**CYP_2C19_inhibition** - Non **CYP_2C9_inhibition** - Non **CYP_2D6_inhibition** - Inhibitor **CYP_2D6_substrate** - Weakly **CYP_3A4_inhibition**- Non **CYP_3A4_substrate** – Substrate	**Plasma_Protein_Binding** =56.997692	**BBB** 5.65674
6958	68mg/kg	Class: 2	inhibitor	**Pure_water_solubility_mg/L**- 0.026083 **Buffer_solubility_mg/L** - 0.123304	**CYP_2C19_inhibition** - Non **CYP_2C9_inhibition** - Inhibitor **CYP_2D6_inhibition**- Non **CYP_2D6_substrate** - Weakly **CYP_3A4_inhibition** - Inhibitor **CYP_3A4_substrate** – Substrate	**Plasma_Protein_Binding** 31.794375	**BBB** - 0.384809
7004	305mg/kg	Class: 4	Non	**Pure_water_solubility_mg/L**- 0.560002 **Buffer_solubility_mg/L**- 0.0796709	**CYP_2C19_inhibition**- Non **CYP_2C9_inhibition**- Inhibitor **CYP_2D6_inhibition** - Non **CYP_2D6_substrate** - Weakly	**Plasma_Protein_Binding**- 12.630945	**BBB**- 0.0348676 *

					CYP_3A4_inhibition - Inhibitor **CYP_3A4_substrate** – Substrate		
7018	68mg/kg	Class: 2	Inhibitor	**Pure_water_solubility_mg/L** - 0.0562501 **Buffer_solubility_mg/L** - 0.533069	**CYP_2C19_inhibition** - Non **CYP_2C9_inhibition** - Inhibitor **CYP_2D6_inhibition** - Non **CYP_2D6_substrate** - Weakly **CYP_3A4_inhibition** - Inhibitor **CYP_3A4_substrate** – Substrate	**Plasma_Protein_Binding** - 19.287388	**BBB** -- 0.158973
7036	305mg/kg	Class: 4	Inhibitor	**Pure_water_solubility_mg/L** - 0.013522 **Buffer_solubility_mg/L-** 14.6265	**CYP_2C19_inhibition**- Non **CYP_2C9_inhibition** - Inhibitor **CYP_2D6_inhibition** - Non **CYP_2D6_substrate** - Weakly **CYP_3A4_inhibition** - Inhibitor **CYP_3A4_substrate** – Substrate	**Plasma_Protein_Binding** 58.641983	**BBB** 0.497633
7112	68mg/kg	Class: 2	Non	**Pure_water_solubility_mg/L** - 0.147502 **Buffer_solubilit**	**CYP_2C19_inhibition** - Non **CYP_2C9_inhibition** - Inhibitor	**Plasma_Protein_Binding** - 11.993057	**BBB** - 0.04299

				y_mg/L - 0.0795257	**CYP_2D6_inhibition** Non **CYP_2D6_substrate** - Weakly **CYP_3A4_inhibition** - Inhibitor **CYP_3A4**_-substrate Substrate		
8266	68mg/kg	Class: 2	Inhibitor	**Pure_water_solubility_mg/L-** 0.0140139 **Buffer_solubility_mg/L-** 0.017051	**CYP_2C19_inhibition**- Non **CYP_2C9_inhibition** - Inhibitor **CYP_2D6_inhibition** - Non **CYP_2D6_substrate** - Weakly **CYP_3A4_inhibition** -- Inhibitor **CYP_3A4_substrate** – Substrate	**Plasma_Protein_ Binding** - 63.999544	**BBB** - 0.386426
9915	68mg/kg	Class: 2	Inhibitor	**Pure_water_solubility_mg/L-** 0.0131937 **Buffer_solubility_mg/L** - 0.0318007	**CYP_2C19_inhibition** - Non **CYP_2C9_inhibition** - Inhibitor **CYP_2D6_inhibition**- Non **CYP_2D6_substrate** Weakly **CYP_3A4_inhibition** - Inhibitor **CYP_3A4_substrate** – Substrate	**Plasma_Protein_ Binding** - 64.715325	**BBB** - 0.0434254

3.1.4. Selection & Procurement of compounds

All the compounds were docked (Autodock 4.2) [12] with PHD-2 protein (PDB ID: 2G19) and about thirteen compounds were found to have good binding energy with PHD-2 protein. After the docking studies compounds were searched for their availability and supply. Various manufacturers and suppliers were contacted. Finally, 3 compounds [NSC-82591 (Voacamine)-80mg, NSC-269619 (Vinkaleukoblastine)-1mg, NSC-608210()-5mg were approved for dispatch from National Cancer Institute, USA (https://dtp.cancer.gov/RequestCompounds/index.xhtml). The compound with NCI ID-NSC-608210 couldnot be transported due to requirement of special storage conditions while compounds second with NCI ID- NSC-269619 was approved in very less quantity as well as its binding energy with PHD2 was less compared to the Voacamine. Finally, Voacamine (ZINC169368472) was selected for further *In Vivio*studies based on its good binding energy and approved quantity.

Upon further literature survey it was found that the drug VOA is an active constituent of plant *Pescheriafuchasiae* folia and already in use for Chloroquine resistant malaria [1]. The drug has been shown its anti-cancer activity in Doxorubicin resistant Osteo Sarcoma U-2 OS cells. The drug is a P-gp inhibitor and can induce apoptosis –independent autophagy cell death in both sensitive and resistant cells [3]. Being a Pgp inhibitor, it can enhance or decrease the intracellular concentration of other drugs like Vincristine and Tamoxifen. Therefore, to confirm the said effect , its combination therapy was also given to the animals during *In vivo* studies.

3.2. *In Vivo* study

3.2.1. Equipments used

Various equipments used in the study are listed in table 3 below

Table 3: List of equipments used

Serial No.	Equipment	Manufacturer and Model
1.	Cooling centrifuge	Eppendorf India Limited, Chennai 5418R
2.	Vortex shaker	Remi Mumbai CM101
3.	Refrigerator	Godrej, Lucknow
4.	Homogenizer	Remi, Mumbai RQT-127A
5.	Microvolume Spectrophotometer	Agilent Technologies, Mumbai Carry 500
6.	Weighing balance	Sartorius, Mumbai BSA224S-CW
7.	pH meter	Labman Scientific Instruments, Lucknow LMPH-10
8	Micropipette	Genetix Biotech Asia Pvt. Ltd. New Delhi
9	Deep freezer	Celfrost, Lucknow
10	Digital biological microscope	N 120, BR-Biochem Life Sciences, New Delhi
11	Microplate Reader	Bio-Rad Laboratories Inc. Model 680XR
12	SDS-PAGE Electrophoresis	Biorad
13	Semidry transfer unit	Biorad
14	Chemidoc XRS+	Biorad
15.	Gas Chromatography	PerkinElmer 480
16.	Bio-amplifier (ML-136) and channel power lab (ML-826)	AD instruments, Australia
17	NMR Spectrophotometer (Bruker 800 MHz)	Bruker India Scientific Pvt. Ltd

3.2.2. Chemicals and Reagents

VIN (Cytocristin-Cipla) and Tamoxifen (TMX) (Tamodex20-Zydus) was purchased from the local market. VOA (NCI-3375-85-5) was obtained from National Cancer Institute (NCI) United States as a drug sample. Dimethyl sulfoxide (DMSO) (Merk), , ponceau S (Himedia.ML045), hematoxylin (Himedia, So58), eosin (Himedia,S007), acrylamide (Genetix-1443c196), transfer buffer (Genetix,GX-9411AR), Glycine (Amresco-0167-kg), ammonium persulfate (APS) (Loba Chemie-LB2282a09), RIPA lysis buffer (Amresco,N653), Tetramethylenediamine (TEMED) (Amresco-0761), Tris Ultrapure (DuchefaBiochemie), Sodium Lauryl Sulfate (SLS) (Lobachemie 56971301), DMBA (Sigma Aldrich,57-97-6), Protein assay kit (Amresco, M173), Bovine serum albumin (BSA) (Genetix,PG-2330). All other chemicals used in this study were purchased from Genetix Asia Pvt. Ltd. New Delhi, India and all are of molecular grade.

3.2.3. DMBA study

3.2.3.1. Experimental animals

Female albino wistar rats were obtained from CDRI Lucknow after the approval of the protocol (UIP/IAEC/May-2016/06). After procurement, animals were kept in the central animal house in the Department of Pharmaceutical Sciences (BBAU). The animals were kept for a 12h light/dark cycle at a stable temperature 22-24°C) and humidity. Also, animals had free access to standard animal feed water *ad libitum*. All the experiments were performed according to the guidelines laid by CPCSEA, Government of India. After one week, animals were randomly selected (in the weight range 100-150g) and divided into seven groups containing eight animal in each: Group 1 (normal control receives normal saline 2ml/kg, p.o.); Group 2 (toxic control receives DMBA 8mg/kg, i.v.); Group 3 (treatment1(T1) receives DMBA 8mg/kg, i.v. + VOA 1mg/kg, s.c.);

Group 4 (treatment2 (T2) receives DMBA 8mg/kg, i.v. + VIN 1mg/kg, i.v.); Group 5(treatment3 (T3) receives DMBA 8mg/kg, i.v. + VOA o.5mg/kg, s.c. + VIN 0.5mg/kg, i.v) ;Group 6 (treatment4 (T4) receives DMBA 8mg/kg, i.v. + VOA 1mg/kg, s.c. + VIN 1mg/kg, i.v); Group 7 (dummy control receives 3% DMSO solution s.c.). DMBA was prepared in a 3% DMSO solution and administered once at the beginning of study. Normal saline, 3% DMSO solution and drug treatment were administered after 15 days of DMBA injection and continued up to one month at a week interval. The study was continued up to 3 months. At the end of study, blood was collected from the retro tail vein in order to study the metabolomics profile of control and treatment groups. After blood withdrawal, animals were sacrificed under mild ether anaesthesia by cervical dislocation. Abdominal cavity was opened though the median incision. Mammary glands were carefully separated from the skin with the help of sharp scissors and forceps and mounted whole on the slide in order to carry out carmine staining [13]. Liver and kidney were also separated and preserved in the -20ºC to be used to assess the toxicity of drug molecules.

3.2.3.2.Hemodynamic analysis

For the assessment of cardiac toxicity due to DMBA, hemodynamic profile was performed using AD Instrument. The animals were mounted on the wax trays after anesthetizing by injecting ketamine hydrochloride (50mg/kg, i.m.) and diazepam (2.5mg/kg, i.m.). In order to record the ECG signals, dorsal and ventral thorax skin was cleaned and sterilized with spirit and then platinum hook electrodes were fixed on it. These electrodes had connections with the Bio-amplifier (ML-136) and channel power lab (ML-136). Both these instruments work together to convert analogue signals into digital signals (AD Instruments, Australia) which were stored in the hard disk of the system. Offline analysis of saved ECG signals was performed with Lab Chart Pro-8 (AD-Instruments, Australia) [14].

Further, ECG signals were also employed for HRV analysis. Firstly, a manual inspection of recorded signals was carried out in order to accurately detect R-waves. Afterward, R waves per unit time were plotted in order to calculate the HR. . Then, HR was calculated by plotting the number of R-waves per unit time. Finally, Lab Chart Pro-8 (AD Instruments) employed to calculate the time and frequency domain parameters of HRV [15, 16].

3.2.3.3. Carmine staining

For mammary gland whole mount analysis, mammary glands tissues were removed from rats and stretched over the glass slides. After drying, slides were placed in the Carnoy's fixative solution [ethanol (60%), chloroform (30%) and glacial acetic acid (10%)] for 2h and then washed with decreasing concentrations of ethanol (90%, 70%, 35%, and 15%) for 1h. The slides were placed in the alum carmine stain (1g carmine dye and 2.5g aluminium potassium sulphate in 500ml distill water) for 2 days. After 2 days, the Carmine stained slides were taken out and dehydrated with increasing concentration of ethanol (70%, 95% and 100%) and the lipids were removed by immersion in xylene for an overnight period of time. After that, slides were examined under the biological microscope at 4X in order to check the presence/absence of alveolar buds (ABs), terminal end duct (TED), terminal end bud (TEB) and lobules (LOs) [17, 18].

3.2.3.4. Histopathological analysis

To examine the morphology of the mammary gland, liver and kidney; Hematoxylin (H) and Eosin (E) staining was performed. Firstly, tissues were placed in 10% formaldehyde fixing solution and then buried inside the wax cubes. Using the microtome, 5µm sections were prepared and stained with H&E. Finally prepared tissue sections were examined under the digital biological microscope (BR-Biochem Life Sciences, N120, New Delhi, India) in order to visualize and imaging stained tissue. Photographs were taken at 4X and 40X [19].

3.2.3.5. Antioxidant markers

Frozen mammary gland tissue samples were thawed, precisely weighed and homogenized in 0.15M KCl. The mixture was centrifuged at 10000 g for 15 min. Supernatants were collected and kept in an ice bath until analysis. The enzymatic assays of catalase, thiobarbituric acid reactive substances (TBARs), superoxide dismutase (SOD), protein carbonyl (PC) and glutathione (GSH) were determined performed according to the method described us earlier [20, 21]. The reactivity of the enzymes with tissue samples was determined spectrophotometrically (UV-Visible spectrophotometer Agilent Technologies, Carry 60).

3.2.3.6. Fatty acid methyl ester (FAME) analysis

Frozen mammary gland tissue was accurately weighed and dissolved in a mixture of chloroform: methanol (2:1) in order to make 0.5% tissue homogenate. The homogenized tissue was further sonicated at 4˚C up to 5 min and then filtered with Whatman filter paper. Methanol added at last to make up the final volume. In the filtrate, 0.2ml double distilled water was added to remove the non fatty components. The resultant mixture was left undisturbed for half an hour. After half an hour, the solution was centrifuged at 5000g for 5min. After centrifugation, the lower lipid containing layer was conserved and the upper non fatty layer was discarded. In the subsequent step, methyl esters of the lipid sample were prepared by stirring the 0.75 gm of the sample with 2ml hexane and 0.2ml methanolic KOH(2N). The resultant mixture was vortexed for 15 min in order to separate into two layers. The FAME was present in the upper layer. It was carefully separated and used to analyze the lipid profile in control, toxic and treatment groups [22, 23].

3.2.3.7. ^{1}H NMR study

^{1}H NMR was performed in blood serum samples. To remove precipitates, serum samples were thawed and then centrifuged. For data acquisition, 220 µl of supernatant was serum taken in the

NMR tubes (Wilmad Glass, USA). To make up the final volume 440µl in the NMR tubes, 220µl NMR buffer solution (sodium phosphate saline of strength 20mm of pH7.4 prepared in D2O) was added. After this , a 2mm sealed tube called co-axial containing a 0.5mM solution of 3-trimethylsilyl-(2,2,3,3-d4)-propionic acid (TSP) was inverted in 5mm NMR tubes and 150µl of the solution poured into it. It worked as an internal reference standard. The prepared samples were analyzed with NMR spectrometer (Bruker NMR spectrometer), 800MHz) and raw spectra were obtained as NMR peaks. Also, CPMG (Carr-Purcell-Meiboom-Gill) NMR spectra was recorded for each serum sample by adopting the Brukers standard pulse programme library sequence (cpmgpr1d) with saturation of the water peaks. The spectrum was further processed in Bruker software Topsin-v2.1 (Bruker BioSpin GmbH, Silberstreifen 476287 Rheinstetten Germany) and AMIX software in order to carry out spectral binning of the CPMG data. The binned data was then further submitted to MetaboAnalyst, in order to carry out multivariate analysis of metabolomic spectral data. Firstly, Principal Component Analysis (PCA) was performed in order to take an initial overview of the metabolites in control, toxic and treatment groups. Next, data again analyzed with Partial Least Squares Discriminant Analysis (PLS-DA) method to bring out the metabolites responsible for class separation and the class separation among the grouped animals. The data was Pareto scaled for both PCA and PLS-DA and strictly validated for statistical significance. The cross validation of the models was described by the R^2 and Q^2 parameters and the p-values ≤0.05 calculated with Mann Whitney test for pairwise comparisons) were assumed to be statistical significance [24, 25].

3.2.3.8. Immunoblotting

For protein sample preparations 500mg mammary gland tissue was weighed and completely homogenized in Radioimmuno precipitation assay buffer (RIPA lysis buffer) and phenylmethy

lsulfonyl fluoride (PMSF). The amount of protein in each sample was quantified with Bradford assay. After quantification, proteins were separated on 12.5% sodium dodecyl sulfate-polyacrylamide gel electrophoresis (SDS-PAGE) gel using the principle of Laemmli. In the subsequent step proteins separated on gel transferred on to the polyvinylidene difluoride (PVDF) membrane (IPVH 00010 Millipore, Bedford, MA USA). Proteins transferred on PVDF membrane with Turbo Transfer assembly (Bio Rad) operated at 25 V, 2A for 15 min at 16^{o}C. The proteins transferred on membrane was blocked for 3h with mixture of 5% BSA and 5% not fat skimmed milk prepared in TBST and followed by incubation at 4ºC with primary antibodies,[SREBP-1c (SC-13551), HIF-1α (SC-13515), FASN (SC-55580), [(PHD2 (SC-67030)] for overnight period. β-actin was used as a standard reference. After overnight incubation with primary antibody, PVDF membrane was wiped three times with TBST and then incubated with HRP conjugated secondary antibodies [anti-mouse (SC-31430, Pierce Thermo Scientific, USA), anti-rabbit (SC-2030), anti-goat (SC-2020)] at room temperature for 3h [9, 26]. At the end, membrane was washed one time with TBST and protein blots were developed and analyzed in ChemiDoc XRS+ (Bio Rad).

3.3. MNU study

3.3.1. Experimental animals

Female albino Wistar rats in the weight range 60-100g were procured from Central Drug Research Institute (CDRI) Lucknow (protocol approval No.UIP/IAEC/May-2016/06). After procurement, animals were kept in the quarantine room of the departmental animal house in order to acclimatize to the laboratory conditions. Tetracycline was administered to the animals for next 7 days through water bottles in order to prevent bacterial infection. Also, 12h light /dark cycle, constant temperature and humidity were maintained along with free access to food water *ad libitum*. All the experiments were performed according to the guidelines laid by CPCSEA, Government of India. After one week, animals were randomly selected (in the weight range 100-

150g) and divided into 7 groups (eight animals in each group) Group1 (normal control receives normal saline 2ml/kg, p.o.); Group 2 (toxic control receives MNU 50mg/kg, i.p., Group 3 (MNU 50mg/kg, i.p. + VOA 1mg/kg, s.c.); Group 4 (MNU 50mg/kg, i.p. + VOA 2mg/kg, s,c.); Group 5 (MNU 50mg/kg, i.p. + TMX 8 mg/kg, p.o.); Group 6 (VOA 1mg/kg, s.c.+ TMX 1mg/kg s.c.) and Group 7 (dummy control receives 3% DMSO solution s.c.). In group 6, a lower dose of VOA and TMX was selected because both drugs are P-glycoprotein inhibitors (efflux pump), hence would enhance each other's intracellular concentration in cancer cells[16][17]. MNU was prepared in a 3% DMSO solution and administered once at the beginning of study. Normal saline, 3% DMSO solution and drugs treatment were administered after 15 days of MNU injection and continued up to one month. The study was continued up to 3 months. One day prior to the study electrocardiographic changes of the experimental animals were recorded. Next day, the animals were anesthetized with a cocktail of diazepam (5mg/kg/i.m.) and ketamine hydrochloride (100mg/kg/i.m.)[18]. Blood was collected from retro orbital plexus in order to study the metabolomics profile of control and treatment groups. After blood withdrawal, animals were sacrificed under mild ether anesthesia by cervical dislocation. Abdominal cavity was opened though the median incision. Mammary glands were carefully separated from the skin with the help of sharp scissors and forceps and mounted whole on the slide in order to carry out carmine staining[19]. Liver and kidney were also separated and preserved in the -20ºC to be used to assess the toxicity of drug molecules.

3.3.2. Hemodynamic analysis

Haemodynamic analysis of experimental animals was performed using an AD Instrument to assess cardiac toxicity due to MNU and VOA. Purposely, ketamine (50mg/kg, i.m.) and diazepam (2.5mg/kg, i.m.) were used to anesthetize the animals and mounted on the wax trays. Platinum hook electrodes were placed at the sterilized dorsal and ventral thorax skin. These electrodes had connections with Bio-amplifier (ML-136) and channel power lab (ML-826,

Australia) which has the capacity to convert analogue signals into digital signals. The electrocardiograph (ECG) signals thus recorded saved on the hard disk which are analyzed offline using Lab Chart Pro-8 (AD-Instruments, Australia)

Additions to this, the above ECG signals were further used for heart rate variability (HRV) analysis. Before this, a raw signal was manually inspected for the correct detection of R waves and from this HR was calculated by plotting the R waves per unit time. Finally, HRV was calculated using Lab Chart Pro-8 (AD-Instruments) after setting of time and frequency parameters[18].

3.3.3. Carmine staining

Carmine staining is an excellent method to view angiogenesis in malignant cancers. Mammary gland tissue was carefully removed and stretched over the glass slides and dried for some time. Afterwards, slides were kept in the Carnoy's fixative solution which was formed by mixing ethanol (60%), chloroform (30%) and glacial acetic acid (10%) continuously for 2hr. Subsequently slides were washed with decreasing concentrations of ethanol (90%, 70%, 35% and 15%) for 1h and then placed in a carmine staining solution for 2days. Carmine staining solution was formed by dissolving 1g carmine and 2.5 gm aluminium potassium sulfate in 500 ml water. After 2 days, slides were dehydrated again dipped in increasing concentration of ethanol (70%, 95% and 100%) and then placed in the xylene to remove the lipid adhesion on the tissue for an overnight period of time. Finally, prepared slides were examined under the biologicalmicroscope and images were taken at 4X resolution[14].

3.3.4. Histopathological analysis

To examine the morphology of the mammary gland; small tissue sections were fixed in a 10% solution of formaldehyde and then embedded in the wax cubes. Using the microtome, 5µm sections were prepared and stained with H&E. Afterwards, tissue sections were visualized and

photographed at 4X and 40X using a digital biological microscope (BR-Biochem Life Sciences, N120, New Delhi, India)[20].

3.3.5. Weight Variation

Constant decrease in body weight has been reported in cancer patients[21]. In the current study, initial body weight and final body of control, toxic and treated groups were measured. Percentage body weight was calculated the below given formulae:-

Percentage (%) decrease in body weight= (Final body weight-initial body weight/Initial body weight) X100.

3.3.6. Antioxidant markers

Tissue samples from each group were precisely weighed and homogenized in 0.15M KCl. The resultant mixture was centrifuged at 10000 rpm for 15 min and supernatants were collected and stored at ice cold water until further analysis. At the time of analysis a fraction of the supernatant was taken and used for the determination of superoxide dismutase (SOD), catalase, thiobarbituric acid reactive substances (TBARs), protein carbonyl (PC) and glutathione (GSH) according to the previous method described elsewhere. The absorbance of the samples was taken through UV-Visible spectrophotometer (Agilent Technologies, Carry 60**)[22].**

3.3.6 ^{1}H NMR study

Serum metabolic profile of experimental rats was analyzed with Bruker NMR spectrometer (Avance-III) operating at frequency of 800 MHz equipped with Cryoprobe. Serum samples was prepared by taking 220µl of serum in NMR tubes (5mm)(Willmadglasss, USA) and final volume is adjusted to 440µl with addition of 220µl of NMR buffer solution which was prepared in D2O by adding sodium phosphate saline of strength 20mm(pH7.4). Into this, 5mm tube, another tube termed as co-axial with diameter 2mm containing 0.5mM solution of 3-trimethylsilyl-(2,2,3,3-

d4)-propionic acid (TSP) was inserted. This acted as external lock and standard for the NMR experiments with reference to the metabolic quantification and assignment. After that, resultant NMR tubes were placed in the analysis point and raw NMR spectra was recorded and stored in the hard disk. The RAW NMR data thus obtained was analyzed with Bruker software Topspin-v2.1 (Bruker BioSpin GmbH, Silberstreifen 476287 Rheinstetten Germany). The spectra corresponding to the signals from lipoproteins, glycoproteins, amino acid, lactate and choline were mainly focused upon. In order to carry out analysis, the CPMG (0.7-8.6) spectra were binned and integrated using AMIX package (Version3.9.15, Bruker). Further, concentration of individual metabolites were determined with Chenomax software [23].

3.3.7. Western blotting

Tissue sample (500gm) was prepared in RIPA lysis buffer and phenylmethylsulfonyl fluoride (PMSF). After protein quantification with Bradford assay, 12.5% SDS-PAGE gel was employed to separate the proteins according to the principle of Laemmle. The separated proteins were transferred on to the PVDF membrane (IPVH00010 Millipore, Bedford, MA USA). Blocking of the transferred proteins was done with a mixture of 5%BSA and 5% non-fat skimmed milk prepared in TBST. After 3hr blocking, membrane was incubated with primary antibodies like FASN (SC-55580), SREBP-1c (SC-13551), PHD2 (SC-67030), HIF-1α (SC-13515) for overnight and then incubated with HRP conjugated secondary antibody [anti-goat (SC-2020)] at room temperature for 3h [14]. In the last, blots were developed with chemiluminescence substrate (Western Bright ECL HRP substrate, Advasnta, Melanopark, California, US) in ChemiDoc XRS+ (Bio Rad) after washing one time with TBST. β-actin was used as a reference standard in the analysis of protein blots.

3.3.8. Statistical analysis

The results were analyzed with Graph Pad Prism software (5.02). The values were presented as mean ± SD and the statistical significance was calculated by one way ANOVA followed by the Bonferroni test. The values less than *p< 0.05, **p<0.01, ***p< 0.001 were considered as statistically significant.

CHAPTER-4

DRUG PROFILE

4. Drug Profile

4.1. Drug 1:

Source: *Pescheria fuchsiae* folia tree

Chemical properties

1. Molecular formulae: $C_{43}H_{52}N_4O_5$
2. Molecular weight:704.9 g/mol
3. Case No: 3371-85-5
4. IUPAC Name: Methyl 12-methoxy-13-(17-methoxy-17-oxovobasan-3-alpha-yl) ibogamine-18-carboxylate
5. Common name: Voacamine
6. Chemical category: Bisindole alkaloid
7. Structure:

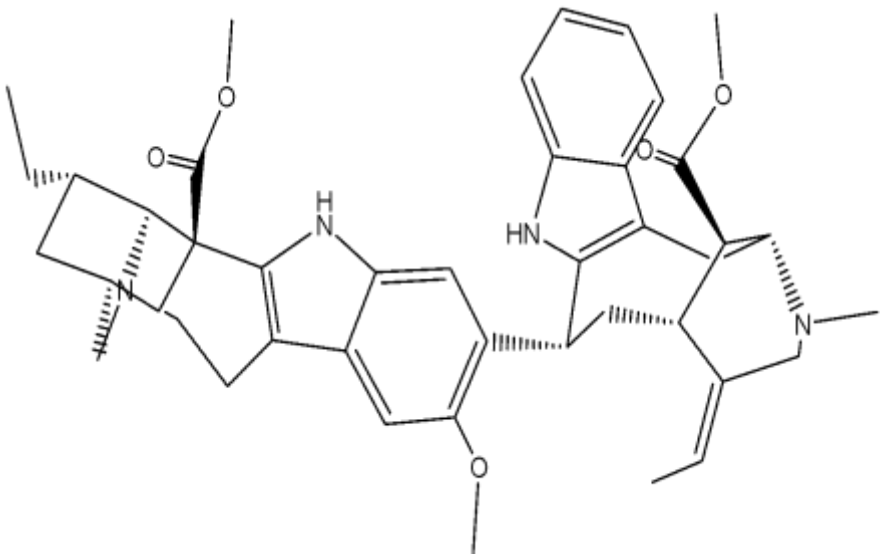

Physical properties

1. Color: Dark brown fine powder
2. Solubility in water: Sparingly soluble in water

4.2. Drug 2:

Source: *Vinca rosea*

Chemical properties

8. **Molecular formulae:** $C_{46}H_{58}N_4O_9$
9. **Molecular weight:**822.9 g/mol
10. **Case No:** 54022-49-0
11. **IUPAC Name**: Vinkaleukoblastin, 4-deoxy-3-epoxy-22-oxo-(3-alpha, 4-alpha)-(9Cl)
12. **Common name**: Vinkaleukoblastine
13. **Chemical category**: Indole alkaloid
14. **Structure:**

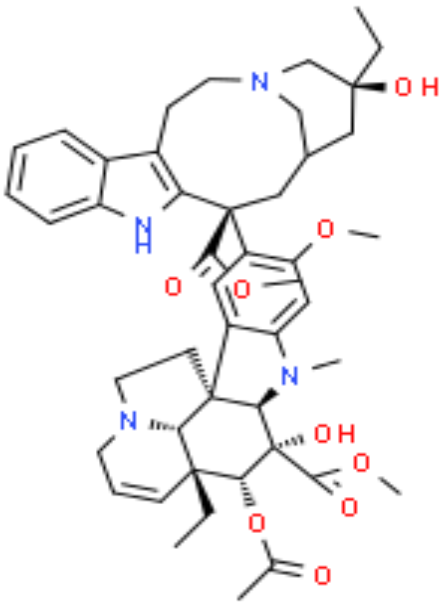

Physical properties

3. Color: Dark brown fine powder
4. Solubility in water: Sparingly soluble in water

CHAPTER 5

RESULTS & DISCUSSION

5. Result & discussion

5.1. *In Silico* study

5.1.1. Virtual screening of compounds

In docking studies, calculated negative energy determines the strength of binding and affinity between the docked ligand and the protein[24]. When VOA docked with PHD-2, the maximum binding energy was found to be -9.46 kcal/mol (**Figure 8**). The docked pose of the VOA had interaction with huge number of amino acids (LEU271, THR218, LEU193, LEU191, HIS282, ARG282, ARG281, ALA190, LEU188, PHE213, GLY213, LEU214, GLU217, ASP278, SER275, and SER214) which further support the stability of protein ligand complex. After docking studies VOA was subjected to calculation of rodent oral toxicity and the calculated LD50 was found to be 68mg/kg[25].

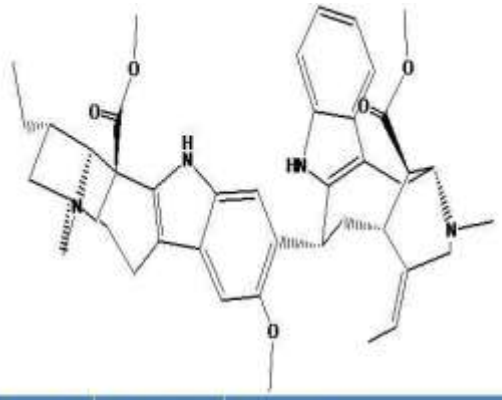

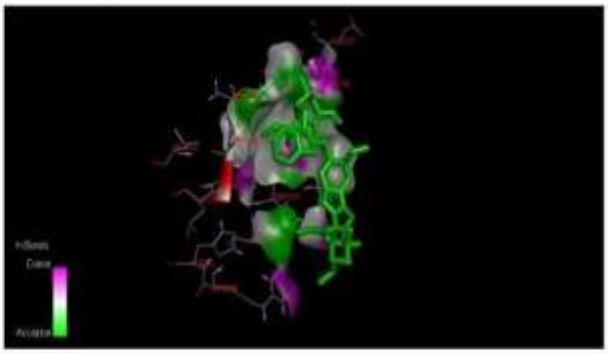

Predicted LD50	Toxicity class	Metabolism	Pgp	Binding energy	Amino acid interaction
68mg/kg	Class:III	**CYP_2C19_inhibition** -Non **CYP_2C9_inhibition** Inhibitor **CYP_2D6_inhibition** Non **CYP_2D6_substrate** Weakly **CYP_3A4_inhibition** Inhibitor **CYP_3A4_substrate** Substrate **Plasma_Protein_Binding** =84.588839 **BBB**-6.73675 **Pure_water_solubility** =0.00868525mg/L **Buffer_solubility**=0.201054mg/L	Inhibitor	-9.46	LEU271,THR218,LEU193,LEU191,HIS282,ARG282,ARG281,ALA190,LEU188,PHE213,GLY213,LEU214,GLU217,ASP278,SER275,SER214,

Figure 8: Docked pose of VOA with PHD-2 and metabolism

The compound belongs to class-III toxicity class. Following toxicity studies, VOA was further subjected *in silico* ADME studies and the results are presented in figure 1. Pharmacokinetic profile of the drugs shows that the drug has high plasma protein binding (84.588839) and has very less solubility in the pure water (water solubility 0.00868525mg/L). The drug also has moderate buffer solubility 0.201054 mg/L. Since the drug is highly lipophilic and crosses the blood brain barrier (BBB- 6.73). The drug VOA is a substrate and inhibitor of CYP-2C9 and CYP-3A4 type of liver enzymes which warns its interaction with all the drugs activating and inhibiting these enzymes. The drug VOA has potential to inhibit PgP-the efflux pump and thus it can potentiate the action as well as increase the toxicity of all those drugs which are effluxed through this pump like doxorubicin, Vincristine and TMX as well[26].

5.2. *In Vivo* study

5.2.1. DMBA induced mammary gland carcinoma

5.2.1.1. Effect of drugs and toxicants upon hemodynamic profile

Hemodynamic profile was measured by ECG **(Figure 9)** and HRV (**Table 4).** The results were analyzed online by MetaboAnalyst selecting PCA from chemometric analyses. 2D score plot of PCA of NC and treatment groups depicted a very good separation among the groups. The DMSO treated group was moving away from the NC group which indicates DMSO administration somehow affecting the cardiac activity. The DMBA administration also displaced the TC control group. Treatment with monotherapy with VOA (T1) and VIN (T2) further displaced away from the NC. But treatment with combination therapy displaced T3 and T4 even far away from the NC that clearly indicates cardiac toxicity of the drug. To further confirm the cardio toxicity of the drugs, data was again analyzed by Box-Cum Whisker plot (**Figure 10**).

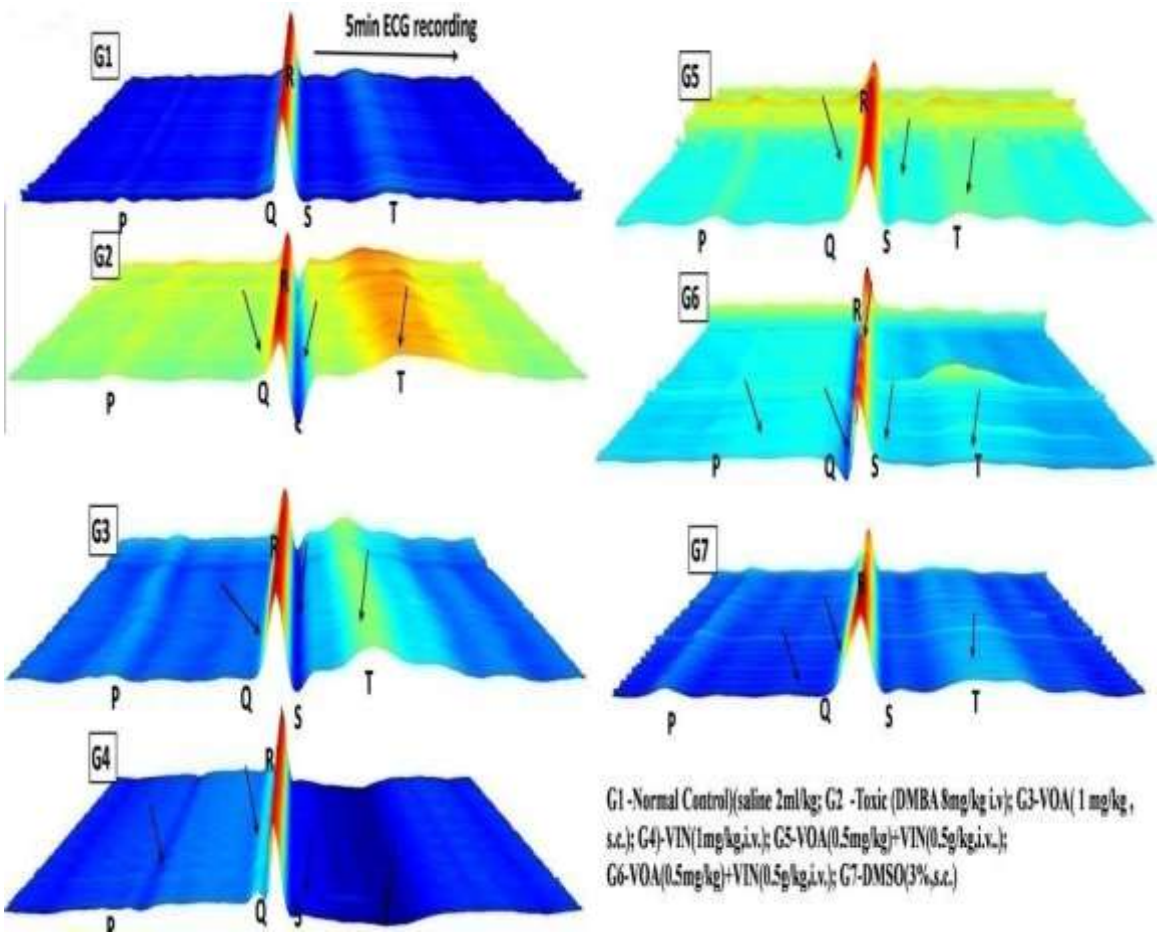

Figure 9: Waterfall map presentation of ECG/HRV recording of experimental animals

In figure, deformities in ECG are pointed by arrows. Groups are G1 -Normal Control saline 2ml/kg); G2 -Toxic (DMBA 8mg/kg i.v); G3-VOA(1 mg/kg , s.c.); G4)-VIN(1mg/kg,i.v.); G5-VOA (0.5mg/kg) + VIN(0.5g/kg,i.v..); G6-VOA (0.5mg/kg) + VIN (0.5g/kg,i.v.); G7-DMSO (3%,s.c.)

A significant difference in R and P amplitude was observed in the TC group when compared to the NC and treatment groups. P amplitude increased in all the groups when compared to the NC group with more pronounced effect in the VIN treated group. Duration of the P wave significantly increased with VOA (T1) but remained the same in all the other groups. PR interval increased with high dose monotherapy of VOA, VIN and with high dose combination therapy when compared to the normal control. QT interval was observed to be decreased in DC, combination low and high dose in TC whereas it was observed to be increased with monotherapy (T1 and T2). A raised level of R amplitude was observed in the TC group when compared to all

the treatment groups. S amplitude was decreased in DC, T1 and T4 while it was found to be increased with VIN high dose treatment group. T amplitude decreased with DMSO treatment but increased with high dose of monotherapy. A small decrease in heart rate was observed with DMSO administered group but sharp decrease in heart rate was observed with DMBA administration in TC group. Heart rate was even more decreased in all the treatment groups (T1, T2, T3, and T4) with the institution of therapy when compared to the NC, DC and TC. JT interval increased with monotherapy but opposite trend of RR interval observed in all the treatment groups. Q amplitude was increased with VIN high dose but no change observed with other treatments. T peak was greatly increased with a high dose of combination therapy but small increase in T peak also observed with monotherapy.

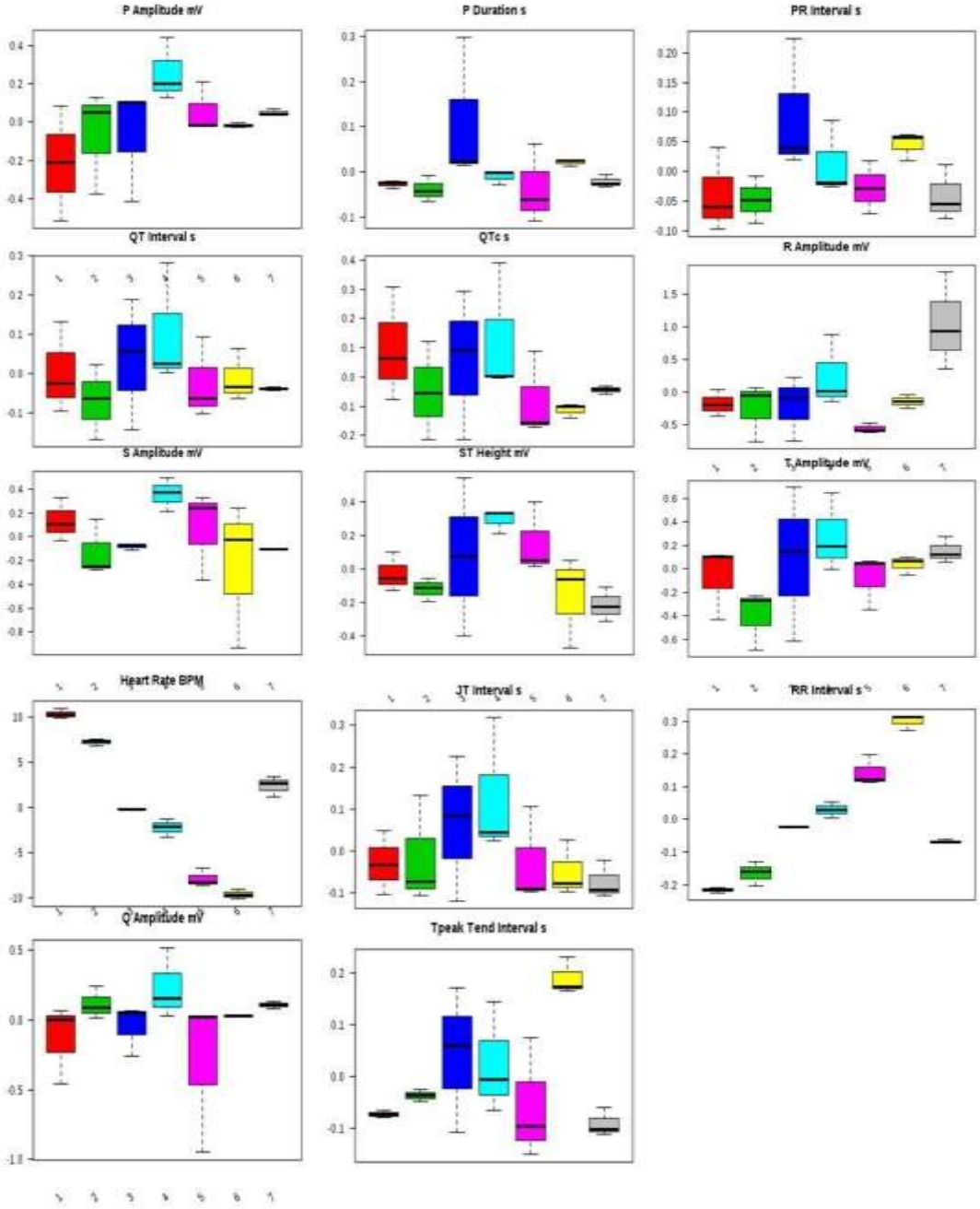

Figure 10: Box cum whisker plot of ECG/HRV recording of experimental animals.

1(Red)-NC (normal saline 2ml/kg,p.o.), 2(Green)-DC (DMSO 3%, 2ml/kg.p.o.), 3(Blue)-T1 (VOA 1mg/kg,s.c), 4(Light green)-T2 (VIN 1mg/kg,i.v.), 5(Pink)-T3 (VOA+VIN (0.5mg/kg), 6 (Yellow)-T4 (VOA+VIN (1mg/kg), 7 (Grey)-TC (DMBA)

Table 4: Effect of VOA and VIN on ECG/HRV of rats.

Groups	G1-NC	G2-TC	G3-T1	G4-T2	G5-T3	G6-T4	G7-DC
Average RR	234.45±22.98	162.35±0.070	244.35±0.07***	154.25±5.30	186.4±4.94**	147.75±4.94	195.9***
Median RR	235±22.62***	163±0.00	246±0.00***	154.5±4.94	185±1.41*	148±1.41	194.5±14.84***
SDRR	3.806±1.66	234.45±22.98***	6.465±0.03	1.40±0.50*	9.145±7.29	1.9±0.71	5.075±0.40
CVRR	0.016±0.00*	0.0465±0.00	0.024±0.002	0.0085±0.00**	0.0475±0.038	0.012±0.004*	0.0255±0.00
Average Rate	257.25±25.24***	370.4±0.14	245.7±0.00***	388.3±11.87	322.9±7.35***	406.15±3.747**	307.25±21.99***
SD Rate	4.465±2.77***	17.635±1.43	3.158±0.031***	3.525±1.08***	15.65±11.74	5.41±2.149**	7.94±0.48*
Frequency domain							
VLF Band	28.425±8.56	30.11±4.31	54.61±2.85*	39.63±17.77	70.43±25.90***	30.67±1.96	64.52±5.71***
LF	10.27±10.13	11.64±2.22	2.64685±1.23	7.045±4.27	11.271±9.20	5.511±0.12	5.09±2.51
HF	44.025±7.67	43.24±3.37	28.995±1.025*	41.265±6.17	15.9435±14.51***	48.505±1.80	23.845±0.37***
LF/HF	0.2156±0.19	0.2795±0.07	0.089±0.04	0.164±0.07	0.75±0.11***	0.111±0.001	0.21±0.09

All values represent Mean ± SD. Comparisons were made on the basis of one-way ANOVA followed by Bonferroni test. All groups were compared to the DMBA treated group. Values *p<0.05, **p<0.01 and ***p<0.001 were considered significant.

5.2.1.2. Morphological analysis

Carmine staining

Carmine staining is a very reliable staining technique to analyze angiogenesis in a malignant tumor. Single dose administration of DMBA caused significant increase in angiogenesis marked by an increase in alveolar buds (AB) and lobules (LO) in the TC group when compared to the NC (**Figure11:A1-G1).** Administration of monotherapy and combination therapy (both low and high dose) of VOA and VIN inhibited angiogenesis in the experimental animals. Moreover, results show that VOA alone (T1) and combination therapy resulted in better inhibition of angiogenesis compared to the VIN (T2) treatment characterized by lower number of AB counts and LO.

Histopathology

H&E staining was performed to view the microscopic architecture of mammary gland tissue of control and toxic treated rats. On DMBA administration, significance damage to the lactiferous duct (LD), adipocytes (AD) along with distorted myoepithelium (ME) and ductal epithelium (DE) was observed in TC group when compared to the NC **(Figure 11:(A2-G2).** On initiation of therapy with VOA and VIN (as monotherapy and combination therapy) granted a significant protection to the mammary gland tissue as evidenced by the regeneration of lactiferous duct (LD), fibrous stromal tissue (FST) and adipocytes. A better improvement was observed with the combination therapy comparable to normal. Not any kind of cellular damage was observed in the DMSO (3%) treated animals. This further gives a clue that DMSO at this concentration has no side effects if used as a solvent.

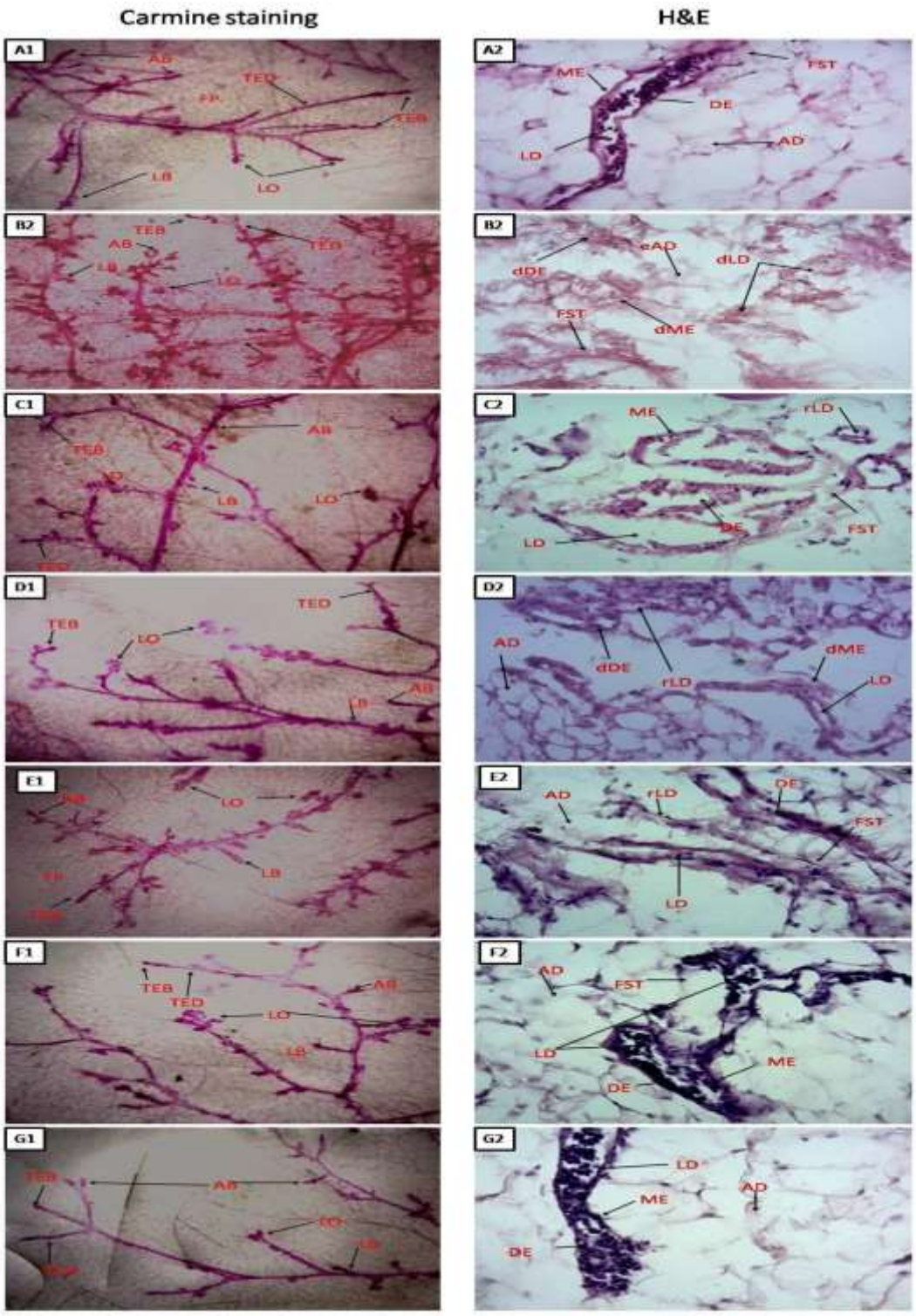

Figure 11: Microscopic examination of rat mammary gland tissue through carmine staining (A1-G1) and H&E staining (A2-G2).

A1 and G1 shows that carmine staining of mammary gland tissue of NC and DMSO treated groups has a lesser number of alveolar buds (AB), lobules (LO), lateral bud (LB) and terminal end duct (TED). B1: DMBA treated TC group showing extensive branching of TED, high

number of AB and LB, with large number of LO, C1-F1:Mammary gland of rats treated with monotherapy and combination therapy of VOA(1mg/kg)and VIN(1mg/kg) showing lesser number of AB counts, LB,TED and LO when compared to TC.

A2 andG2:H&E staining of mammary gland tissue of NC group showing normal architecture of lactiferous duct (LD), adipose tissue (AT), myoepithelial tissue (ME), ductal epithelium (DE) along with fibrous stromal tissue (FST), B2:H&E staining of mammary gland tissue of DMBA treated group showing distorted architecture of lactiferous duct (dLD), damaged myoepithelium and damaged ductal epithelium (dME&dDE), C2-F2:treatment with monotherapy and combination therapy of VOA(1mg/kg) and VIN(1mg/kg) significantly protected further damage to the mammary tissue as evidenced by the restoration of normal architecture LD,AT,DC ME.

5.2.1.3. H&E staining of liver and kidney tissue

Results of H&E staining of rats treated with DMBA caused significant damage to the Bowman's capsule (BC) and glomerulus (G) (**Figure 12).** The space between BC and G was observed to be increased and the structure of proximal convoluted tubules (PCT) and distal convoluted tubules (DCT) observed to be largely distorted in TC when compared to the NC **(Figure 12: B1, B2**). Normal architecture of renal tissue was observed in the VOA treated group. But treatment with monotherapy of VIN caused significant damage to BC and G along destruction of microtubules (PCT & DCT) **(Figure 12: D1, D2)**. Extensive damage of BC, G, PCT and DCT was observed in treatment groups treated with combination therapy of VOA and VIN (**Figure 12: E1, E2 and F1, F2**). Normal architecture of renal tissue was observed in the DMSO treated group.

Liver histology of DMBA treated TC showed damage to liver sinusoids and dilation of central vein and resultant disruption of lobular architecture when compared with normal (**Figure 13:B1 & B2).** Relative small destruction of liver architecture was observed with monotherapy of VOA and VIN (**Figure 13: C1-C2 & D1-D2**). But extensive damage to lobular structure was observed with both low and dose of combination therapy evidenced by large damage to hepatocytes, sinusoids and dilatation of central vein **(Figure 13:E1, E2, F1, F2).** No damage to liver structure was observed with DMSO administration.

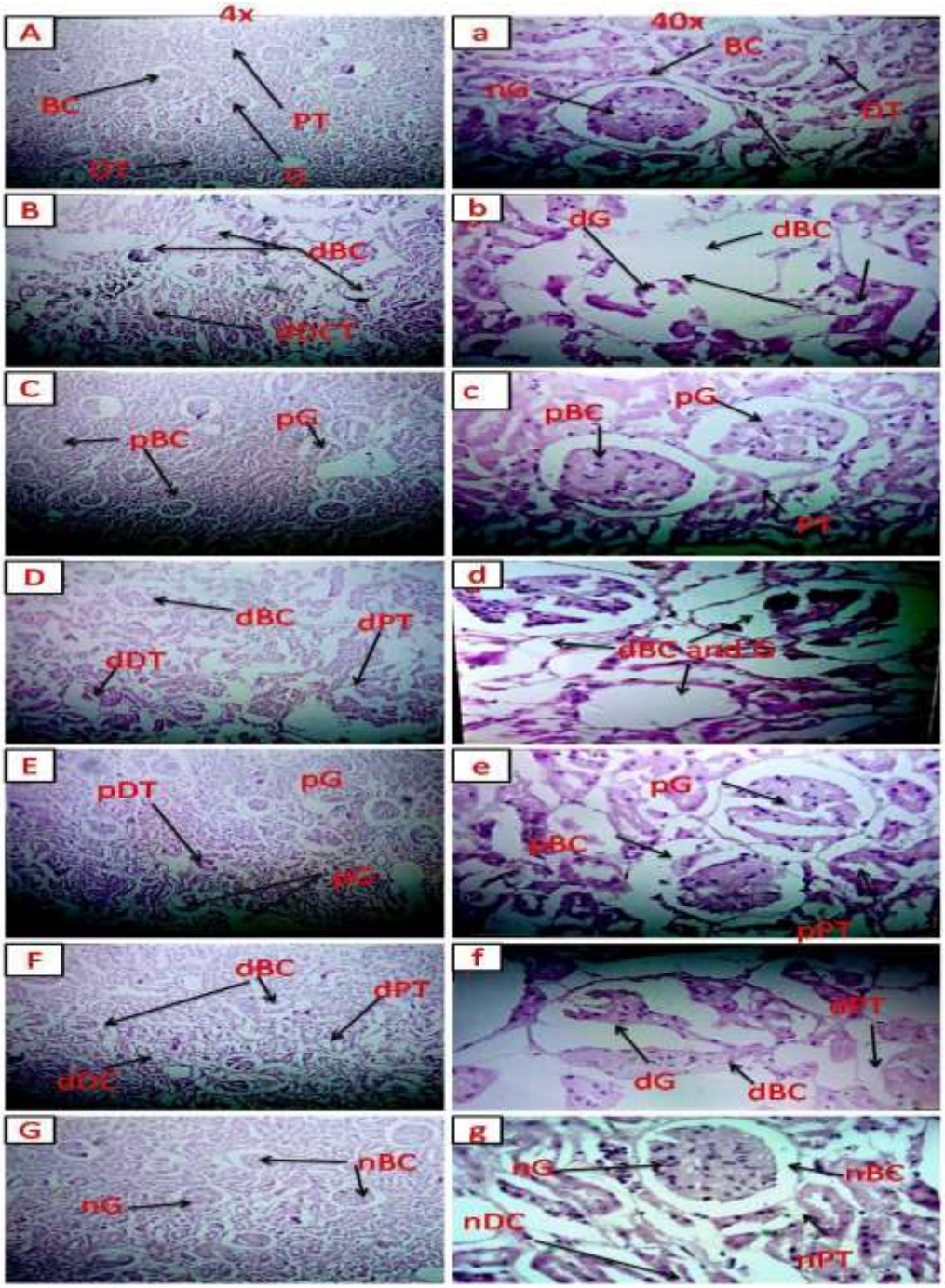

Figure 12: Effect of VOA and VIN therapy on rat kidney

A-G&a-g: kidney section of rat treated with VOA and VIN at 4X and 40 X magnifications.

A,a-Renal of normal rats showing normal architecture of BC,G,PCT and DCT; B,b-TC rat kidney showing dBC,dG, distorted architecture of PCT and DCT; C,c-VOA treated rat kidney showing normal architecture of BC,G,PCT and DCT; VIN treated rat kidney showing extensive damage to BC,G,PCT and DCT; Ee&F,f- kidney of rats treated with combination therapy of VOA and VIN showing even more damage to BC,G, and to microtubules(PCT DCT); G,g-

kidney of rat treated 3%DMSo showing normal architecture of kidney. dBC- damaged bowman's capsule, dG-damaged glomerulus, PCT-proximal convoluted tubule, DCT-distal convoluted tubule.

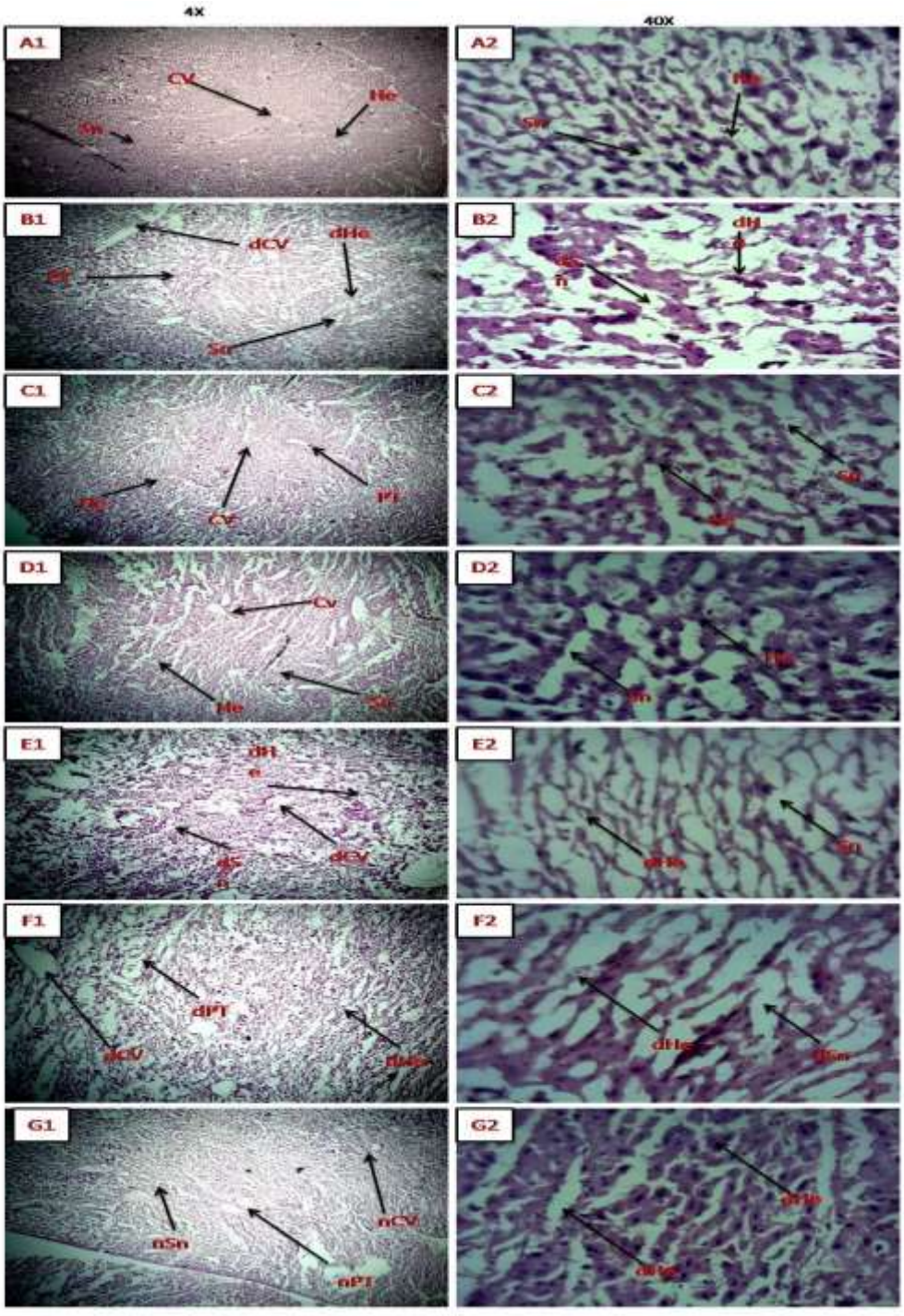

Figure 13: Effect of VOA and VIN therapy on rat Liver]

A1-G1&A2-G2-Histology of rats treated with VOA and VIN at 4Xand 40X.

A1-A2-liver section of NC rat showing normal architecture of liver lobules(Lo), hepatocytes(He), sinusoids(Sn) and central vein(CV); B1-B2-liver section of TC rats showing dilated central vein, damaged He, distorted Sn and Lo, C1-C2-liver section of VOA treated rat

showing little dilation of CV, intact lobular structure, no distortion of Sn and with normal He, D1-D2-liver section of VIN treated rats showing dilated CV, distended portal triads(PT), enhancement in sinusoidal space; E1-E2 and F1-F2-liver section of rat treated with low and high dose combination therapy of VAO and VIN showing extensive distortion of Sn, damage to He, enlargement of central and portal triads and disruption of lobular structure; G1-G2-liver section of rat treated with 3%DMSo showing normal liver architecture like normal.

5.2.1.4. Oxidative stress marker

Single dose administration of DMBA significantly increased the level of TBARs in TC (0.65±0.184 and 119.46± 6.58) group when compared to the NC (0.13±0.032 and 72.007***±6.64) group (**Table 5).** Treatment with monotherapy of VOA and VIN worked well to keep the level of TBARs and PC to minimum level in treatment groups (T1-0.27±0.20***, T2-0.32±0.118***, T3-0.138±0.046***, T4-0.17±0.017*** and T1-67.87±4.76***, T2-41.29± 10.66***, T3-67.38±10.93***, T4-44.92 ±12.40***). Interestingly, treatment with combination low dose therapy provided a better improvement in the level of TBARs whereas in case of PC better restoration of activity was observed with VOA monotherapy and combination low dose. GSH, SOD and catalase is a group of enzymes which work together to neutralize the harmful reactive oxygen species (ROS) generated in the body. The level of SOD, catalase and GSH was significantly decreased after DMBA administration in TC (GSH-0.12±0.005, SOD-0.014±0.002, Catalase-0.29±0.064) group when compared to the NC (GSH-0.36±0.002, SOD-0.058±0.006, catalase-0.72±0.004) group. It can be observed in table 1 that the level of all three enzymes significantly increased after treatment with monotherapy and combination therapy of VOA and VIN. The combination therapy also imparted a better antioxidant activity**.**

Table 5: Effect of VOA/VIN on oxidative stress markers

Groups	TBARS (nM of MDA/µg of protein)	GSH (mg %)	SOD(Units of SOD/mg of protein)	Catalase (nM of H2O2/min/mg of protein)	PC (nM/ml unit)
NC	0.13±0.032	0.36±0.002	0.058±0.006	0.72±0.004	72.007***±6.64
TC	0.65±0.184	0.12±0.005	0.014±0.002	0.29±0.064	119.46± 6.58
T1	0.27±0.20***	0.25±0.030	0.034***±0.002	0.51±0.123***	67.87±4.76***
T2	0.32±0.118***	0.21±0.002***	0.041±0.009***	0.45±0.08***	41.29± 10.66***
T3	0.138±0.046***	0.27±0.001***	0.039±0.002***	0.53±0.084***	67.38±10.93***
T4	0.17±0.017***	0.29±0.008***	0.048±0.001***	0.57±018***	44.92 ±12.40***
DC	0.13±0.046***	0.39±0.007***	0.059±0.001***	0.77±0.004***	75.25 ±3.11***

All values represent mean ± SD. Comparisons were made on the basis of one-way ANOVA followed by Bonferroni test. All groups were compared to the DMBA treated group. Values *p<0.05, **p<0.01 and ***p<0.001 were considered significant. NC-Normal control (normal saline 3ml/kg,o.p.),TC-Toxic control (DMBA 8 mg/kg, i.v.),T1-Treatment 1 (VOA 1mg/kg, s.c.), T2-Treatment 2 (VIN 1mg/kg, i.v.), T3-Treatment 3 (VOA 0.5mg/kg, s.c.+ VIN 0.5mg/kg, i.v.), T4-Treatment 4 (VOA 1mg/kg, s.c.+ VIN 1mg/kg, i.v.),), DC-Dummy control (DMSO).

5.2.1.5. NMR

The collected serum samples were analysed in 1H NMR to predict change in serum metabolomics and the resultant peaks are shown by stock plot **(Figure 14).** A total of 23 markers namely Glucose, Citrate, Acetate, Lactate, Glycerol, Betaine, Choline, Vakine, Proline, Leucine, Isoleucine, PUFA, Low density lipoproteins (LDL),Very low density lipoproteins (VLDL), Glutamate, Formate, Tyrosine, Fumarate, Phenylalanine, Urea and Histidine were found **(Table 6**). The initial analysis of metabolites was performed with 2D PLS-DA score plots (**Figure 15).** The combined 2D PLS-DA score plots between the groups clearly depict that the DMBA induced metabolic changes are largely resetting back to their normal level after VOA and VIN treatment in monotherapy and with combined therapy of both drugs as inferred by the decreased separation between treated and normal control groups.

Further, analysis of metabolites was performed with Box-Cum Whisker plot (**Figure 16).** The Box-Cum plot of metabolites documented significant raised levels of Glucose, Lactate, Acetate, Glutamate, Fumarate and PUFAs were observed in the TC group when compared to the normal. A significant reduction in aforesaid metabolites observed in the treatment groups with the institution of therapy. Acetate level was reverted back to normal in all the treated groups while level of Lactate was significantly reduced by the combination therapy (favorably with higher dose combination). Monotherapy also worked well in lactate reduction but no significant change in lactate was observed. The level of Glutamate was reduced in T1, T2 and T3 but increased in T4. Glutamine remained unchanged in T1 but reduced in T2, T3and T4. As far as PUFAs are considered, a linearity pattern of reduction was observed with monotherapy and combination therapy.

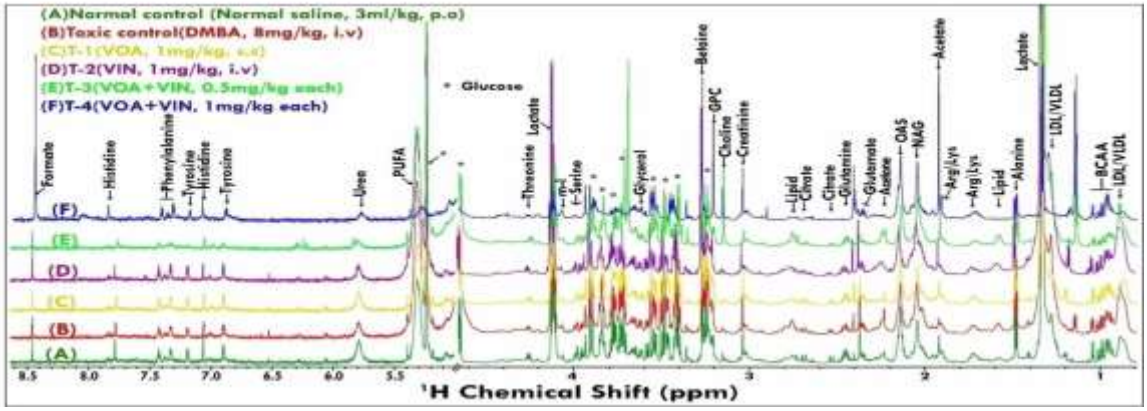

Figure 14: Stock plot representation of 1D-H-NMRc of serum metabolites of experimental rats: NMR spectra of serum samples are represented in distinguished color formats (A, B, C, D, E, and F shown in above figure). The peaks annotated in the figure below shows the assignments of serum metabolites.

The abbreviations used are: LDL/VLDL: Low/very-low density lipoproteins; PUFA: polyunsaturated fatty acids; BCAA: Branch chain amino acids; Leu: Leucine, NAG: N-acetyl glycoproteins; Arg: Arginine; Lys: Lysine; m-I: myo-Inositol; GPC: glycerophosphocholine; and Glucose resonances have been indicated using symbol asterisk "*"

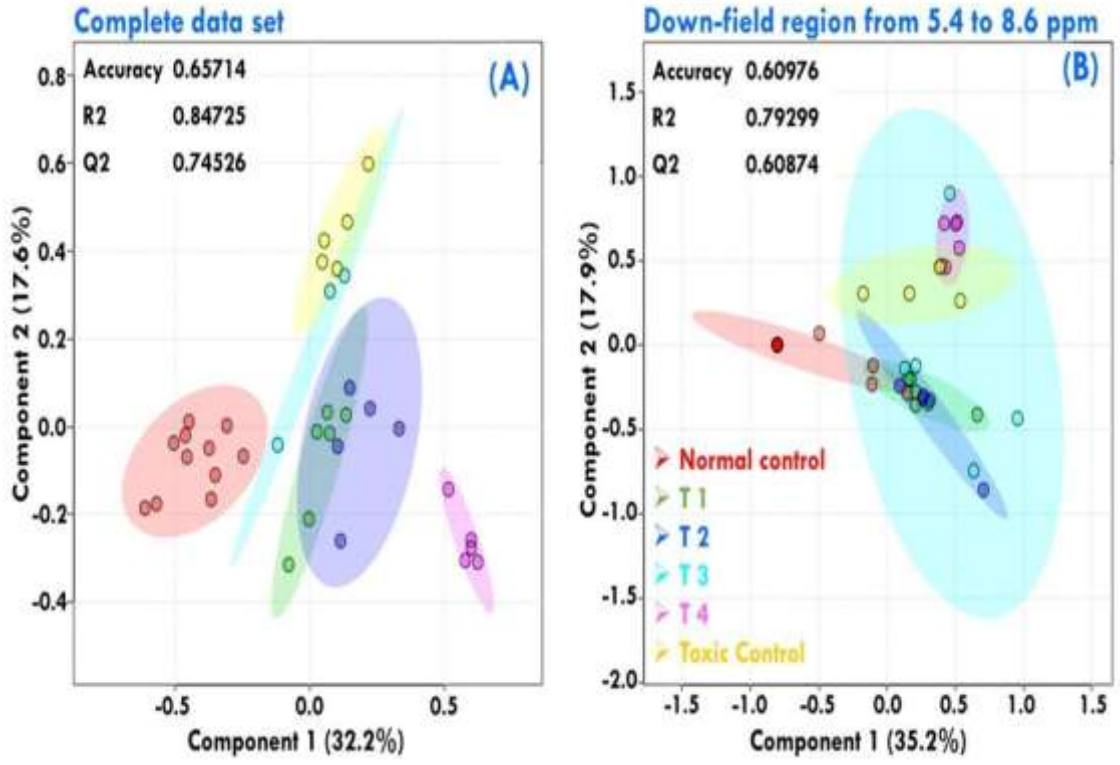

Figure 15: 2D-PLS-DA score plot of rat serum metabolites

The combined 2D PLS-DA score plots between the groups clearly depicting that the DMBA induced metabolic changes are largely resetting back to their normal level after Vaocamine and Vincristine treatment in monotherapy and with combined therapy of both drugs as inferred by the decreased separation between treated and normal control groups. In (A), the complete CPMG data matrix is used for PLS-DA modeling; (B) the up-field spectral region (from 5.4 to 8.6 ppm, aromatic region) was excluded from the data matrix to evaluate the discriminatory significance of aromatic residues. The 10 fold validation parameters (R2, Q2 and accuracy) for the resulting PLS-DA model are shown in the inset**.**

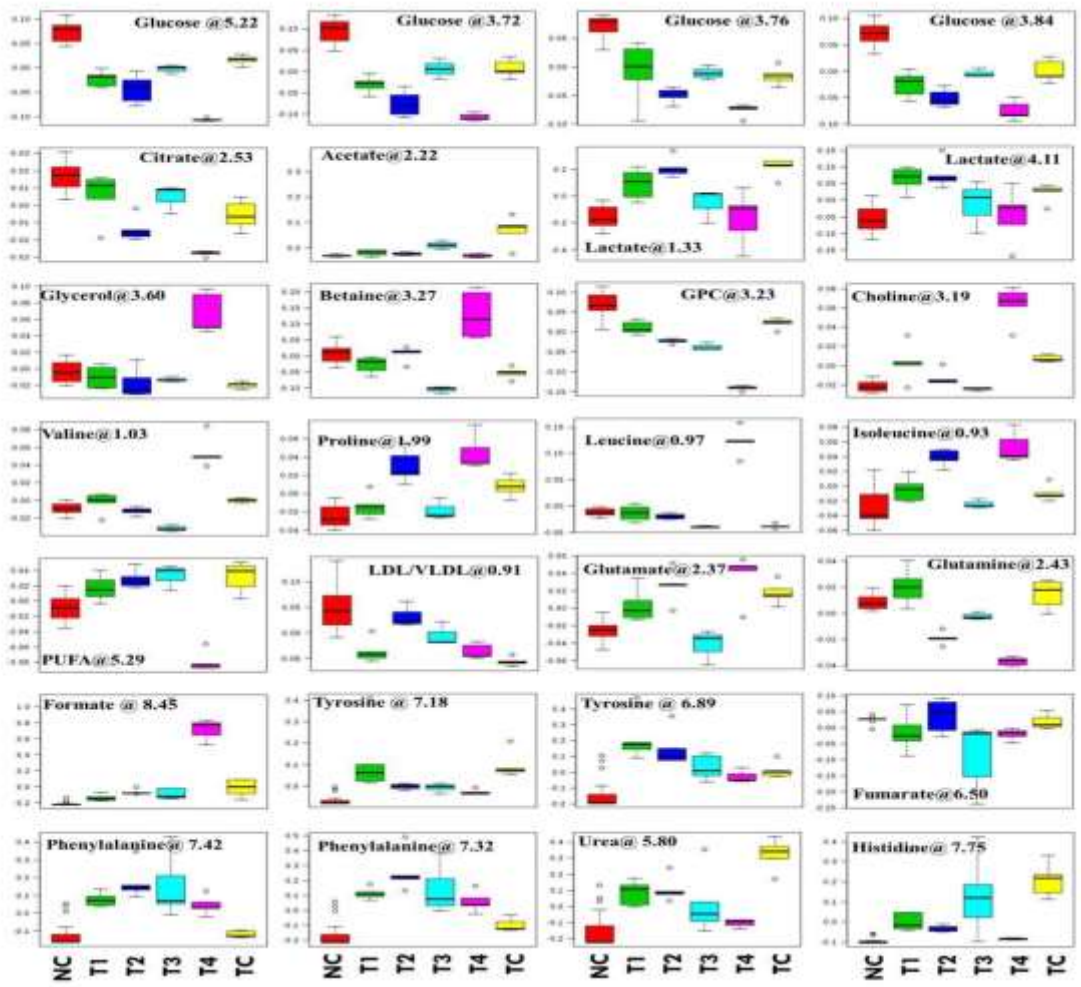

Figure 16: Box-cum whisker plot of rat serum metabolites

Representative box-cum whisker plots showing quantitative variation of relative signal integrals for serum metabolites. For presented metabolite entities, the VIP score>1 and statistical significance is at the level of $p \leq 0.05$. In the box plots, the boxes denote the interquartile ranges, horizontal lines inside the boxes denote the median and bottom and top boundaries of boxes are 25^{th} and 75^{th} percentiles, respectively. Lowe and upper whiskers are 5^{th} and 95^{th} percentiles, respectively.

Table 6: List of cross analysed metabolites

S.No	Metabolites	ppm Values	NC vs TC	NC vs T1	NC vs T2	NC vs T3	NC vs T4
1	Isoleucine	0.93 (t), 1.01 (d)	↑	↑	↓	↓	↑
2	Leucine	0.95 (d), 0.96 (d)	↓	↑	↓	↓	↑
3	Valine	0.98 (d), 1.04 (d)	↑	↑	↓	↓	↑
4	Lactate	1.33 (d), 4.12 (q)	↑	↑	↑	↑	
5	Alanine	1.46(d)	↑	↑	↑	↑	↑
6	Acetate	1.91 (s)	↑	↑	↑	↑	↓
7	NAG	2.04 (m)	↑	↓	↓	↓	↓
8	Glutamate	2.07(m), 2.34(m)	↑	↑	↑	↓	↓
9	Glutamine	2.11(m), 2.43(m)	↑	↑	↓	↓	↑
10	Citrate	2.53 (d), 2.69 (d)	↓	↓	↓	↓	↓
11	Proline	2.01(m), 1.99(m)	↑	↑	↑	↑	↑
12	Choline	3.20 (s), 4.02(m)	↑	↑	↑	↓	↑
13	GPC	3.228(s), 4.34(m)	↓	↓	↓	↓	↓
14	Glycine	3.55 (s)	↓	↓	↓	↓	↓
15	Glycerol	3.56, 3.65 (d)	↓	↓	↓	↓	↑
16	Betaine	3.268	↓	↓	↓	↓	↑
17	Glucose	3.24(t), 3.53(q), 3.49(t), 3.71(t), 3.40(t), 3.41(t) 3.46(m), 3.83(m) 3.72(q), 3.76(q), 3.84(q), 3.90(q)	↓	↓	↓	↓	↓
18	α-Glucose	4.65(d)	↓	↓	↓	↓	↓
19	β-Glucose	5.23(d)	↓	↓	↓	↓	↓
20	Serine	3.94, 3.98 (tt)	↑	↓	↓	↑	↓
21	PUFA	5.29	↑	↑	↑	↑	↓
22	Urea	5.80	↑	↑	↑	↑	↑
23	Tyrosine	6.89 (d), 7.18 (d)	↑	↑	↑	↑	↑

24	Phenylalanine	7.32(d), 7.35(t) 7.42 (d)	↑	↑	↑	↑	↑
25	Histidine	7.05 (s), 7.76 (s)	↑	↑	↑	↑	**NA**
26	Formate	8.45 (s)	↑	↑	↑	↑	↓
27	LDL/VLDL	0.88, 0.91,	↓	↓	↓	↓	↓

The list of metabolites responsible for variation and class separation between normal control vs toxic control and Normal control vs treatment groups (T1, T2, T3 and T4). The metabolic biomarkers were screened based upon the VIP score values > 1.0 (derived from PLS-DA modeling, showing discrimination significance) and then tested (using univariate and student t-test) for statistical significance based on p-value < 0.05. The up (↑) and down (↓) arrows represent, respectively, increased and decreased metabolite levels within the groups compared to controls.

5.2.1.6. Gas chromatography

FAME analysis of mammary gland tissue of control and treatment groups was analyzed by GC-FID as mentioned in the material and method section. A significant change in fatty acid composition of TC animals was observed when compared with NC. Higher levels of PUFAs were observed in TC after DMBA administration. On treatment with VOA and VIN monotherapy as well as with combination therapy, a significant reduction in synthesis of PUFAs was noted (**Figure 17).**

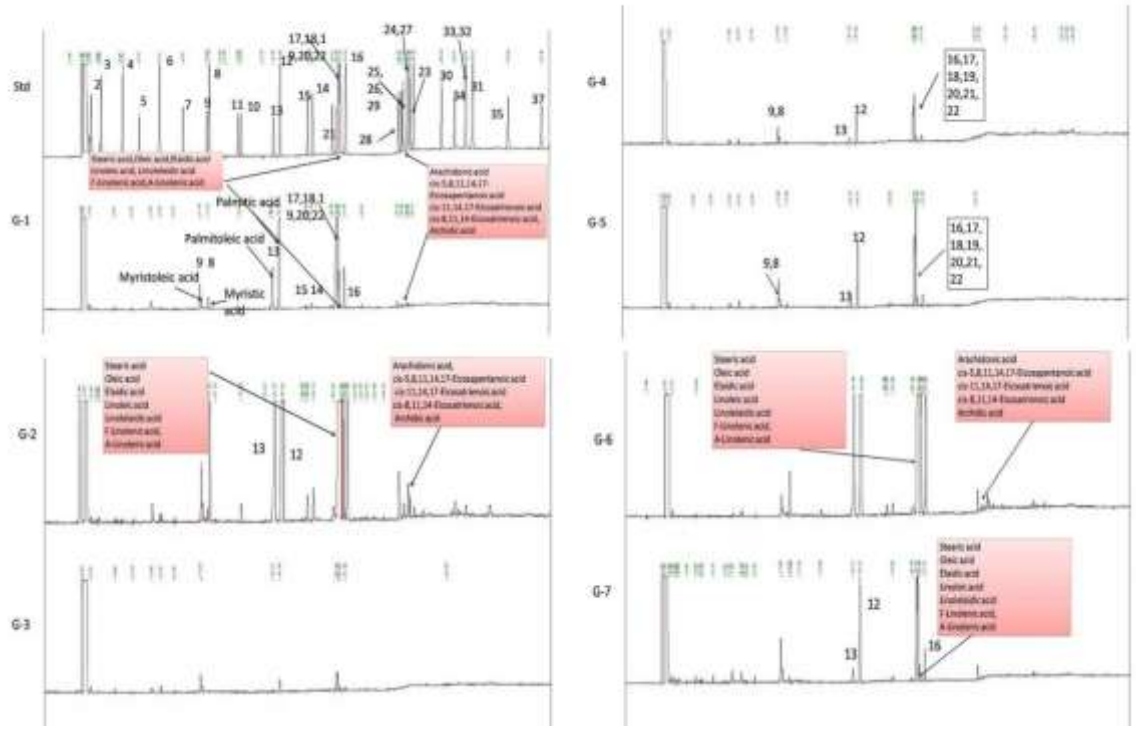

Figure 17: Effect of VOA and VIN on fatty acid composition of mammary gland tissue

Std-Standard (Supelco FAME 37component, Sigma Aldrich), G1-Normal control (saline 2ml/kg); G2-Toxic control (DMBA 8mg/kg,i.v.),G3-Voacamine (VOA) (1mg/kg,s.c.), G4-Vincristine (VIN) (1mg/kg,i.v.), G5-VOA (0.5mg/kg,s.c) + VIN (0.5mg/kg,i.v.), G6-VOA (1mg/kg,s.c.) + VIN (1mg/kg, i.v.), G7-DC-DMSO 3% (2ml/kg)]

5.2.1.7. Western Blotting

Both, combination and monotherapy with VOA and VIN suppressed the expression of HIF-1α, SREBP-1c and FASN. Monotherpy with VOA(T1) 1mg/kg) caused a significant reduction in HIF-1α, FASN and SREBP-1c level when compared to the toxic group while at the same time PHD2 level was observed to be increased. Similarly VIN 1mg (T2) also provided better inhibition of HIF-1α, FASN and SREBP-1c in comparison to VOA 1mg group **(Figure 18).** Combination therapy of VOA and VIN both low (T3) and high dose (T4) significantly reduced the expression of HIF-1α, SREBP-1c and FASN in comparison to toxic groups. Interestingly, both doses of combination therapy significantly enhanced the PHD2 expression. The results are

consistent with the silico docking studies. Also, better activation of PHD2 was observed with the high dose (T4) of combination therapy.

After DMBA administration, a significant change in expression of anti-apoptotic (Bcl-XL) and pro-apoptotic (BAD, BAX) proteins were noted in toxic control animals. Also, the increased expression of VDAC, Apaf-1, and Caspase 9 were observed in toxic control. But VOA and VIN therapy imparted significant protection, worked well to restore the changes (**Figure 20**).

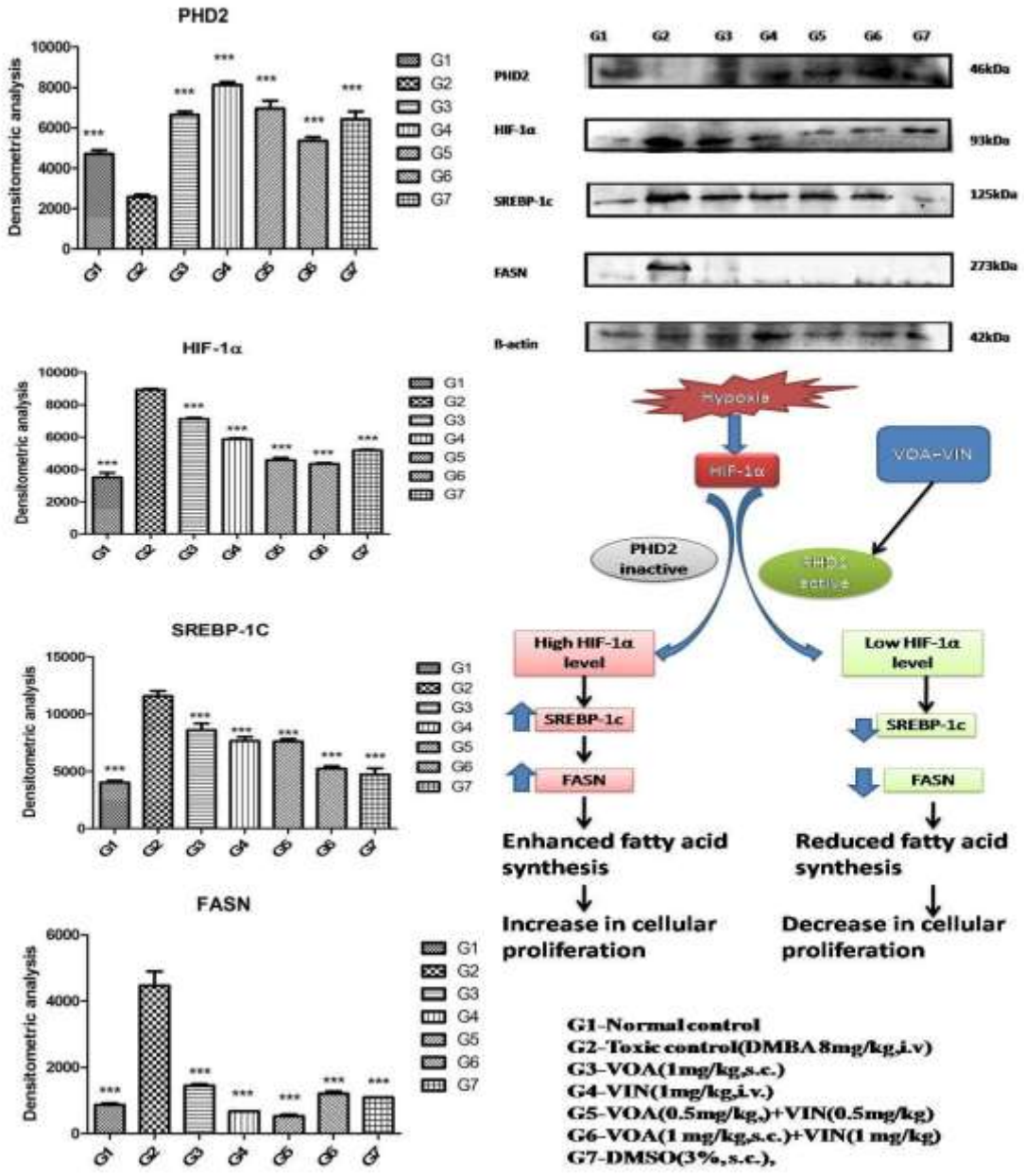

Figure 18: Effect of VOA and VIN on hypoxic markers and fatty acid synthesis markers.

Immunoblotting of respective group [NC-Normal control (saline 2ml/kg); TC-Toxic control (DMBA 8mg/kg,i.v.), T1-Voacamine (VOA) (1mg/kg,s.c.), T2-Vincristine (VIN) (1mg/kg,i.v.), T3-VOA (0.5mg/kg,s.c) + VIN (0.5mg/kg,i.v.), T4-VOA (1mg/kg,s.c.) + VIN (1mg/kg, i.v.), DC-DMSO 3% (2ml/kg)] for HIF-1α, PHD2, SREBP-1c and FASN concluded the hypoxic microenvironment after DMBA administration. Values are presented as mean + SD. Comparisons were made on the basis of one way ANOVA followed by Bonferroni multiple tests. All groups were compared to the DMBA treated group (*p<0.05, **p<0.01, ***p<0.001).

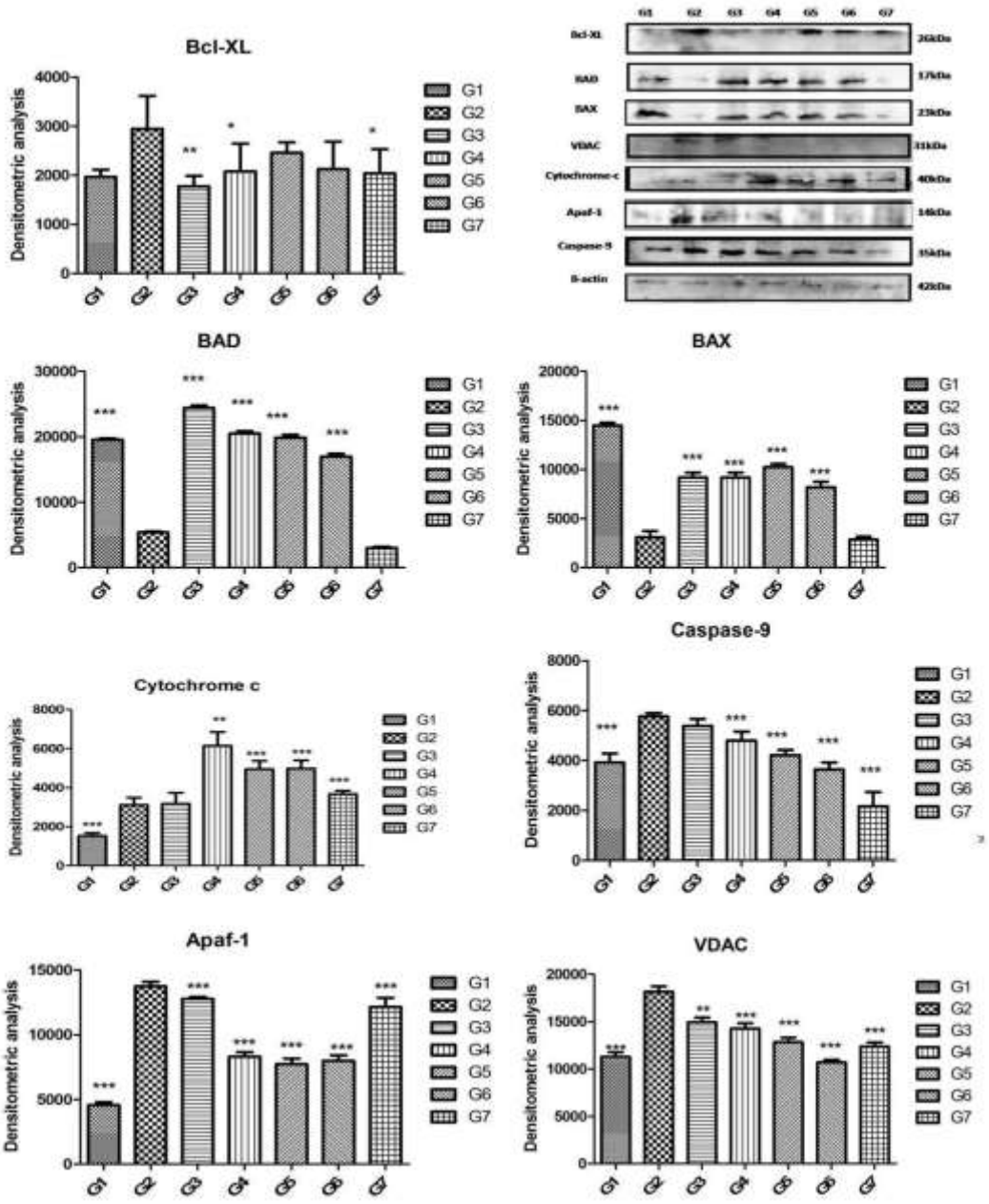

Figure 19: Effect of VOA and VIN on mitochondrial apoptotic markers.

Values are presented as mean + SD. Comparisons were made on the basis of one way ANOVA followed by Bonferroni multiple tests. All groups were compared to the DMBA treated group (*p<0.05, **p<0.01, ***p<0.001).

5.2.1.8. Discussion

PUFAs are crucial for plasma membrane synthesis in rapidly dividing cancer cells of mammary gland tissue and dietary sources alone are insufficient to accomplish this [27]. Therefore, cancer cells must take over an alternative fatty acid synthesis pathway and HIF-1α helps them to adapt this [28]. Previous studies have reported that HIF-1α acts in a very smart way and modifies the tumor microenvironment in such a way that it indirectly enhances the fatty acid synthesis, required for the synthesis of plasma membrane and to furnish other purposes in cancer cells [29]. Considering the role of HIF-1α and FASN, the present study was undertaken to downregulate HIF-1α by activating PHD-2 with natural drugs VOA alone and in combination with VIN.

Cardiac toxicity is a very common risk factor in mammary gland carcinoma patients. For the analysis of cardiac toxicity, hemodynamic profile of animals was performed **(Figure 11, Table 3).** Normal ECG and HRV was recorded in case of NC groups when administered by vehicle for 3 months. DMSO is a universal solvent for hydrophobic drugs and its cardio toxic effect is well established [30]. DMSO administration decreased the heart rate, S, ST and T interval and increased the RR and P amplitude in the DMSO control group. Decrease in HRV after VIN treatment is already reported in previous studies [31] and the same was also reflected in the present study. A large perturbation in ECG and HRV parameters were observed with both low and high doses of combination therapy. Hence, the concomitant administration of VOA with VIN/DMSO would have further exacerbated the cardiotoxic effect (Figure 1C).

Hypoxia in solid tumors plays an important role in angiogenesis which is necessary to accomplish increasing demand of oxygen and other nutrients. Various studies have already reported that increased levels of HIF-1α stimulates angiogenesis in tumor cells [32, 33]. In the present study, results of the carmine staining manifest an increase in the AB count and lobules in

the toxic control group which clearly depicts the formation of neovascularization **(Figure 12:A1-G1).** But treatment with monotherapy and combination therapy of VOA and VIN reduced the AB count and no of lobules in the experimental animals which indicates suppression of angiogenesis after initiation of therapy. Therapy with VOA and VIN might have regulated the HIF-1α pathway to abolish angiogenesis.

Histopathology of mammary gland tissue of carcinogen treated rats have shown extensive damage to the lactiferous duct (LD), adipocytes (AD), ductal epithelium (DE) and myoepithelium as reported in the previous studies [34]. Extensive damage to the micro architecture of mammary tissue like LD, AD, DE and myoepithelium was observed after DMBA administration in TC control (**Figure 12:A2-G2**). A revert effect upon the same was exhibited with VOA and VIN treatment. This indicates VOA and VIN would be working at cellular level to stop tumor progression. Histopathological examination of mammary gland tissue further witnesses the protective action of therapy.

Liver and kidney is the vital and sensitive organ in the body which are responsible for the detoxification and excretion of drugs. Continuous detoxification and excretion of harmful drug molecules, especially those which belong to the anticancer class, can cause harm to these organs and ultimately becomes the reason of nephrotoxicity and hepatotoxicity if dose is not monitored adequately. Most of the anticancer drugs are reported to have varying degrees of nephrotoxicity and hepatotoxicity in patients taking them [35]. Nephrotoxicity due to chemotherapy is marked by the necrosis of the proximal convoluted tubule (PCT), distal convoluted tubule (DCT) epithelial cells and injury to the Bowman's capsule, ultimately kidney failure [36]. Histopathological examination of mammary glands of treated rats revealed the same type of damage to the microarchitecture of the kidney after DMBA administration (**Figure 13**). Subsequent treatment with VIN monotherapy further exacerbated the renal toxicity as evidenced

by the greater damage to the PCT, DCT and Bowman's capsule as its nephrotoxicity is already reported [37]. It would be pertinent to mention that no renal toxicity was noted in rats treated with monotherapy of VOA which confirms its safety in renal failure. Even more damage to the kidney was exhibited by both low and high dose of combination therapy marked by the necrosis of the renal tubular epithelial cell, loop of Henle, and glomerulus attributed to the high drug accumulation, either of the two. Since, VOA is already known to have Pgp (efflux pump) inhibitory effect [38], it might have helped intracellular pooling of VIN in the nephron of experimental animals, and can be the one possible cause of nephrotoxicity .

Liver is the site where most of the drugs undergo their first pass metabolism (except from those administered through parenteral route [39]. Normal functioning of the liver is affected due to continuous exposure to high concentration of cytotoxic substances which then leads to liver failure in some patients. Liver toxicity is marked by dilation of the central vein, damages to hepatocytes (He), distorted sinusoids (Sn), and lobules (Lo) which is very well evident in DMBA treated animals (**Figure 14).** Monotherapy of VOA and VIN worked well to stop further damage to the liver of experimental animals which documents the liver safety of both drugs at the given dose. But histology of combination therapy treated rat's depicted large damage to the liver organ which again proves the VIN /VOA accumulation, or either of two into the hepatocytes and consequently resulting hepatotoxicity.

Various studies have reported the role of ROS in development of cancer manifested by the increase in TBARs, PC and reduction in the activity of SOD, GSH and Catalase [40, 41]. Same type of manifestations in the antioxidant markers were also noted in DMBA treated rats. Interestingly, both monotherapy as well as combination therapy effectively restored the TBARs, SOD and other associated antioxidant markers. From this we can expect, restoration of

antioxidant activity could be the one possible mechanism behind the anticancer potential of the drug (**Table 5).**

Numerous studies have reported that myriad changes occur in a biological system under disease conditions which can be detected in biological fluids like blood serum. With this goal serum metabolic study was carried out to extract biomarkers and to understand the interplay between molecular and cellular components (**Figure 17)** [42, 43]. Previous studies have demonstrated that a hypoxic tumor cell utilizes more and more glucose to meet its energy and for biomass accumulation [44, 45]. Several studies have reported that tumor cells produce high amounts of lactate and glutamate that impart benefit to the tumor cells in various ways like fatty acid biosynthesis, immune protection, angiogenesis and invasiveness [46]. The metabolic profile of DMBA treated rats have shown high levels of lactate and glutamate and that of PUFAs which is in accordance to the previous studies i.e excess lactate/glutamate is converted into fatty acids. Decreased level of glucose further affirms the above findings. Interestingly, reverse chronological order of above metabolites were observed with VOA and VIN (monotherapy as well as with combination therapy) i.e. decreased level of lactate, glutamate and PUFAs were noted all in the treatment groups. It would be pertinent to mention that monotherapy with VOA and high dose combination therapy of VOA(1mg/kg) and VIN(1mg/kg) provided much better fatty acid synthesis inhibitory action compared to the VIN monotherapy and combination low dose. Serum metabolomics analysis of present clearly established a relationship between glycolysis, lactate, glutamate and fatty acid synthesis production **(Table 6).**

We further performed the FAME analysis of mammary gland tissue to affirm the raised level of fatty acids after DMBA, VOA and VIN treatment. Similar story was also observed in the FAME analysis of mammary gland tissue i.e high level PUFAs were detected toxic control and very low level of PUFAS were noted in the treatment groups **(Figure 18).** Results of FAME analysis

further evidence that excess lactate was utilized in fatty acid synthesis. No PUFAs like toxic control were observed in FAME analysis of treated animals which clearly indicates VOA and VIN have an inhibitory action on fatty acid synthesis.

Immunoblotting was further performed to investigate the effect of therapy on the proteins of hypoxic and fatty acid synthetic pathways. Several studies have confirmed that the expression of HIF-1α increases in oxygen scarcity which enhances the expression of other genes that indirectly benefits the tumor cells in various ways [47, 48]. A study conducted by P.Maxwell et al on the wild type (wt) Hepa-1 cells and derivatives c4,c31 and Rc4 proved that HIF-1α plays a crucial role in GLUT one transporter and VEGF [48]. Another study conducted by Wendi Sun et al on HeLa, HCT116 and on cultured human primary epithelial cells showed that HIF-1α increased the level of SREBP-1c and FASN [49]. Intriguingly, a similar type of trend was also observed in the present study i.e. the level of HIF-1α, SREBP and FASN expression was up regulated while PHD2 expression was down regulated after DMBA treatment (**Figure 19).** An opposite effect on the same was observed after the initiation of VOA/VIN therapy. It is already reported that PHD2 is a negative regulator of HIF-1α and activation of PHD2 alone can downregulate all its downstream effects [50]. This affirms that VOA and VIN might have activated PHD2 and subsequently the level of HIF-1α along with FASN proteins would have dwindled as it was hypothesized.

Several studies have reported that failure of apoptosis in normal cells is an indication of cancer transformation [51-53]. Decrease in anti-apoptotic proteins (Bcl-XL and Bcl-2) and increase in pro-apoptotic proteins (BAD,BAX) indicates normal functioning mitochondrial apoptotic pathway [7]. Result of immunoblotting shows increase in expression of Bcl-XL and decrease in BAX and BAD proteins in toxic control after DMBA administration. Furthermore, expressions of VDAC, Apaf-1 and caspase9 were also found elevated which proves the failure of

mitochondrial apoptotic pathway. Treatment with monotherapy as well as with combination therapy of VOA and VIN restored the apoptotic pathway in treatment groups which is evidenced by the increased level of cytochrome-c as well (**Figure 19).**

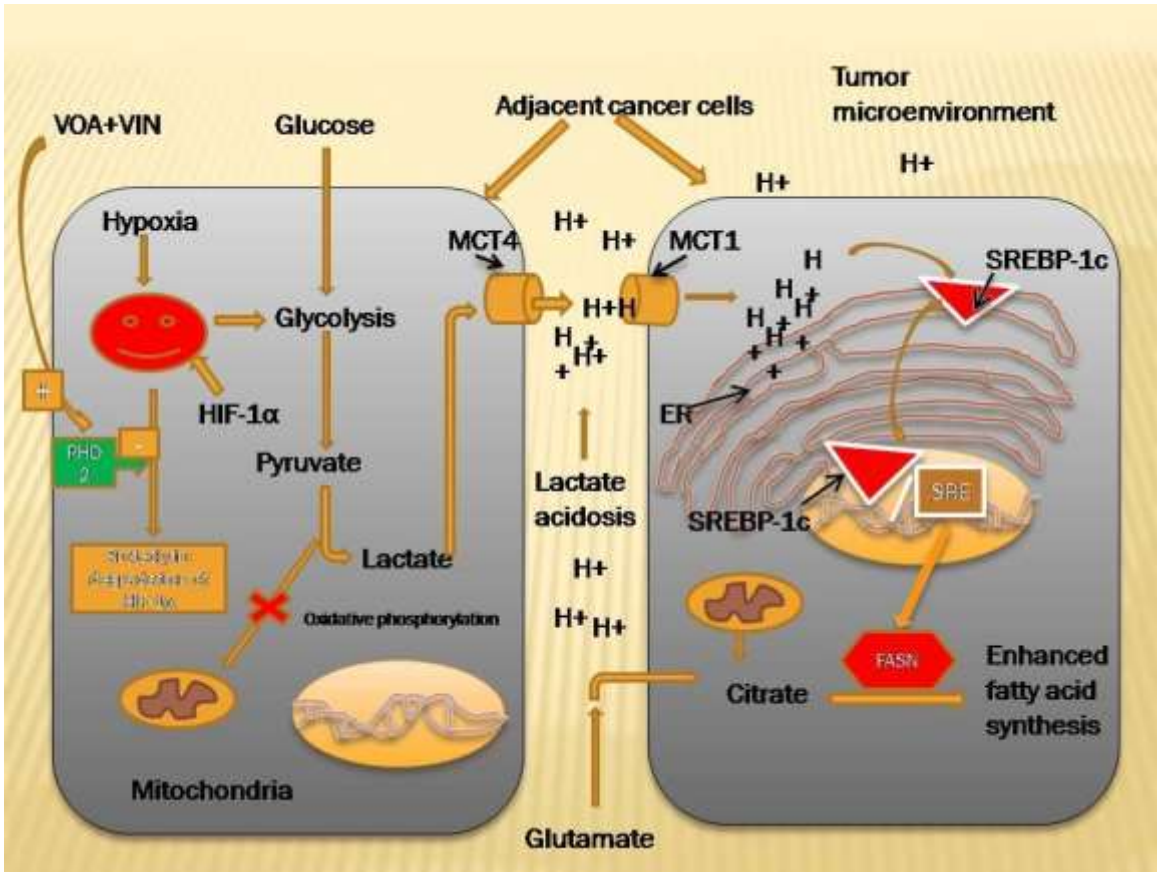

Figure 20: Mechanism of VOA and VIN to inhibit fatty acid synthesis in DMBA induced mammary gland carcinoma of albino wistar rats.

Hypoxia activated HIF-1α enhances lactate acidosis in tumor microenvironments. Dysregulated pH in tumor microenvironment activated SREBP-1cand FASN expression to speed up fatty synthesis required for plasma membrane synthesis in rapidly proliferating cells. VOA and VIN activated PHD2 enhanced proteolytic degradation of HIF and thus inhibited fatty acid synthesis.

HIF-1α hypoxia inducible factor-1α, SREBP-1c-sterol regulatory element binding protein-1c, cFASN: fatty acid synthesis, PHD2-prolyl hydroxylase2

5.2.2. MNU study

Following the DMBA study, anti-cancer potential of VOA was further validated with MNU induced mammary gland carcinoma in albino Wistar rats. Mammary gland carcinoma was

induced with single dose administration of MNU (50 mg.kg, i.p.) and treatment with VOA was started 15 days after MNU injection and stopped after one month. In this study, TMX was used as a standard drug. Upon the completion of study after 3 months, various experiments were performed to assess the efficacy and safety of treatment.

5.2.2.1. Effect of VOA/TMX therapy on cardiac function of experimental animals

First of all, we performed ECG of experimental animals to assess cardiac-toxicity if any with the current treatment drugs. Cardio-toxicity with anti-cancer drugs is an associated risk factor and can be monitored with ECG parameters like P,Q,R,T and S waves at the preclinical studies. Various studies have reported cardio toxicity with anti-cancer drugs[27][28]. Therefore, ECG of experimental animals was recorded to assess the cardio toxicity due to VOA and TMX with AD Instrument **(Figure 21).** Normal ECG was recorded in normal group animals as only vehicles were administered up to the end of study. But a significant change in ECG parameters like increase in PR interval, Q amplitude, HR, ST height, JT interval, R amplitude, QT interval, T amplitude, QTc interval observed after MNU administration. Also, a decrease in RR, QRS interval was observed in the same group when compared with the normal rats (**Figure 22**). A sharp increase in Q amplitude, small increase in HR and T amplitude was observed in VOA low dose treated groups whereas no significant change was noted in JT interval, R-amplitude, Q-interval, QTc and ST height. Also, no change in S amplitude, ST height, JT-interval, and R amplitude was observed like toxic control animals after VOA low dose treatment and an ECG comparable to that of normal rat was observed

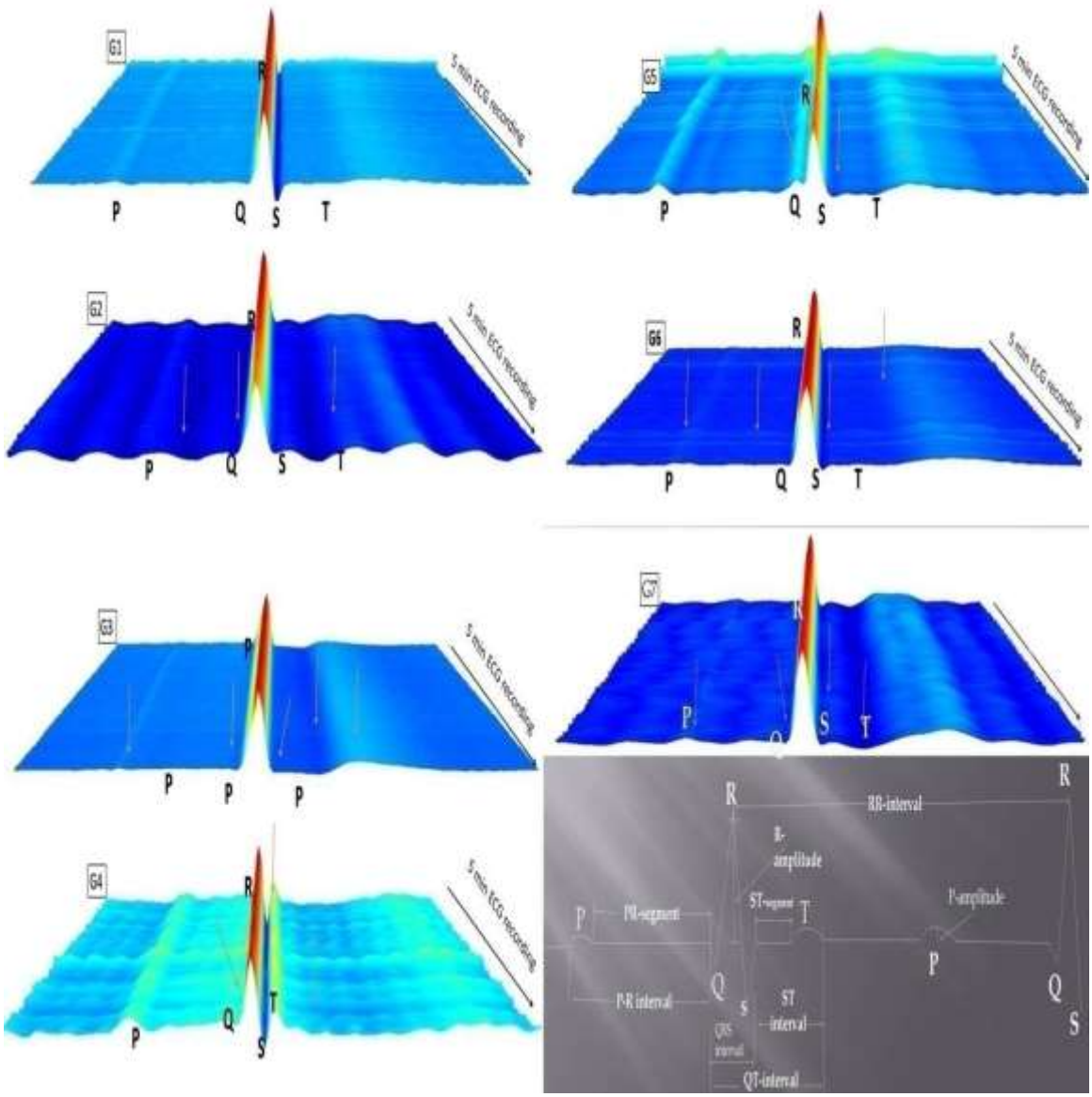

Figure 21: Waterfall map presentation of 5 min ECG recording of experimental animals

G1-Normal control (saline 2ml/kg), G2-Toxic control-MNU (50 mg/kg, i.p), G3-VOA low dose (1mg/kg, s.c.), VOA high dose (2mg/kg, s.c.), G5-TMX (8mg/kg, p.o.), G6-VOA (1mg/kgs.c.)+TMX (8mg/kg, p.o.), G7-DMSO 3% (3ml/kg, s.c.).

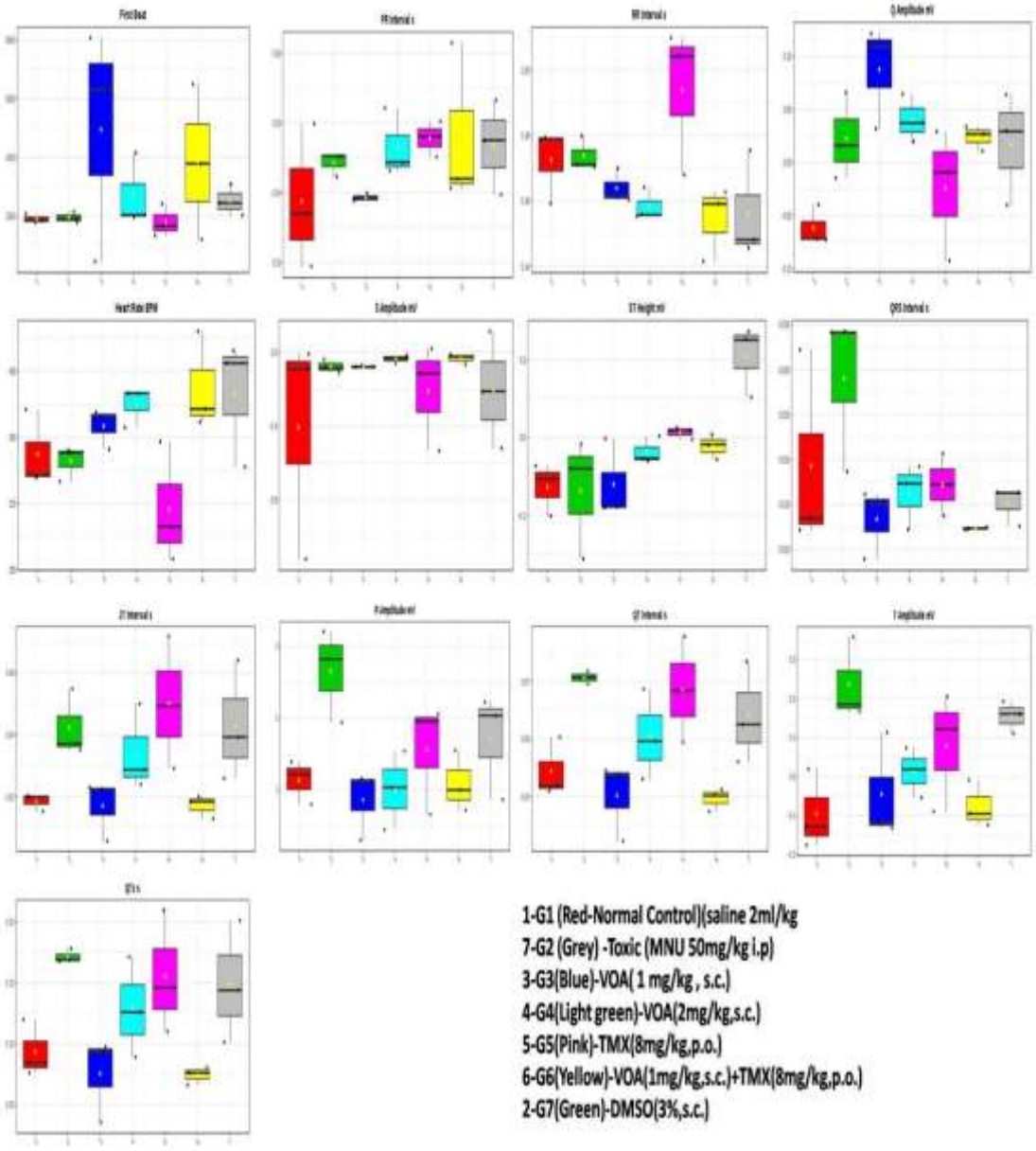

Figure 22: Box –Cum whisker plot of ECG recording of VOA treated on experimental animals

Red-G1-Normal control (saline 2ml/kg), Grey-G2-Toxic control-MNU (50 mg/kg, i.p), Blue-G3-VOA low dose (1mg/kg, s.c), Light green-G4-VOA high dose (2mg/kg, s.c.), Pink-G5-TMX(8mg/kg,p.o.),Yellow-G6-VOA(1mg/kg,s.c.)+TMX(8mg/kg,p.o.),
GreenG7-DMSO 3% (3ml/kg, s.c.).

Table 7: Effect of VOA and TMX on rat HRV parameters

Groups	G1	G2	G3	G4	G5	G6	G7
			Time domain				
Average RR	161.65±3.46	146.90± 1.83	172.15±11.10***	160.8±0.56	155.6±0.42	291.15±34.011***	160.9±2.40
SD RR	3.18±2.73	2.39±1.45	2.22±1.64	7.68±0.13*	5.34±5.36	6.42±0.91	4.18± 0.465
Average Rate	371.4±7.63	408.6±5.23	22.55±1.27***	386.35±0.21**	386.35±0.21	207.55±24.25***	373.15 ±5.44***
SD Rate	7.061±5.79	6.70±4.15	4.287±2.90	18.35±0.388*	13.367±13.45	4.53±0.36	9.50±0.56
			Frequency domain				
VLF	44.97±20.194	36.23±34.23	60.46±6.68	45.66±9.079	52.79±54.92	49.48±3.40**	62.41±4.27
LF	5.85±4.48	4.32±2.46	5.96±0.73	6.31±1.24	4.97±3.98	20.28±14.03	7.93±5.44
HF	39.53±21.44	31.53±8.37	26.20±7.38	45.45±7.22	39.82±49.04	24.96±11.92	26.52±1.03
LH/HF	0.13±0.038	0.14±0.11	0.24±0.095	0.13±0.004	0.24±0.20	1.06±1.07*	0.29±0.22

Values are represented as Mean ± SD, each group contains 6 animals. Comparisons were made on the basis of the one-way ANOVA followed by Bonferroni test. All groups were compared to the toxic control group (*p<0.05, **p<0.01, ***p<0.001).

with a low dose of VOA. But on treatment with a high dose of VOA a very small reduction in PR interval, Heart rats, ST height, JT interval, QT interval, T amplitude and QTc interval was observed when compared to the toxic control. Standard therapy with TMX significantly increased the PR interval, RR interval, Q amplitude, ST height, QRS complex, JT interval,

QT intervals, T amplitude and QTc intervals but a sharp decrease in Heart rate were noted when compared with normal rats. A sharp decrease in RR interval, Q-amplitude, Heart rate and ST height while a decrease in RR interval, JT height, R amplitude and QRS interval observed with combination therapy. A significant change in QRS interval, JT interval amplitude, QT interval amplitude, QTc interval but no significant change in Heart rate, S amplitude and ST height were noted with DMSO treatment when compared with normal control. As far as toxic control, standard group and DMSO group were considered, a similar trends in ECG parameters like JT interval, R amplitude, QT interval, T amplitude and QTc were observed.

HRV analysis of toxic control rats showed decrease in Average RR and Average rate when compared other treatment groups, No significant change in SD rate, SDRR, LF,HF and LF/HF ratio were noted(**Table 6**)

5.2.2.2. Effect of VOA therapy on morphology of mammary glands

Carmine staining:

Having determined the cardiac safety of treatment drugs, next we performed carmine staining to assess the anti-angiogenic potential of VOA/TMX therapy. Angiogenesis is the characteristic feature of malignant tumours[29]. Therefore, carmine staining was performed to study the anti-angiogenic effect of the VOA therapy and change in the development of micro ducts of

mammary glands were compared in toxic and control animals.

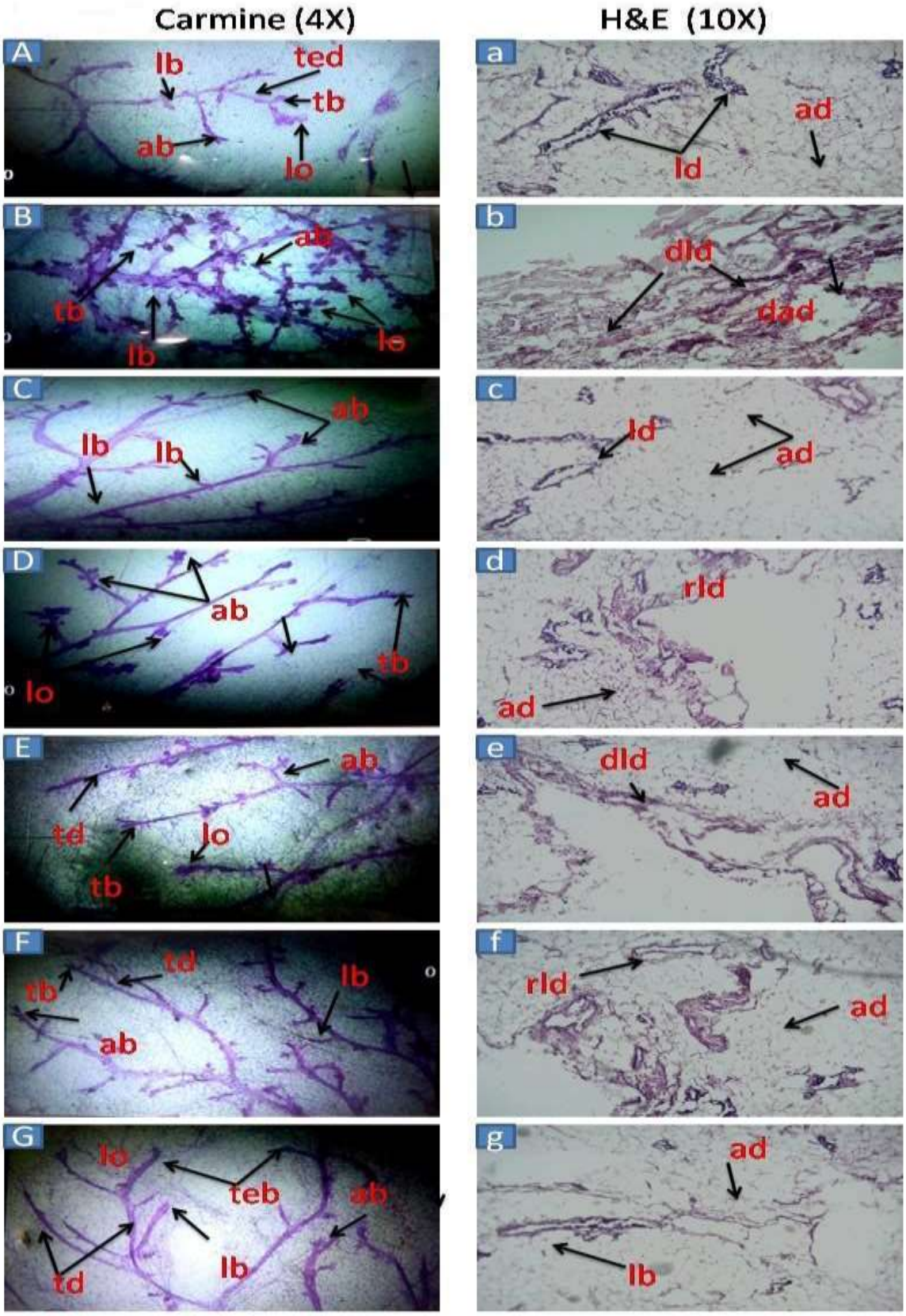

Figure 23: Effect of VOA on the morphology of mammary gland

Carmine staining: A-G

A & G-Carmine staining of normal control (G1) and DMSO (G7) administered rats showing very less branching of ducts , **terminal end duct (ted),terminal bud (tb),** normal **lateral bud (lb), alveolar buds** (**ab), B-**Carmine staining toxic control (G2) rats showing excessive branching of mammary gland ducts, high number of **ab** and **lobules (lo**) along with **tb** and **lb**. **C-G3** rats treated with low dose of VOA showing very less branching of mammary gland ducts and few number of **ab** and no **lo** formation was noted, **D-G4**-Rats treated with high dose of VOA showing **tb, lb, ab** and **lo**, **E-G5**-Rats treated with TMX showing **lb, tb, ab** and lo, **F-G6**-Rats treated with combination therapy of VOA and TMX showing along **tb, lb, ted** and **ab** only**.**

H&E staining:a&g-Histology of G1 and G7 rats showing normal shape and of lactiferous duct (ld) and adipocytes, B-G2-Histology of rats showing **damaged lactiferous duct (dld)** and distorted shape of **adipocytes (ad**), C-G3-Rats showing normal shape of ld and ad, D-G4-VOA high dose treated rats showing regenerated **lactiferous duct (rld**) and **ad**, E-Rats treated with TMX showing **rld** and ad, F-G6-VOA and TMX treated rats showing normal shape of **ld** and **ad**.

Carmine staining of normal control animals witnessed the normal growth and differentiation of mammary glands tissue. A very few no. of lobules (lo), alveolar buds (ab), terminal end duct (ted), lateral bud

(lb) and terminal bud (tb) were observed in this group as only vehicles were administered up to the end of study. No significant change in the DMSO treated group was observed. Excessive branching of mammary gland ducts, tb, lb, high no of ab and lb formation was observed in the MNU treated animals when compared with normal control animals. A significant

reduction in lb, tb, ab and lo formation was observed after VOA low dose and high dose of VOA. Also, a better anti-angiogenic potential was observed with high dose. Standard therapy also worked well and imparted mammary gland protection comparable to the high dose of VOA. Combination therapy VOA with TMX showed anti-angiogenic potential comparable to the low dose of VOA i.e very less branching of mammary gland ducts and few numbers of lo were observed (**Figure 23:A-G).**

H&E staining:

Further, H&E staining of mammary gland tissues was performed to validate the results of carmine staining. Normal shape and structure of lactiferous duct and adipocytes were noted in

the normal group animals (**Figure 23: a-g).** A significant damage to lactiferous duct (dld) and distorted shape of adipocyte(dad) were manifested in MNU treated animals. Treatment with low dose of VOA imparted significant protection to the mammary gland tissue as normal architecture of adipocytes and lactiferous ducts comparable to the normal control animals were observed in this group. Histology of VOA high dose treated animals also imparted protection evidenced by the appearance of presence of some of the normal lactiferous duct but not up to the extent of low dose. Standard therapy with TMX imparted very little protection as evidenced by large damage to ld and da. Significantly, good results were observed with combination therapy compared to the standard therapy as evidenced by the regeneration of lactiferous duct (rld) and normal shape of adipocytes

5.2.2.3. Changes recorded upon body weight of animals after VOA treatment

Cachexia is very common in cancer patients due to alteration of metabolism. Therefore, in the next step we determined body weight of experimental animals up tothe end of study and percentage decrease in body weight was calculated and shown in **Figure 24.** A continuous increase in body weight of normal control and DMSO treated animals were observed as only vehicles were administered up to the end of study. A significant decrease in body weight [30] of toxic control animals was recorded in comparison to the control animals. Upon treatment with low dose of VOA, a significant increase in body weight of animals was noted but treatment with high dose of VOA caused an unexpected decrease in body of animals like toxic control. TMX being a well known anticancer drug stopped further decrease in body weight of animals, rather increased comparable to normal controls. Combination therapy with VOA and TMX also worked well and provided significant protection from decreasing body weight.

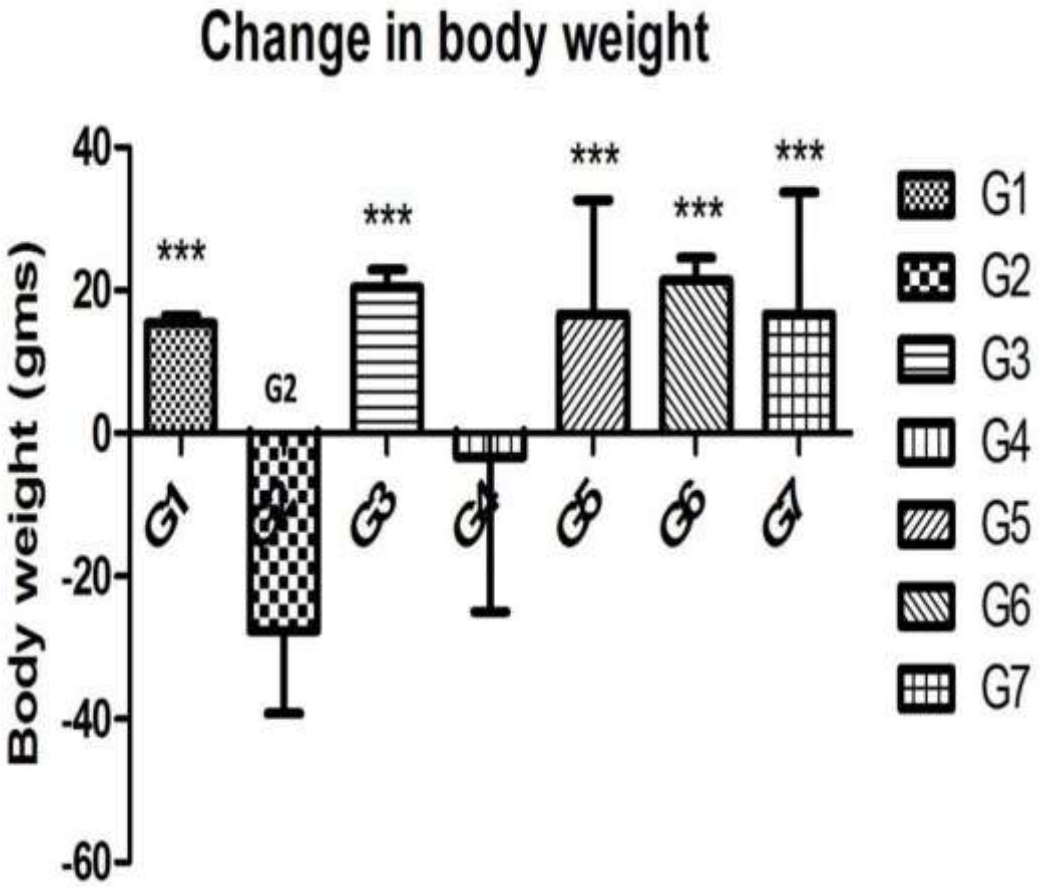

Figure 24: Effect of VOA on body weight of experimental animals

Cachexia is the hallmark of cancer. Continuous loss in body weight after MNU treatment was observed in toxic control (G2). Treatment with low dose of VOA (G3), TMX treatment (G5) and combination therapy of VOA and TMX (G6) stopped further loss of body weight like normal control rats(G1,G7). Continuous loss in body weight was also observed in VOA high dose (2mg/kg,s.c.) treatment which indicates VOA at this has toxic consequences.

G1-Normal control (saline 2ml/kg), G2-Toxic control-MNU (50 mg/kg, i.p), G3-VOA low dose (1mg/kg, s.c.), VOA high dose (2mg/kg, s.c.), G5-TMX (8mg/kg, p.o.), G6-VOA (1mg/kgs.c.)+TMX (8mg/kg, p.o.), G7-DMSO 3% (3ml/kg, s.c.).

5.2.2.4. Effect of VOA on antioxidant markers

Next we assessed the free radical scavenging mechanism of MNU treated rats because failure to neutralize free radicals can damage DNA and subsequently mammary gland carcinoma. Antioxidant markers like TBARs, PC, SOD, catalase and GSH play an important role by neutralizing free radicals generated in the body **(Table 8).** Levels of these can increase or decrease in deceased conditions. A significant increase in TBARs and PC level was observed in toxic control (868.6±67.31, 57.08±7.34) when compared with the normal control (479.70±56.4***, 21.30±6.4***). When therapy was started with a low dose of VOA, significant moderate decrease in TBARs and PC was observed with VOA high dose and standard therapy.

SOD, catalase and GSH level was significantly reduced in the toxic control (0.022±0.001, 0.19±0.03, 0.63±0.03) group. Treatment with low dose of VOA significantly increased the level of SOD, catalase and GSH (0.037±0.004**, 0.34±0.02*). Only, moderate increase in

SOD, catalase and GSH were observed with high doses of VOA. Standard therapy with TMX significantly raised the level of SOD, catalase and GSH (0.034±0.005**, 0.34±0.12, 0.80±0.09). Combination of VOA and TMX worked well and significantly upraised the level of SOD, catalase and GSH (0.07±0.004**, 0.56±0.06*, 1.9±0.09***).

Table 8: Effect of VOA and TMX on antioxidant markers

Groups	TBAR's (nm of MDA/µg of protein	GSH (mg %)	SOD (units of SOD/mg of protein)	CATALASE (nm of H_2O_2/ min/mg of protein)	PROTEIN CARBONYL nmol/mg of protein
G1	489.70±56.4***	0.71±0.3***	0.03±0.01***	0.43±0.2***	21.30±6.4***
G2	868.6±67.31	0.63±0.03	0.022±0.00	0.19±0.036	57.08±7.34
G3	304.5±54.9***	1.4±0.09***	0.04±0.00**	0.34±0.02*	24.4±3.4***
G4	698.56±90***	0.72±0.09	0.021±0.00	0.28±0.06	45.3±0.4
G5	592.4±25.8***	0.80±0.09	0.034±0.001**	0.34±0.12	35.6±0.6
G6	207.5±54.9***	1.9±0.09***	0.07±0.00**	0.56±0.06*	27.3±0.4***
G7	379.70±56.4***	0.71±0.3***	0.06±0.01*	0.45±0.2***	23.30±6.4***

Values are represented as Mean ± SD, each group contains 6 animals. Comparisons were made on the basis of the one-way ANOVA followed by Bonferroni test. All groups were compared to the toxic control group (*p<0.05, **p<0.01, ***p<0.001).

5.2.2.5. Metabolomics changes after treatment with VOA

Having determined the oxidative stress in experimental animals, next we analysed their serum metabolomic profile because a stressed tissue produces abnormal serum metabolites[31][32]. Purposely, Serum samples from all the groups were collected and subjected to H^1-NMR analysis in order to compare the metabolomic profile of experimental animals **(Figure 25 and 26).**

A total of 34 metabolites were analysed in the serum samples out of which major perturbation were observed in glucose, lactate, pyruvate, and citrate along with amino acids leucine, isoleucine, threonine, tyrosine and proline. A significant change in glucose, pyruvate, lactate, citrate, succinate, leucine, isoleucine, threonine, tyrosine and proline in MNU treated toxic control rats were observed when compared to the normal rats **(Figure 27).**

The recorded serum metabolomic data was first analysed with combined 2D PLS-DA in order to see the variation in the principle components. The 2D PLS score plots of toxic control (Group 2) showed a clear separation from the G1, G3 (VOA low dose), G5 (TMX treated) and with combination of both of these drugs (Groups 6). Metabolic profile of Group 4 animals was observed like that of toxic control animals after treatment with a high dose of VOA which indicates its toxicity at this dose. This indicates VOA low dose and its combination with somehow resetting back the perturbed metabolites as a result of MNU administration.

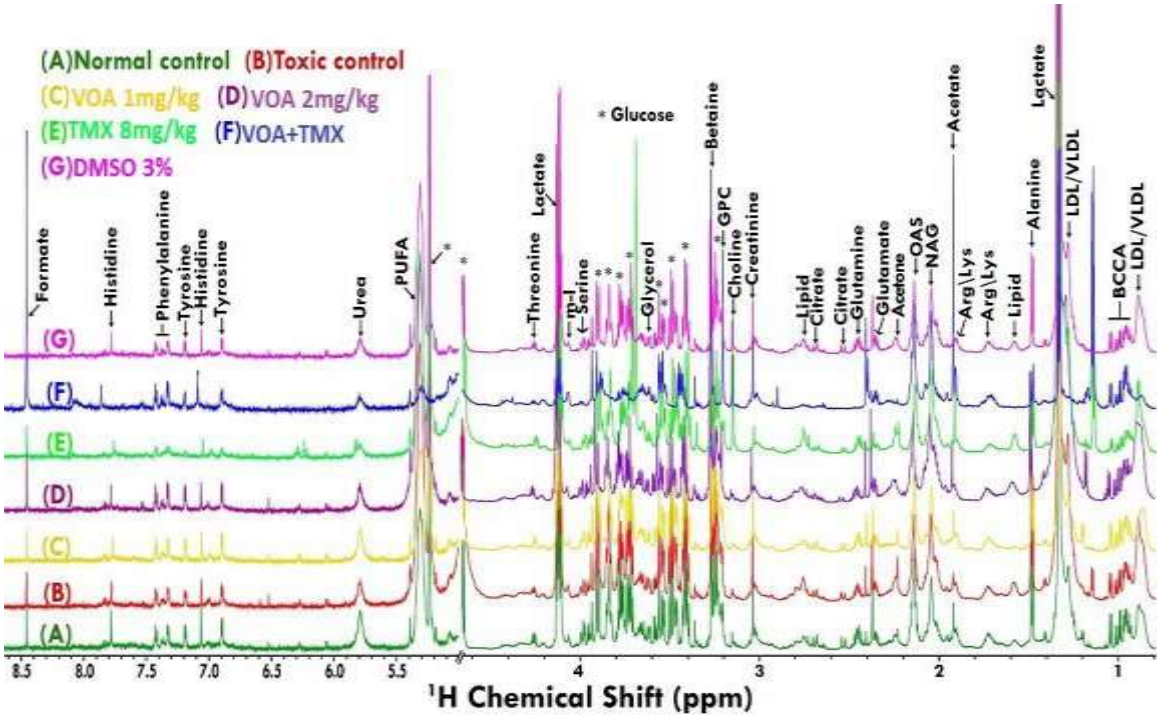

Figure 25: Stack plot of representation of H [1] NMR peaks of serum metabolites.

The peaks annotated in the Figure show the assignments of serum metabolites. The abbreviations used are: LDL/VLDL: Low/very-low-density lipoproteins; PUFA: polyunsaturated fatty acids; Ile: isoleucine; Leu: leucine; Val: Valine, Pyr: pyruvate; Ch: choline; GPC: glycerophosphocholine; Glucose resonances have been indicated using symbol asterisk "*";

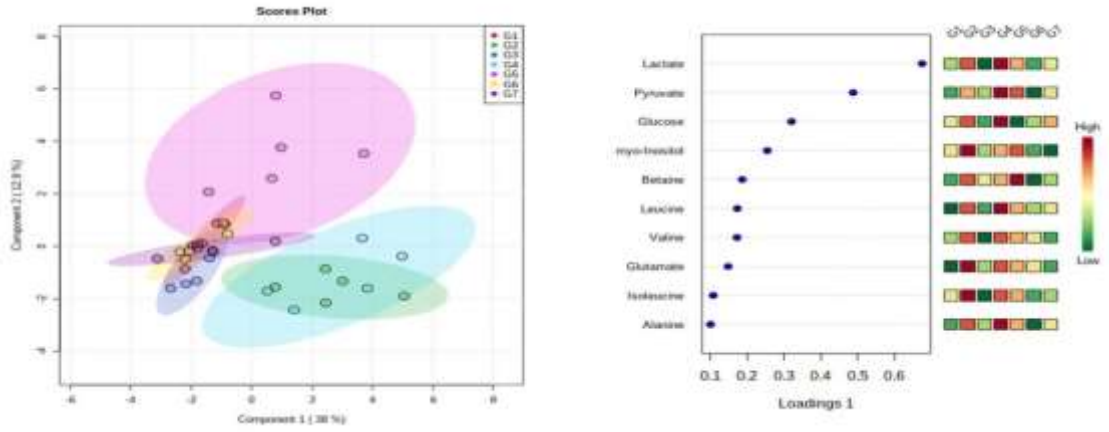

Figure 26: 2D-PLS-DA score plot of rat serum metabolites treated with MNU

The recorded serum metabolomic data was first analyzed with combined 2D PLS-DA in order to see the variation in the principle components. The 2D PLS score plots of toxic control (Group 2) and that Group 4 animals treated with MNU dose depicting a clear separation from the normal,

VOA low dose (G3), TMX treated(Group 5) and with combination of both of these drugs (Groups 6). Metabolic profile of Group 4 animals was observed like that of toxic control animals after treatment with high dose of VOA which indicates its toxicity at this dose. This indicates VOA low dose and its combination with somehow resetting back the perturbed metabolites as a result of MNU administration. Excluded from the data matrix to evaluate the discriminatory significance of aromatic residues.

A significant reduction in glucose, pyruvate, lactate ,citrate succinate, along with amino acids threonine, leucine, isoleucine and tyrosine were observed with low dose of VOA but opposite trend in these metabolites were observed with high dose of VOA. A very small decrease in aforesaid metabolites was observed with the standard therapy. Combined therapy of VOA with TMX worked very well, reducing serum concentration of glucose, lactate, pyruvate, citrate, succinate, threonine tyrosine, leucine, isoleucine like VOA low dose treatment. Normal metabolic profile was observed with DMSO treatment. No significant alteration in above metabolite was observed when compared with normal control upon treatment with DMSO.

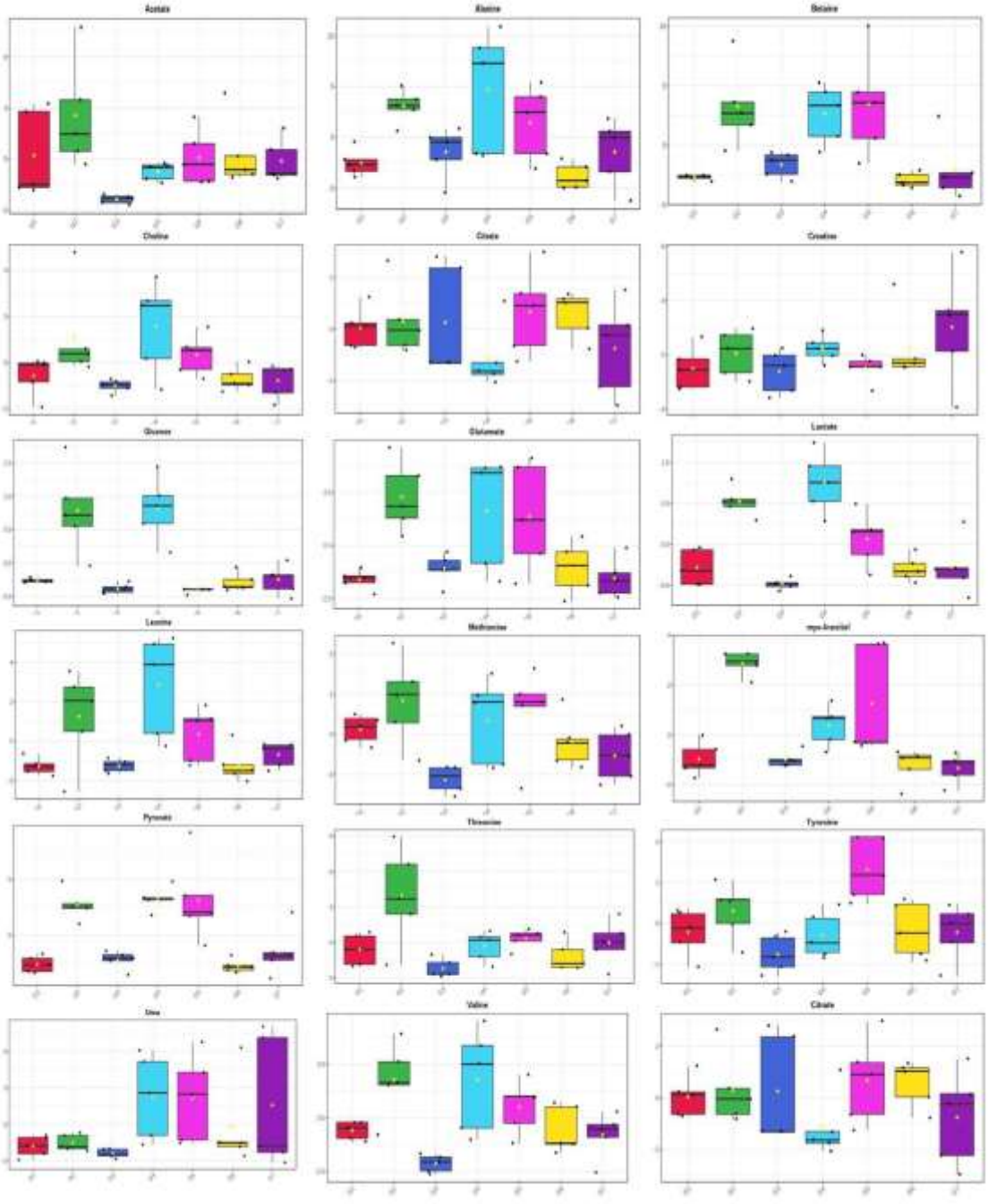

Figure 27: Box cum whisker plot of rat serum metabolites of experimental animals after treatment with VOA/TMX.

Representative box-cum whisker plots showing quantitative variation of relative signal integrals for serum metabolites. For presented metabolite entities, the VIP score>1 and statistical significance is at the level of $p \leq 0.05$. In the box plots, the boxes denote the interquartile ranges, horizontal lines inside the boxes denote the median and bottom and top boundaries of boxes are 25^{th} and 75^{th} percentiles, respectively. Lowe and upper whiskers are 5^{th} and 95^{th} percentiles, respectively.

5.2.2.6. Western blotting

Metabolomic profile confirmed alteration of cellular proteins at molecular level. Therefore, in subsequent steps we performed western blotting of major proteins in order to validate the above findings. MNU administration significantly increased the level of HIF-1α, SREBP-1c, and FASN and decreased the expression of PHD-2 when trend was compared within normal control, toxic control and treated animals groups.

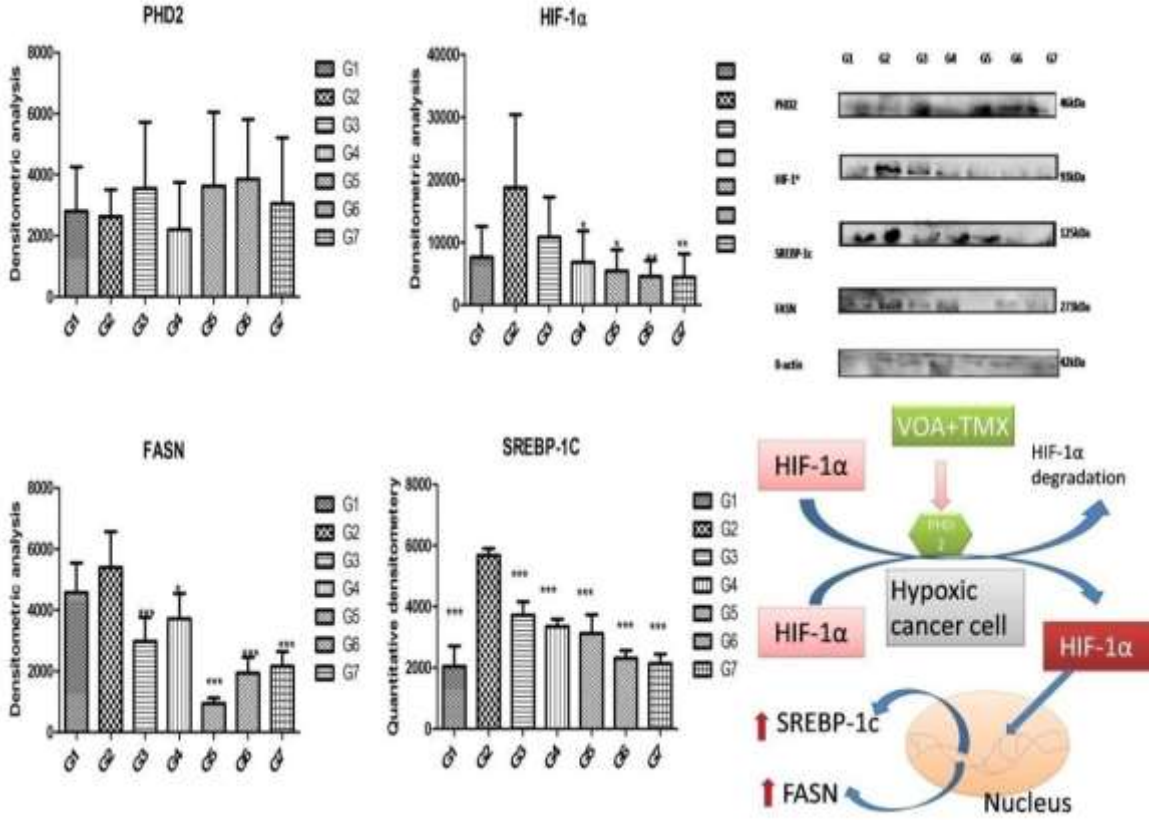

Figure 28: Effect of VOA/TMX on proteins of hypoxic pathway

Hypoxia in cancer cells activated hypoxia inducible factor-1α (HIF-1α) which enhanced the cellular expression of sterol regulatory element binding protein-1c (SREBP-1c) and fatty acid synthase (FASN) and thus fatty acid synthesis in toxic control. Prolyl hydroxylase -2 (PHD-2) is a negative regulator of HIF-1α and its expression downregulated in hypoxic environments. Treatment with VOA upregulated PHD-2 activity and downregulated HIF-1α an reverted back its downstream effects.

G1-Normal control (saline 3ml/kg,p.o), **G2**-Toxic control (MNU-50mg/kg,i.v.),**G3**-VOA(img/kg,s.c), **G4**-VOA (2mg/kg,s.c.), **G5**-TMX (8mg/kg,p.o.), **G6**-VOA(1mg/kg)+TMX(8mg/kg,p.o., **G7**-DMSO (3%)

Treatment with both low and high doses of VOA significantly reduced the expression of HIF-1α, SREBP-1c and FASN when compared with toxic control animals[33] (**Figure 28).** Increase in PHD2 expression was observed only with low dose but no significant change in PHD2 expression was observed with high dose. Treatment with TMX also enhanced the PHD2 expression and reduced the HIF-1α, SREBP-1c and FASN level. Combination therapy with VOA and TMX worked well and significantly reduced HIF-1α, SREBP-1c and FASN and enhanced PHD2 expression. No change in above proteins was noted in DMSO treated animals which indicates DMSO does not interfere with protein expression at molecular level.

5.2.2.7. Discussion

MNU is a well known carcinogenic agent for mammary gland carcinoma. Being an alkylating agent, bind with the guanine base pair of DNA and form two intermediate compounds -one short lived *N*-methyl guanine and second long lived O-methyl guanine. Due to methylation the O-position of guanine alters its hydrogen bonding properties and ultimately damages the DNA of mammary glands cells[34]. The cells with damaged DNA start dividing in an uncontrolled way and develop hypoxia as they move away from blood vessels.

Hypoxia activates HIF-1α in solid tumors of mammary glands which helps in the furbishing of cancer cells even in oxygen scarcity[35]. It guards the glucose metabolism chiefly through glycolysis which enhances lactate acidosis in the tumor microenvironment which indirectly benefits the cancer cells in many ways[36]. For instance it signals for metastasis, invasiveness, and angiogenesis. It also enhances fatty acid synthesis required for plasma membrane synthesis. It is already reported in previous studies that cancer cells remain in high demand of fatty acid which is required for plasma membrane synthesis[13]. HIF-1α induced lactate acidosis helps the cancer cells to attain this adaptation. PHD-2 is a negative regulator of HIF-1α which becomes inactive in hypoxic environments and its chemical activation can retrograde all its effect along with inhibition of fatty acid synthesis[37]. A recent study conducted by *Manjari et al* has already

proved that PHD-2 activation by BBAP-1 downregulated HIF-1α and reduced expression of FASN in ER (+) ve mammary gland carcinoma[34].

In the present study, VOA is targeted to activate PHD-2 and consequently down regulation of HIF-1α guided fatty acid synthesis to fight mammary gland carcinoma. Results of the study are discussed in the preceding section to validate the fatty acid synthesis inhibitory potential of VOA. Along with this, results of ECG and HRV have been discussed to ensure the safety of drugs in cardiac patients.

HIF-1α promotes formation of neovascularization in solid tumors in order to accomplish nutrient and oxygen supply to the rapidly dividing cancer cells [38][39]. Excessive angiogenesis was observed after MNU treatment characterized by alveolar bud (ab), lobules (lo), terminal end bud (teb) and lateral buds which are according to the previous studies. Further increase in blood vessels formation was terminated upon treatment with low dose VOA and TMX. It would be pertinent to mention that better anti-angiogenic action was observed with low dose of VOA (**Figure 23:A-B).**

Histopathology of mammary gland tissue was further performed to confirm the morphological changes in MNU and VOA treated rats. Extreme damage to lactiferous damage (dld) and distortion of adipocytes (ad) was observed which is corresponding to the previous studies [19]. No lolular and ab formation along with ted, teb like MNU treated rats were seen after treatment with VOA and TMX therapy, Better protection to mammary gland was imparted by the low dose of VOA and combination therapy (VOA+TMX) as evidenced by the lower number of teb, ted, lb. No lo formation was noted in these animals (**Figure 23:a-g).**

Cachexia in advanced cancers of mammary gland is another encountered problem and various studies have reported progressive loss of weight in cancer [40][30]. *Lee et al* reported that loss of body weight in cancer is different from that is faced by the people on hunger strike [41]. Similar results were also observed in the current study after treatment with MNU. MNU treated

the rat's documented constant decrease in body weight which is consistent with the previous studies **(Figure 24).** Further decrease in body weight was prevented by the low dose of VOA, TMX and combination therapy but excessive decrease in body weight like toxic control was observed with high dose of VOA which indicates its toxicity at high dose.

Mammary gland carcinogenesis is associated with free radical oxidative stress and SOD, Catalase and GSH are family enzymes which work in tandem to fight against this oxidative stress. Excess of H2O2 produced in breast cancer may be due to the increased production of superoxide anions (O^{2-})[14]. MNU treatment decreased the enzymatic activity of SOD, GSH and Catalase which clearly indicates development of oxidative stress and VOA and TMX restored the enzymatic back to normal **(Table 7).** Increased activity of TBARS and Protein carbonyl is described as the indicator oxidation of lipid membrane. Same was also observed in the current study and the level of the same was also restored back to normal upon initiation of therapy with VOA and TMX .

Metabolomic alteration in the hypoxic environment is the hallmark of cancer. Several studies have reported that cancer cells utilized more glucose even in presence of oxygen and consequently more pyruvate and lactate is produced which accumulate in the extracellular tumormicroenvironment[42]. Similar type of perturbation was also observed in the experimental animals after MNU administration. Increase in glucose, pyruvate and lactate in serum of toxic control evidenced the metabolism of glucose only through glycolysis **(Figure 30).**

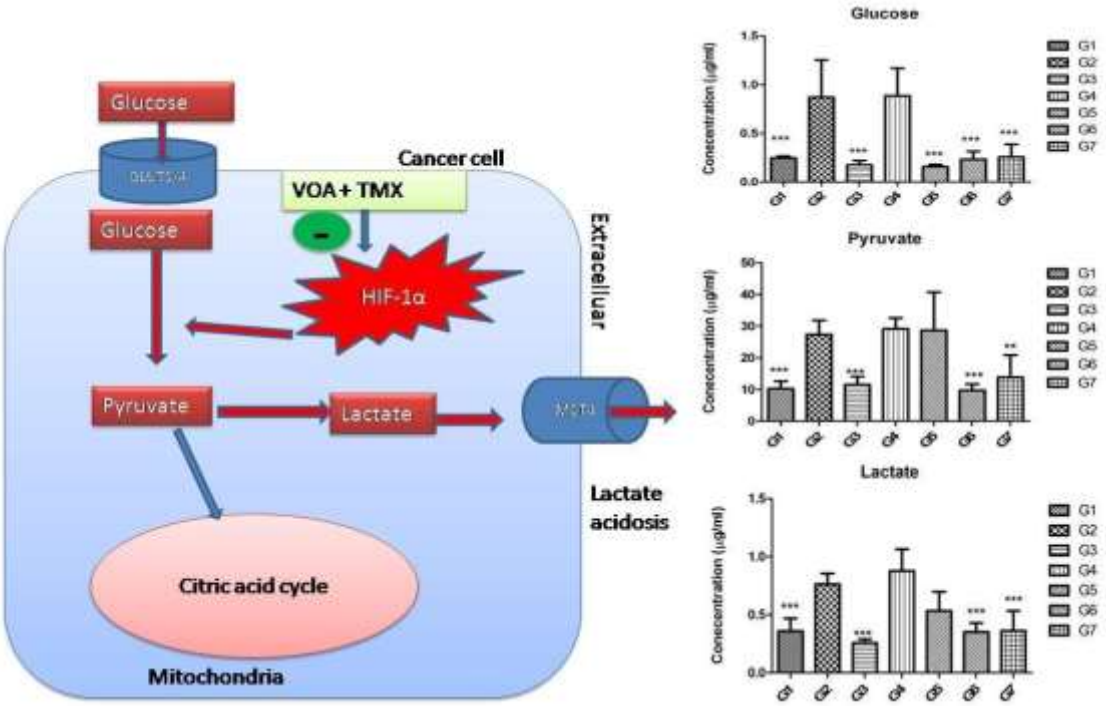

Figure 29: Effect of VOA/TMX therapy on hypoxia induced metabolic reprogramming of serum metabolites involved in glucose metabolism.

In response to hypoxia, cancer cells utilize more and more glucose which not used in oxidative phosphorylation in mitochondria and as result excess pyruvate accumulates in the cells. Accumulated pyruvate then converted into lactate which is expelled out through MCT4 transporter into the tumor microenvironment and makes the extracellular environment which is exploited in various ways by the cancer cell. Treatment with VOA/TMX caused activation of prolyl hydroxylase-2 (PHD-2) which carried out the hydroxylation and finally proteolytic degradation of hypoxia inducible factor -1α (HIF-1α). Inactivation of HIF-1α ultimately reduced the glucose utilization and lactate acidosis in tumor microenvironment.

G1-Normal control (saline 3ml/kg,p.o), **G2**-Toxic control (MNU-50mg/kg,i.v.),**G3**-VOA(img/kg,s.c), **G4**-VOA (2mg/kg,s.c.), **G5**-TMX (8mg/kg,p.o.), **G6**-VOA(1mg/kg)+TMX(1mg/kg,p.o., **G7**-DMSO (3%)

Upon treatment with VOA low dose, TMX and combination of both of these drugs decreased glucose , pyruvate and lactate that validated the efficacy of these drugs in mammary gland carcinoma prevention. Also, even more high levels of glucose, pyruvate and lactate was observed in VOA in high dose treated groups which pointed to its toxicity at this dose.

Various studies have reported that lactate acidosis accomplishes many functions for the cancer cells. Its role in alteration of fatty acid metabolism[43], induction of angiogenesis, invasiveness

is already reported in previous studies [44,45]. Angiogenesis is necessary for new blood vessel formation in order to re-establish nutrient supply and enhanced fatty acid would be used for plasma membrane synthesis of rapidly dividing cancer cells [35][14]. Enhanced angiogenesis in toxic control already discussed in the above section that might be initiated by the lactate acidosis. Abrupt fatty acid synthesis in response to hypoxia is previously reported in numerous studies [46]. In, this study, serum metabolomics analysis of experimental rats have shown upsurge level of choline, betaine, myo-inositol, acetate, along with glucose, pyruvate and lactate which validates the role of hypoxia in reprogramming of fatty acids. Rapidly dividing cancer cells remain in high demand of saturated and polyunsaturated fatty acids which is required for plasma membrane synthesis [11]**.** Therefore, hypoxia activated HIF-1α might have activated enzymes involved in the fatty acid synthesis (*de novo*) pathway like FASN. For, synthesis of plasma membrane phospholipids,like-phosphatidylcholine and phosphatidylinositol , choline and myo-inositol must be present in adequate amounts. Choline is supplied through dietary sources and through catabolism of body phospholipids while glycerol and myo-inositol is supplied by the glycolysis, this is why cancer cells adopt glycolytic pathways. To be converted into phospholipids, fatty acids, glycerol, choline and myo-inositol accumulate on the cytosolic side of the endoplasmic reticulum and newly synthesized phospholipids are incorporated into the growing plasma membrane (**Figure 30**)**.** The increased level of above said metabolites in response to hypoxia is in line with the previous findings. It would be pertinent to mention here that treatment with VOA low dose and combination with TMX worked well and re-established the metabolic profile of fatty acid.

But, on treatment with VOA high dose even more accumulation was noted like the toxic which indicates its toxicity at this dose and monotherapy with TMX Along with fatty acids, demand of amino acids is equally important in cancer cells needed for the cell plasma membrane proteins, enzymes and signaling molecules. Perturbation in serum amino acids like threonine, isoleucine,

leucine, tyrosine, glutamine, and alanine was observed in response to hypoxia in the current study after MNU administration **(Figure 31).** Low dose VOA and its

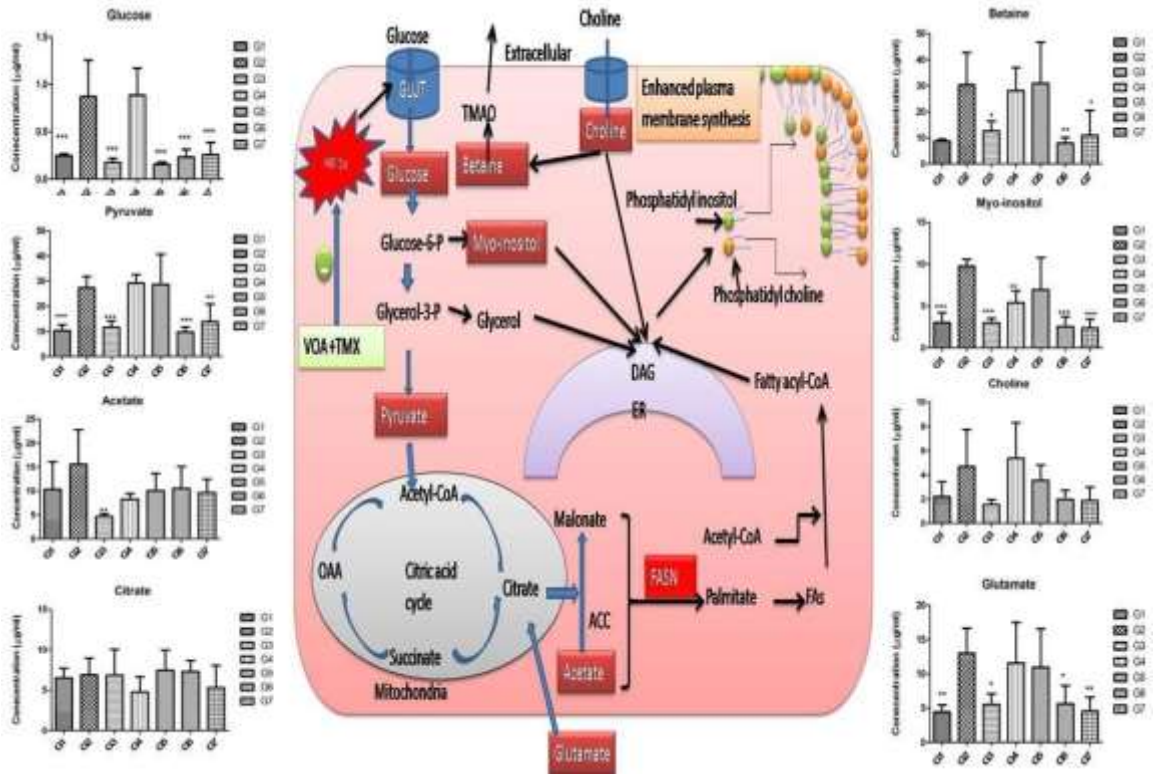

Figure 30: Effect of VOA/TMX on hypoxia induced metabolic reprogramming of serum fatty acids

Cancer cells remain in high demand of fatty acids which are required for plasma membrane synthesis. Consequently glycolysis is upregulated to enhance de novo fatty acid synthesis. Glutamate from extracellular regions also helps in de novo fatty acid synthesis. To form plasma phospholipids, choline and myo-inositol processed in the endoplasmic reticulum. Phosphatidylcholine and phosphatidylinositol are thus incorporated into the newly synthesized plasma membrane. Glycerol and myo-inositol are supplied by the glycolysis and choline is supplied from the dietary sources or from degradation of plasma lipids. Treatment with low dose of VOA, and its combination with TMX, restored the perturbed metabolic profile of

experimental animals. Also, metabolic profiles like that of toxic control animals were observed in VOA high dose and with monotherapy of TMX.

G1-Normal control (saline 3ml/kg,p.o), G2-Toxic control (MNU-50mg/kg,i.v.),G3-VOA(img/kg,s.c), G4-VOA (2mg/kg,s.c.), G5-TMX (8mg/kg,p.o.), G6-VOA(1mg/kg)+TMX(8mg/kg,p.o., G7-DMSO (3%)

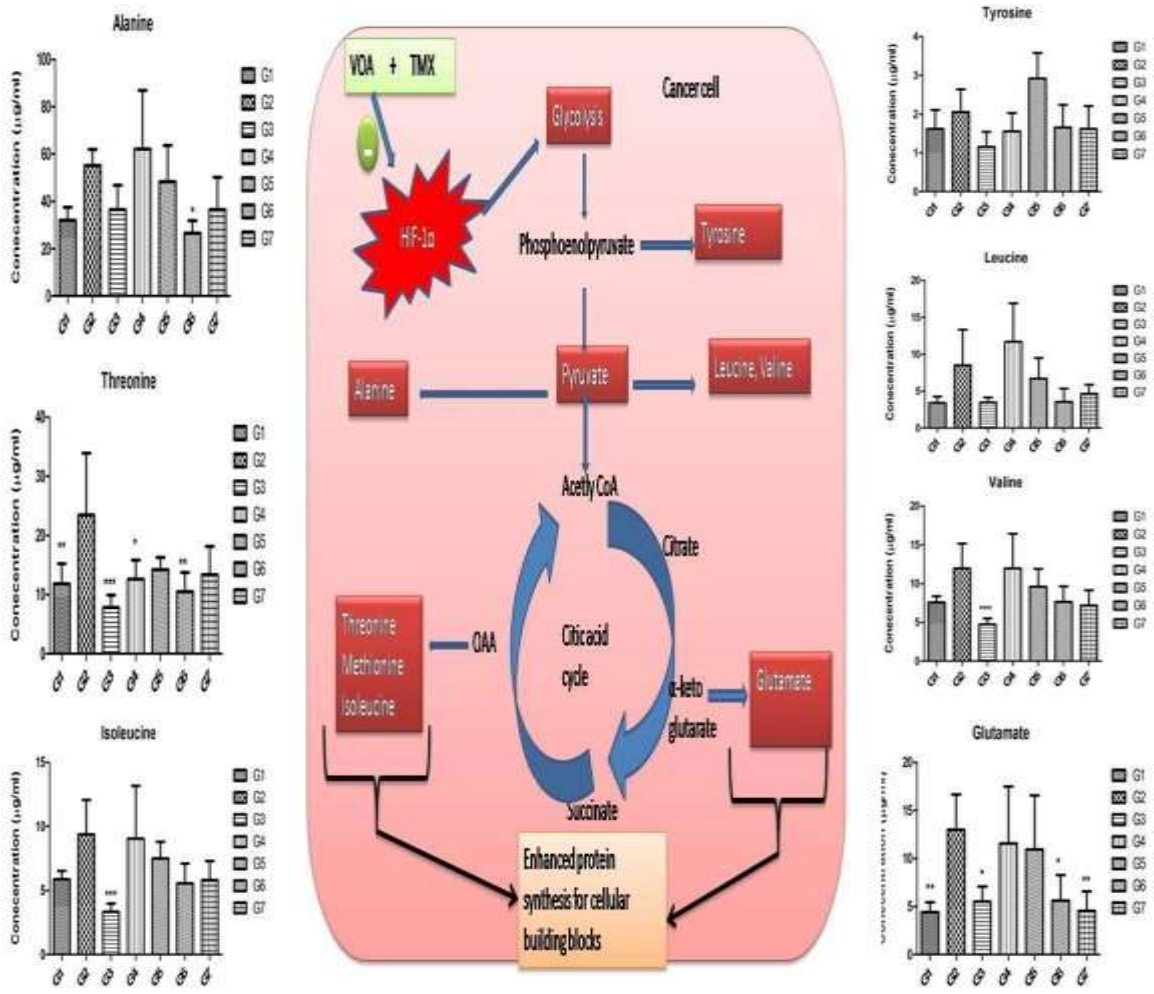

Figure 31: Effect of VOA /TAM therapy on hypoxia induced metabolic reprogramming of serum amino acids

After MNU administration, hypoxia developed in the cancer cells which enhanced the glycolytic pathways. As a result of this, amino acid metabolism was reprogrammed. Due to an increase in biosynthesis of amino acids like alanine, threonine, tyrosine, leucine, isoleucine and glutamate, excess polypeptides are formed to be incorporated into plasma membranes of rapidly dividing cells. Glutamate also acts as a substrate in fatty acid synthesis.

G1-Normal control (saline 3ml/kg,p.o), **G2**-Toxic control (MNU-50mg/kg,i.v.),**G3**- VOA (img/kg,s.c), **G4**-VOA (2mg/kg,s.c.), **G5**-TMX (8mg/kg,p.o.), **G6**-VOA (1mg/kg) +TMX (8mg/kg,p.o., **G7**-DMSO (3%)

combination therapy restored the perturbed amino acid metabolism. The collective analysis of serum metabolites involved in glycolytic pathway, protein synthesis pathways and that of fatty acid synthesis pathway shows that cancer cells speed up glucose metabolism in order to meet increasing demands of fatty acids along with amino acids needed for plasma membrane synthesis. Treatment with low dose of VOA and TMX restored the metabolic perturbation back to normal. Also, toxic effects rather than the favourable outcomes were observed with high doses of VOA.

Western blotting was performed to further evaluate the effect of the drug at the molecular level. Immunoblotting of previous studies have reported large increase in cellular expression of HIF-1α, SREBP-1c, FASN and diminished expression of PHD-2 in solid tumors of the mammary gland [47]. Similar kinds of manifestations were also noted in toxic control after MNU administration i.e. the increase in HIF-1α, SREBP-1c, FASN but a decrease in PHD-2 which indicated development of cancer hypoxia in these animals **(Figure 29).** The aforesaid changes might be required to meet out the high demand of fatty acids to be used for plasma membrane synthesis at this point [48]. On the other hand opposite trend in the expression of HIF-1α, SREBP-1c, FASN and PHD2 indicated that VOA and TMX treatment activated PHD-2 which enhanced the proteolytic degradation of HIF-1α and thus reverted all its downward effects.

CHAPTER 6

SUMMARY & CONCLUSION

6. Summary & Conclusion

The current study is ventured to delineate anti-cancer potential of Voacamine (VOA) in DMBA and MNU induced mammary gland carcinoma. The drug was selected on the basis of docking studies and obtained as a drug sample from National Cancer Institute (USA). A library of natural compounds similar in structure with Vincristine (VIN) was downloaded from ZINC database and then docked with PHD-2, VOA was one of them. In silico, toxicity (LD50) and ADME studies were performed with online software and afterward *In Vivo* studies were performed in albino wistar rats after the approval of protocol. Animals were divided into 7 groups in both the studies and treated with low and high doses of VOA alone and in combination with VIN and TMX. After the completion of the experiment, ECG and HRV of animals were recorded prior to the end of study. Afterward animals were sacrificed with cervical dislocation under ether anesthesia, blood and vital organs were collected and preserved in formalin (10%) in order to evaluate the histopathological changes. Mammary gland tissue was stretched on to the glass slide to perform carmine staining to evaluate the anti-angiogenic potential of the drug. Mammary gland tissue was also collected and stored in the -20 to carry out western blotting, gas chromatography and in vivo antioxidant biochemicals like TBARS, Protein carbonyl, SOD and Catalase. The collected blood was centrifuged and serum was carefully separated and used for serum metabolomic analysis. The result of both the studies have evidenced the mammary gland inhibitory potential of the VOA and discussed summarized in the preceding section separately.

In the DMBA study, results of western blotting shows that HIF-1α, SREBP-1c and FASN were significantly raised in TC groups that were observed to be decreased in subsequent

treatment groups (treated with VOA and VIN). At the same time a raised level of PHD2 was found in treatment groups (with combination low and high dose therapy of VOA and VIN). It means treatment with VOA and VIN somehow enhancing protein expression of PHD2 and decreasing protein expression of HIF-1α, SREBP-1c and FASN. Metabolomic profile of TC control group shows a decreased level of glucose and increased level of lactate, glutamate and PUFAs that indicates excess glucose was converted into lactate which is true according to Warburg effect that cancerous cells prefer glycolytic pathway compared to oxidative pathway (Citric acid cycle) in hypoxic conditions. Excess of lactate formed disturbed the intra and extracellular pH in tumor cells. Disturbed pH in the intra and extracellular environment activated the SREBP-1c present in the endoplasmic reticulum. Western blotting has evidenced the increased expression of SREBP-1c which then enhanced the FASN expression and as result of this more and more synthesis of PUFAs resulted to construct the plasma membrane and to meet energy requirements. Treatment with VOA and VIN decreased in level of lactate, glutamate. From this it can be concluded that HIF-1α increased the intracellular lactate acidosis to activate SREBP-1c in order to enhance fatty acid synthesis that was reverted back when HIF-1α went degradation upon PHD2 to activation with VOA and VIN therapy. All in all, VOA and VIN activated PHD2 which down regulated HIF-1α, reduced lactate acidosis, inactivated SREBP-1c and FASN to check fatty acid synthesis needed for plasma membrane synthesis by the rapidly dividing breast cancer cells (Figure13). Further, decreased levels of TBARS, SOD, Catalase, and GSH evidenced the protective mechanism of VOA therapy. Combination therapy imparted much better protection compared to monotherapy of VOA and VIN. FAME analysis of mammary gland tissue also showed higher levels of polyunsaturated

fatty acid (PUFA) level in DMBA treated toxic treated groups which was also subsided back to normal. Carmine staining showed higher branching of mammary gland ducts, alveolar buds (ABs), lobules (Lo) and terminal end buds (TEB) that clearly demarcated the angiogenesis after DMBA administration. Very less branching of mammary gland ducts, ABs, TEB were observed in VOA and VIN treated groups which further support the anti-angiogenic potential of said therapy. Histopathology of mammary gland tissue further supported the anti-cancer potential of VOA alone and combination therapy with VIN. Excessive distortion of ductal epithelium (DE), myoepithelium (ME), and lactiferous ducts (LD) as observed in toxic control was not observed in treated groups which indicate VOA and VIN therapy in combination blocked further damage to the mammary gland tissue. Histopathology of vital organs like liver and kidney showed excessive damage to the Bowman's capsule, Glomerulus, proximal convoluted tubule (PCT) case of kidney and excessive damage to lobules (lo), enlargement of central vein (CV) and damage to sinusoids (dSn) indicates that combination therapy of VOA with VIN should be advocated cautiously in patients with renal and liver complications. Cardiotoxicity of drugs was assessed with ECG and HRV recording and large ECG changes like increase in P amplitude, R amplitude, T amplitude, Heart rate were noted after DMBA administration. Large increases in the same parameters were observed after the initiation of therapy which marked the cardio toxic potential of current therapy. Conclusively, combination therapy with (both low and high dose) VOA and VIN imparted much better protection to the mammary gland tissue but at the same time it caused noteworthy renal, liver and cardio toxicity. As far as monotherapy with VOA high dose was considered, it not only imparted

protection to the mammary gland tissue but also caused negligible renal, liver and cardio toxicity.

In MNU study, MNU administration manifested an increase in expression of HIF-1α, SREBP-1c, FASN and reduced expression of PHD-2 which indicated development of severe hypoxia. Upon treatment with VOA and TMX the opposite relationship is obtained in the above proteins. Again, this indicated HIF-1α somehow increasing expression of SREBP-1c and FASN in order to increase fatty acid synthesis. The above finding was further supported by the serum metabolomic analysis of rats. High Glucose, lactate, Glutamate, Choline ,Betaine and myo-inositol were detected in toxic control which are very well known to enhance fatty acid required for plasma membrane of rapidly dividing cancer cells. From these findings it can be concluded that severe hypoxia activated HIF-1α which directed metabolism of glucose mainly through glycolysis due to lactate concentration was increased after MNU administration. Along with lactate, elevated levels of glutamate, choline, betaine and myo-inositol was also observed in the toxic group which clearly indicates that lactate somehow increases the rate of fatty acid synthesis. These changes were further supported that HIF-1α increased the lactate acidosis to enhance fatty acid synthesis in cancer cells under hypoxia. Interestingly, perturbed metabolites were restored back to normal upon initiation of therapy with VOA low dose, TMX and with combination therapy of both of these drugs which clearly indicates that VOA in low dose as well as in combination with TMX somehow reducing the level of HIF-1α, the ultimate culprit. Above we have already talked about the increased expression of PHD-2 in treatment groups treated with VOA low dose, TMX and combination of these two drugs. PHD-2 is a negative regulator of HIF-1α; it causes hydroxylation and the proteolytic

degradation in normoxic cells but becomes inactive in hypoxia. From, it can be concluded that VOA and TMX monotherapy and combination therapy activated the PHD-2 in a hypoxic medium which enhanced the proteolytic degradation of HIF-1α and subsequently level of lactate and rate of glycolysis was subsided back to normal. Biochemical analysis further supported the above finding. Higher level of TBARS, protein carbonyl was observed in MNU treated toxic groups which was restored back to normal. SOD, catalase and GSH are a group of enzymes which work together to keep the free radical level to minimum. Decreased level of SOD, catalase and GSH in toxic and increased level after treatment evidenced the antioxidant potential of therapy. Anti-angiogenic potential of therapy was evaluated by carmine staining. Results of carmine staining showed excessive branching of the mammary gland ductal tree after MNU administration which indicates initiation of angiogenesis in toxic control. Comparatively very less branching of mammary gland tissue was observed in treatment groups treated with VOA low dose, TMX and their combination evidenced by less number of AB, TEBs and lateral buds (Lb). Histopathological examination of mammary gland tissue further supports the above finding. Distorted arrangement of adipocytes, and lactiferous duct was observed in toxic control group animals after MNU treatment. Normal architecture of adipocytes and lactiferous duct in treatment groups shows that therapy with VOA low dose, TMX and combination of these two drugs worked well to protect the mammary gland tissue. ECG and HRV also recorded to assess the cardio toxic potential of therapy. Normal ECG and HRV were recorded in normal group rat but large ECG changes like increase in PR interval, QT interval, ST height, and JT interval were noted in toxic control which was found even more increased with VOA high doe, TMX and DMSO. From this it can be

concluded that VOA high, TMX and DMSO somehow cause cardiac toxicity because increased ST height, JT interval and QT interval are associated with myocardial infarction. An ECG like normal rats were recorded in rats treated with low dose of VOA, and with combination therapy which indicates VOA is safe at this dose and can be used in heart patients also.

Cachexia in advanced cancers of mammary gland is another encountered problem and various studies have reported progressive loss of weight in cancer. MNU treated rat's documented constant decrease in body weight which is consistent with the previous studies (Figure 3). Further decrease in body weight was prevented by the low dose of VOA, TMX and combination therapy but excessive decrease in body weight like toxic control was observed with high dose of VOA which indicates its toxicity at high dose. Conclusively, we can say that VOA low dose is a comparatively safe and better drug to combat mammary gland carcinoma as well. Results of MNU study also proved that VOA has a potential to activate PHD-2 and which can further down regulate HIF-1α and its subsequent effect on fatty acid synthesis.

CHAPTER-7

REFERENCES

References

1 Al-Dujaili, Z. et al. (2017) Skin cancer concerns particular to women. *International journal of women's dermat ology* 3 (1), S49-S51

2 Becker, A. et al. (2016) Extracellular vesicles in cancer: cell-to-cell mediators of metastasis. *Cancer cell* 30 (6), 836-848

3 Torre, L.A. et al. (2015) Global cancer statistics, 2012. *CA: a cancer journal for clinicians* 65 (2), 87-108

4 Muz, B. et al. (2015) The role of hypoxia in cancer progression, angiogenesis, metastasis, and resistance to therapy. *Hypoxia* 3, 83

5 Fan, L. et al. (2014) The hypoxia-inducible factor pathway, prolyl hydroxylase domain protein inhibitors, and their roles in bone repair and regeneration. *BioMed research international* 2014

6 Sadri, N. and Zhang, P.J. (2013) Hypoxia-inducible factors: mediators of cancer progression; prognostic and therapeutic targets in soft tissue sarcomas. *Cancers* 5 (2), 320-333

7 Tanimoto, K. (2017) Genetics of the hypoxia-inducible factors in human cancers. *Experimental Cell Research*

8 Park, J.S. et al. (2015) Hypoxia-induced IL-32β increases glycolysis in breast cancer cells. *Cancer letters* 356 (2), 800-808

9 Barrett, T.D. et al. (2015) Prolyl hydroxylase inhibition corrects functional iron deficiency and inflammation-induced anaemia in rats. *British journal of pharmacology* 172 (16), 4078-4088

10 Lowry, M.C. and O'Driscoll, L. (2018) Can hi-jacking hypoxia inhibit extracellular vesicles in cancer? *Drug discovery today*

11 Armitage, E.G. et al. (2014) Cancer hypoxia and the tumour microenvironment as effectors of cancer metabolism. In *Correlation-based network analysis of cancer metabolism*, pp. 7-14, Springer

12 Nagy, M. (2011) HIF-1 is the Commander of Gateways to Cancer. *J Cancer Sci Ther* 3 (2), 35-40

13 Niecknig, H. et al. (2012) Role of reactive oxygen species in the regulation of HIF-1 by prolyl hydroxylase 2 under mild hypoxia. *Free radical research* 46 (6), 705-717

14 Kant, R. et al. (2013) Prolyl 4 hydroxylase: a critical target in the pathophysiology of diseases. *The Korean Journal of Physiology & Pharmacology* 17 (2), 111-120

15 Dumas, J.-F. et al. (2017) Metabolic reprogramming in cancer cells, consequences on pH and tumour progression: Integrated therapeutic perspectives with dietary lipids as adjuvant to anticancer treatment. In *Seminars in Cancer Biology*, Elsevier

16 Kollmann, K. et al. (2013) A kinase-independent function of CDK6 links the cell cycle to tumor angiogenesis. *Cancer cell* 24 (2), 167-181

17 Thompson, C.B. (2016) Into thin air: how we sense and respond to hypoxia. *Cell* 167 (1), 9-11

18 Wong, B.W. et al. (2013) Emerging novel functions of the oxygen-sensing prolyl hydroxylase domain enzymes. *Trends in biochemical sciences* 38 (1), 3-11

19 Na, Y.-R. et al. (2016) Pyrithione Zn selectively inhibits hypoxia-inducible factor prolyl hydroxylase PHD3. *Biochemical and biophysical research communications* 472 (2), 313-318

20 Nguyen, L.K. et al. (2015) A dynamic model of the hypoxia-inducible factor 1a (HIF-1a) network. *J Cell Sci* 128 (2), 422-422

21 Meneses, A.M. and Wielockx, B. (2016) PHD2: from hypoxia regulation to disease progression. *Hypoxia* 4, 53

22 Nandal, A. et al. (2011) Activation of the HIF prolyl hydroxylase by the iron chaperones PCBP1 and PCBP2. *Cell metabolism* 14 (5), 647-657

23 Badawi, Y. and Shi, H. (2017) Relative Contribution of Prolyl Hydroxylase-Dependent and-Independent Degradation of HIF-1alpha by Proteasomal Pathways in Cerebral Ischemia. *Frontiers in neuroscience* 11

24 Tarhonskaya, H. et al. (2015) Kinetic investigations of the role of factor inhibiting Hypoxia-inducible factor (FIH) as an oxygen sensor. *Journal of Biological Chemistry* 290 (32), 19726-19742

25 Tekade, R.K. and Sun, X. (2017) The Warburg effect and glucose-derived cancer theranostics. *Drug discovery today*

26 Forgan, L.G. (2009) Influence of Oxygen Supply on Metabolism and Energetics in FishMuscles.

27 Lyssiotis, C.A. and Kimmelman, A.C. (2017) Metabolic interactions in the tumor microenvironment. *Trends in cell biology*

28 Vaupel, P. et al. (1989) Blood flow, oxygen and nutrient supply, and metabolic microenvironment of human tumors: a review. *Cancer Research* 49 (23), 6449-6465

29 Jose, C. et al. (2011) Choosing between glycolysis and oxidative phosphorylation: a tumor's dilemma? *Biochimica et Biophysica Acta (BBA)-Bioenergetics* 1807 (6), 552-561

30 Gottfried, E. et al. (2012) Tumor metabolism as modulator of immune response and tumor progression. In *Seminars in cancer biology* (Vol. 22), pp. 335-341, Elsevier

31 Zeng, W. et al. (2015) Hypoxia and hypoxia inducible factors in tumor metabolism. *Cancer letters* 356 (2), 263-267

32 Quaegebeur, A. et al. (2016) Deletion or inhibition of the oxygen sensor PHD1 protects against ischemic stroke via reprogramming of neuronal metabolism. *Cell metabolism* 23 (2), 280-291

33 Masson, N. and Ratcliffe, P.J. (2014) Hypoxia signaling pathways in cancer metabolism: the importance of co-selecting interconnected physiological pathways. *Cancer & metabolism* 2 (1), 3

34 Solaini, G. et al. (2010) Hypoxia and mitochondrial oxidative metabolism. *Biochimica et Biophysica Acta (BBA)-Bioenergetics* 1797 (6), 1171-1177

35 Palazon, A. et al. (2017) An HIF-1α/VEGF-A Axis in Cytotoxic T Cells Regulates Tumor Progression. *Cancer cell* 32 (5), 669-683. e665

36 Justus, C.R. et al. (2015) Molecular connections between cancer cell metabolism and the tumor microenvironment. *International journal of molecular sciences* 16 (5), 11055-11086

37 Xu, J. et al. (2016) Na+/H+ exchanger 1, Na+/Ca 2+ exchanger 1 and calmodulin complex regulates interleukin 6-mediated cellular behavior of human hepatocellular carcinoma. *Carcinogenesis* 37 (3), 290-300

38 Eales, K. et al. (2016) Hypoxia and metabolic adaptation of cancer cells. *Oncogenesis* 5 (1), e190

39 DeBerardinis, R.J. and Chandel, N.S. (2016) Fundamentals of cancer metabolism. *Science advances* 2 (5), e1600200

40 Yang, K. et al. (2015) Intracellular pH-triggered, targeted drug delivery to cancer cells by multifunctional envelope-type mesoporous silica nanocontainers. *ACS applied materials & interfaces* 7 (31), 17399-17407

41 Stransky, L. et al. (2016) The function of V-ATPases in cancer. *Physiological reviews* 96 (3), 1071-1091

42 Cotter, K. et al. (2015) Activity of plasma membrane V-ATPases is critical for the invasion of MDA-MB231 breast cancer cells. *Journal of Biological Chemistry* 290 (6), 3680-3692

43 Avnet, S. et al. (2014) Proton channels and exchangers in cancer☆,☆☆.

44 Cardone, R.A. et al. (2015) A novel NHE1-centered signaling cassette drives epidermal growth factor receptor–dependent pancreatic tumor metastasis and is a target for combination therapy. *Neoplasia* 17 (2), 155-166

45 Romero-Garcia, S. et al. (2016) Lactate contribution to the tumor microenvironment: mechanisms, effects on immune cells and therapeutic relevance. *Frontiers in immunology* 7

46 Draoui, N. and Feron, O. (2011) Lactate shuttles at a glance: from physiological paradigms to anti-cancer treatments. *Disease models & mechanisms* 4 (6), 727-732

47 Abaza, M. and Luqmani, Y.A. (2013) The influence of pH and hypoxia on tumor metastasis. *Expert review of anticancer therapy* 13 (10), 1229-1242

48 Flaveny, C.A. et al. (2015) Broad anti-tumor activity of a small molecule that selectively targets the Warburg effect and lipogenesis. *Cancer cell* 28 (1), 42-56

49 Zechner, R. (2015) FAT FLUX: enzymes, regulators, and pathophysiology of intracellular lipolysis. *EMBO molecular medicine* 7 (4), 359-362

50 Nomura, D.K. and Cravatt, B.F. (2013) Lipid metabolism in cancer. Elsevier

51 Harjes, U. et al. (2016) Targeting fatty acid metabolism in cancer and endothelial cells. *Critical reviews in oncology/hematology* 97, 15-21

52 Luo, X. et al. (2017) Emerging roles of lipid metabolism in cancer metastasis. *Molecular cancer* 16 (1), 76

53 Bensaad, K. et al. (2014) Fatty acid uptake and lipid storage induced by HIF-1α contribute to cell growth and survival after hypoxia-reoxygenation. *Cell reports* 9 (1), 349-365

54 Roy, S. et al. (2017) Alpha-linolenic acid stabilizes HIF-1 α and downregulates FASN to promote mitochondrial apoptosis for mammary gland chemoprevention. *Oncotarget* 8 (41), 70049

55 Lau, B.Y. et al. (2013) Investigating the role of polyunsaturated fatty acids in bone development using animal models. *Molecules* 18 (11), 14203-14227

56 Huang, D. et al. (2014) HIF-1-mediated suppression of acyl-CoA dehydrogenases and fatty acid oxidation is critical for cancer progression. *Cell reports* 8 (6), 1930-1942

57 Kuzu, O.F. et al. (2016) The role of cholesterol in cancer. *Cancer Research* 76 (8), 2063-2070

58 Sau, S. et al. (2018) A tumor multicomponent targeting chemoimmune drug delivery system for reprograming the tumor microenvironment and personalized cancer therapy. *Drug discovery today*

59 Kondo, A. et al. (2017) Extracellular Acidic pH Activates the Sterol Regulatory Element-Binding Protein 2 to Promote Tumor Progression. *Cell reports* 18 (9), 2228-2242

60 Weiszenstein, M. et al. (2016) Adipogenesis, lipogenesis and lipolysis is stimulated by mild but not severe hypoxia in 3T3-L1 cells. *Biochemical and biophysical research communications* 478 (2), 727-732

61. Zhang, J. *et al.* Prevalence and characterization of BRCA1 and BRCA2 germline mutations in Chinese women with familial breast cancer. *Breast Cancer Res. Treat.*132, 421–428 (2012).

62. Ciriello, G. *et al.* Comprehensive Molecular Portraits of Invasive Lobular Breast Cancer. *Cell*163, 506–519 (2015).

63. Marcotte, R. *et al.* Functional Genomic Landscape of Human Breast Cancer Drivers, Vulnerabilities, and Resistance. *Cell*164, 293–309 (2016).

64. Guo, J. *et al.* Mechanisms of resistance to chemotherapy and radiotherapy in hepatocellular carcinoma. *Transl. Cancer Res.*7, 765–781 (2018).

65. Al Tameemi, W., Dale, T. P., Al-Jumaily, R. M. K. & Forsyth, N. R. Hypoxia-Modified Cancer Cell Metabolism. *Front. Cell Dev. Biol.*7, 1–15 (2019).

66. Singh, L., Aldosary, S., Saeedan, A. S., Ansari, M. N. & Kaithwas, G. Prolyl hydroxylase 2: a promising target to inhibit hypoxia-induced cellular metabolism in cancer cells. *Drug Discov. Today*23, 1873–1882 (2018).

67. Sun, W. *et al.* Interaction between von Hippel-Lindau Protein and Fatty Acid Synthase Modulates Hypoxia Target Gene Expression. *Sci. Rep.*7, 1–11 (2017).

68. Ratcliffe, P. *et al.* Update on hypoxia-inducible factors and hydroxylases in oxygen regulatory pathways: from physiology to therapeutics. *Hypoxia*Volume 5, 11–20 (2017).

69. Singh, M., Devi, U., Roy, S., Gupta, P. S. & Kaithwas, G. Chemical activation of prolyl hydroxylase-2 by BBAP-1 down regulates hypoxia inducible factor-1α and

fatty acid synthase for mammary gland chemoprevention. *RSC Adv.*8, 12848–12860 (2018).

70. Gautam, S. *et al.* DuCLOX-2/5 inhibition attenuates inflammatory response and induces mitochondrial apoptosis for mammary gland chemoprevention. *Front. Pharmacol.*9, 1–17 (2018).

71. Roy, S. *et al.* Alpha-linolenic acid stabilizes HIF-1 α and downregulates FASN to promote mitochondrial apoptosis for mammary gland chemoprevention. *Oncotarget*8, 70049–70071 (2017).

72. Tucker, D. K., Bouknight, S. H., Brar, S. S., Kissling, G. E. & Fenton, S. E. Evaluation of prenatal exposure to bisphenol analogues on development and long-term health of the mammary gland in female mice. *Environ. Health Perspect.*126, (2018).

73. Singh, M. *et al.* Repurposing mechanistic insight of PDE-5 inhibitor in cancer chemoprevention through mitochondrial-oxidative stress intervention and blockade of DuCLOX signalling. *BMC Cancer*19, 1–15 (2019).

74. Mesilati-stahy, R. & Id, N. A. Changes in lipid droplets morphometric features in mammary epithelial cells upon exposure to non-esterified free fatty acids compared with VLDL. 1–17 (2018).

75. Silva, R. A., Pereira, T. C. S., Souza, A. R. & Ribeiro, P. R. 1H NMR-based metabolite profiling for biomarker identification. *Clin. Chim. Acta* 1–11 (2019) doi:10.1016/j.cca.2019.11.015.

76. Roy, S. *et al.* GLA supplementation regulates PHD2 mediated hypoxia and mitochondrial apoptosis in DMBA induced mammary gland carcinoma. *Int. J. Biochem. Cell Biol.*96, 51–62 (2018).

77. Santos, C. R. & Schulze, A. Lipid metabolism in cancer. *FEBS J.*279, 2610–2623 (2012).

78. Bensaad, K. *et al.* Fatty acid uptake and lipid storage induced by HIF-1α contribute to cell growth and survival after hypoxia-reoxygenation. *Cell Rep.*9, 349–365 (2014).

79. Furuta, E. *et al.* Fatty acid synthase gene is up-regulated by hypoxia via activation of Akt and sterol regulatory element binding protein-1. *Cancer Res.*68, 1003–1011 (2008).

80. Kramer, K. *et al.* Effect of dimethyl sulfoxide (DMSO) on the electrocardiogram (ECG) in freely moving male Balb/c mice. *Gen. Pharmacol.*26, 1403–1407 (1995).

81. Uni-, T. T. & Oja, R. Power Spectrum. 650–650 (2011) doi:10.1007/978-90-481-

3585-1_781.

82. Veschini, L. *et al.* Hypoxia-inducible transcription factor-1 alpha determines sensitivity of endothelial cells to the proteosome inhibitor bortezomib. *Blood*109, 2565–2570 (2007).

83. Sonveaux, P. *et al.* Targeting the lactate transporter MCT1 in endothelial cells inhibits lactate-induced HIF-1 activation and tumor angiogenesis. *PLoS One*7, (2012).

84. Hoshino, A. *et al.* Effects of BRCA1 transgene expression on murine mammary gland development and mutagen-induced mammary neoplasia. *Int. J. Biol. Sci.*3, 281–291 (2007).

85. Małyszko, J., Kozłowska, K., Kozłowski, L. & Małyszko, J. Nephrotoxicity of anticancer treatment. *Nephrol. Dial. Transplant.*32, 924–936 (2017).

86. Perazella, M. A. Onco-nephrology: Renal toxicities of chemotherapeutic agents. *Clin. J. Am. Soc. Nephrol.*7, 1713–1721 (2012).

87. Aitchison, R. G., Reilly, I. A. G., Morgan, A. G. & Russell, N. H. Vincristine, adriamycin and high dose steroids in myeloma complicated by renal failure. *Br. J. Cancer*61, 765–766 (1990).

88. Condello, M. *et al.* Voacamine modulates the sensitivity to doxorubicin of resistant osteosarcoma and melanoma cells and does not induce toxicity in normal fibroblasts. *J. Nat. Prod.*77, 855–862 (2014).

89. Maor, Y. & Malnick, S. Liver Injury Induced by Anticancer Chemotherapy and Radiation Therapy. *Int. J. Hepatol.*2013, 1–8 (2013).

90. Manuscript, A. Oxidative stress, inflammation, and cancer. *Free Radic Biol Med*49, 1603–1616 (2011).

91. Hecht, F. *et al.* The role of oxidative stress on breast cancer development and therapy. *Tumor Biol.*37, 4281–4291 (2016).

92. Shang, L. & Wang, M. Molecular alterations and clinical relevance in esophageal squamous cell carcinoma. *Front. Med. China*7, 401–410 (2013).

93. Hu, J. M. & Sun, H. T. Serum proton NMR metabolomics analysis of human lung cancer following microwave ablation. *Radiat. Oncol.*13, 1–10 (2018).

94. Sormendi, S. & Wielockx, B. Hypoxia pathway proteins as central mediators of metabolism in the tumor cells and their microenvironment. *Front. Immunol.*9, 1–19 (2018).

95. Netea-Maier, R. T., Smit, J. W. A. & Netea, M. G. Metabolic changes in tumor

cells and tumor-associated macrophages: A mutual relationship. *Cancer Lett.*413, 102–109 (2018).

96. Cairns, R. A., Papandreou, I., Sutphin, P. D. & Denko, N. C. Metabolic targeting of hypoxia and HIF1 in solid tumors can enhance cytotoxic chemotherapy. *Proc. Natl. Acad. Sci. U. S. A.*104, 9445–9450 (2007).

97. Palazon, A. *et al.* An HIF-1α/VEGF-A Axis in Cytotoxic T Cells Regulates Tumor Progression. *Cancer Cell*32, 669-683.e5 (2017).

98. Sonveaux, P. *et al.* Targeting lactate-fueled respiration selectively kills hypoxic tumor cells in mice. *J. Clin. Invest.*118, 3930–3942 (2008).

99. Dales, J. P. *et al.* Overexpression of hypoxia-inducible factor HIF-1α predicts early relapse in breast cancer: Retrospective study in a series of 745 patients. *Int. J. Cancer*116, 734–739 (2005).

100. Maxwell, P. H. *et al.* Hypoxia-inducible factor-1 modulates gene expression in solid tumors and influences both angiogenesis and tumor growth. *Proc. Natl. Acad. Sci. U. S. A.*94, 8104–8109 (1997).

101. Chen, T. *et al.* MiR-17/20 controls prolyl hydroxylase 2 (PHD2)/hypoxia-inducible factor 1 (HIF1) to regulate pulmonary artery smooth muscle cell proliferation. *J. Am. Heart Assoc.*5, (2016).

ANNEXURE-I

ANIMAL APPROVAL

UNITED INSTITUTE OF PHARMACY, UCER
A-31/1, UPSIDC Industrial Area, Naini, Allahabad - 211010
Ph. : 0532 - 2101568, 2101569 Fax : 0532 - 2687142

INSTITUTIONAL ANIMAL ETHICAL COMMITTEE (IAEC)

REG. No. 1451/PO/E/11/CPCSEA Dated 04/05/2014 UNDER RULE 13 OF THE "BREENDING OF AND EXPERIMENTS ON ANIMALS (CONTROL AND SUPERVISION) RULES 1998"

UIP/IAEC/May -2016/06 **DATE: 07/05/2016**

CERTIFICATE

This is to certify that Mr. /Mrs. /Ms. **Lakhveer**, student of M. Pharm. / Ph. D. is permitted / not permitted to carry out experiments for the dissertation / thesis work entitled **"Upregulating PHD_2 activity to down regulate HIF-1 alfa and subsequently FASN in mammary gland carcinoma"** as per the details mentioned and after observing the usual formalities laid down by IAEC as per the provisions made by CPCSEA.

ANNEXURE-II

PLAGIARISM REPORT

Urkund Analysis Result

Analysed Document: Lakhveer PhD thesis_merged.pdf (D78433926)
Submitted: 9/1/2020 7:24:00 AM
Submitted By: gbl.bbau@gmail.com
Significance: 8 %

Sources included in the report:

Manjari Singh.pdf (D37177659)
Subhadeep thesis.pdf (D38548886)
subhadeep.docx (D30973724)
Subhadeep Roy.pdf (D37272493)
Swetlana.docx (D37658022)
Swetlana plagiarism check.docx (D38427680)
plagiarism check for swetlana.docx (D43086427)
manjari 1.docx (D30973722)
manjari 2.docx (D30973723)
manuscript.docx (D30977155)
Swetlana_Frontiers.pdf (D38427682)
Swetlana Manuscript .docx (D30973725)
https://patents.google.com/patent/WO2017046747A1/en
https://www.ncbi.nlm.nih.gov/pmc/articles/PMC6814136/
https://pubs.rsc.org/en/content/articlehtml/2018/ra/c7ra09689e

Instances where selected sources appear:

309

ANNEXURE-III

PUBLICATIONS

Prolyl hydroxylase 2: a promising target to inhibit hypoxia-induced cellular metabolism in cancer cells

Lakhveer Singh[1], Sara Aldosary[2], Abdulaziz S. Saeedan[3], Mohd. Nazam Ansari[3] and Gaurav Kaithwas[1]

[1] Department of Pharmaceutical Sciences, School of Biosciences and Biotechnology, Babasaheb Bhimrao Ambedkar University, Vidya Vihar, Raebareli Road, Lucknow 226025, U.P., India
[2] Department of Pharmaceutical Sciences, King Faisal University, Al-Ahsa, Saudi Arabia
[3] Department of Pharmacology, College of Pharmacy, Prince Sattam Bin Abdulaziz University, Al-Kharj, Saudi Arabia

Hypoxia-inducible factor-1α (HIF-1α) shifts the metabolism of glucose from highly efficient oxidative phosphorylation to less efficient glycolysis. Pyruvic acid thus accumulated is oxidized to lactic acid which is pumped out in the tumor microenvironment. Protons generated from the pentose phosphate pathway (PPP) and upon hydrolysis of ATP further enhance the acidity in the tumor microenvironment. The resultant pH in the tumor microenvironment activates an endoplasmic reticulum protein: sterol regulatory element binding protein-1c (SREBP-1c), which once activated enhances proliferation of the tumor cell. Prolyl hydroxylase 2 (PHD2) is a negative regulator of HIF-1α and causes degradation of HIF-1α in the presence of oxygen. Chemical activation of PHD2 can downregulate HIF-1α and thus restore all its effects. The present review is an attempt to describe PHD2 as the target to combat cancer hypoxia and consequential cellular and metabolic alterations.

Introduction

Cancer, medically known as malignant neoplasm, occurs when cellular proliferation in normal cells is no longer under normal control owing to genetic mutations primarily caused by environmental factors [1]. This uncontrolled growth and division of cells eventually forms a mass of cells termed the tumor, which interferes with the normal functioning of the organs, either at the site of origin or through spreading to other parts of the body [2]. Tumors can be further differentiated into benign and malignant tumors. A benign tumor remains localized to the organ of origin and does not grow uncontrollably but malignant tumors are metastatic in nature, invade the nearby organs and blood vessels and are transmitted to the distant organs. They are fatal and difficult to manage.

Treatment strategies for malignant tumors include surgery, radiotherapy, chemotherapy, hormone therapy, immune therapy and targeted drug therapy (drugs that interfere with tumor cell growth by targeting specific molecules) [3]. Most of the early tumors respond well to radiotherapy and chemotherapy. However, failure of radiotherapy and chemotherapy in most of the solid tumors has been observed owing to hypoxia, a condition characterized by low oxygen concentration in solid tumors as a consequence of cellular proliferation and angiogenesis (abnormal blood vessel formation) [4,5]. Tumor cells in this situation extract energy mainly from glycolysis (anaerobic mode of energy production) which makes the tumor microenvironment more acidic, further enhancing the resistance to radiotherapy and chemotherapy.

Tumor hypoxia is not only the biggest prohibition in the path of tumor therapy but it also helps the tumor cell in attaining the most hostile environment for proper growth and development [6]. In the hypoxic environment, tumor cells cause activation of a cytoplasmic protein known as hypoxia-inducible factor-1α (HIF-1α). HIF-1α, once activated, enhances the expression of numerous genes assisting the endurance of cancer cells in anoxic conditions. HIF-1α upregulates the genes for angiogenesis, metastasis, invasiveness, metabolic reprogramming, changes in extracellular pH

Corresponding author: Aldosary, S. (saldossary@kfu.edu.sa), Saeedan, A.S. (a.binsaeedan@psau.edu.sa), Ansari, M.N. (m.ansari@psau.edu.sa), Kaithwas, G. (gauravk@bbau.ac.in), (gauravpharm@hotmail.com)

https://doi.org/10.1016/j.drudis.2018.05.016

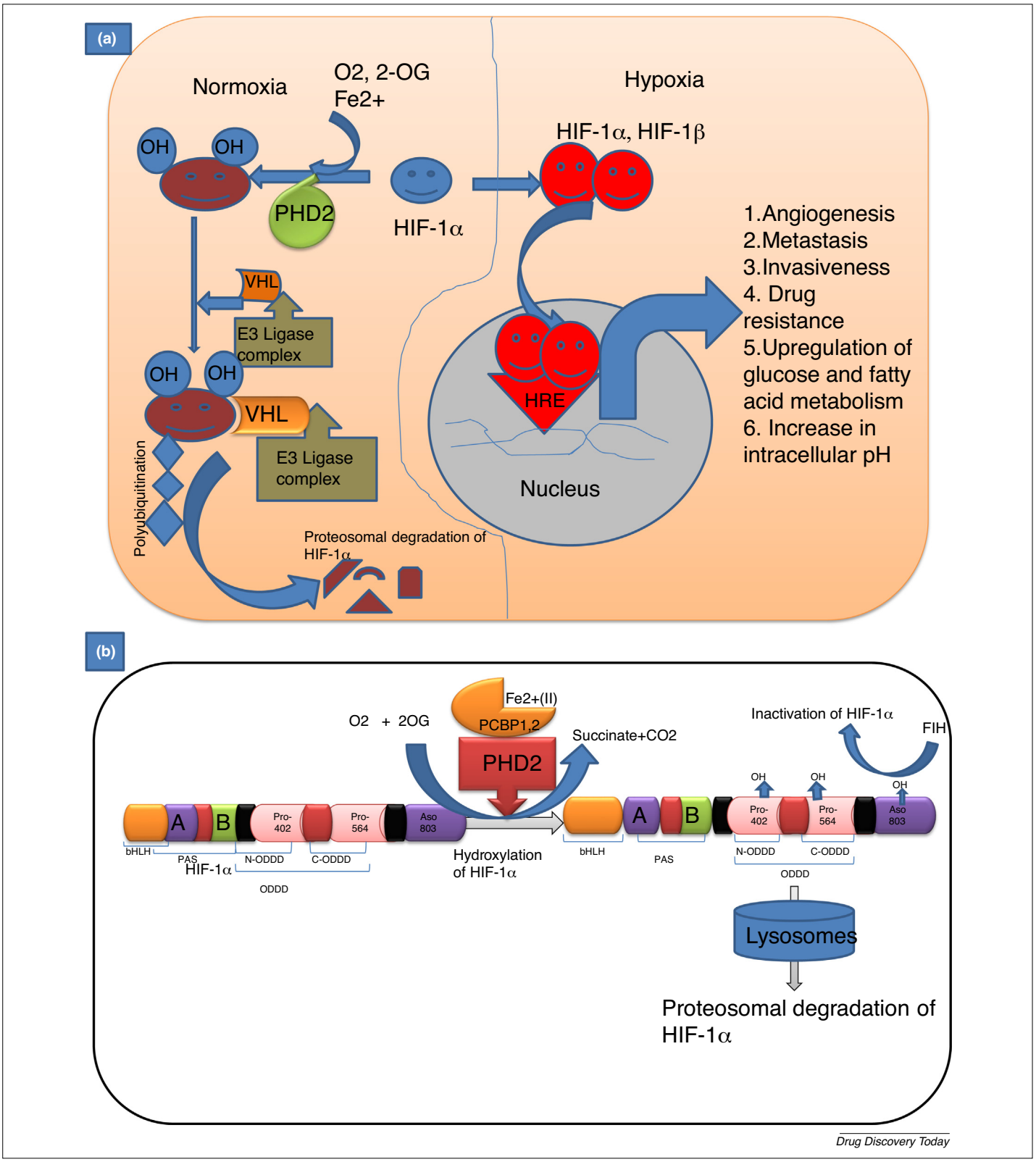

FIGURE 1

(a) Effect of normoxic and hypoxic conditions on hypoxia-inducible factor (HIF)-1α. In normoxic conditions HIF-1α is hydroxylated by prolyl hydroxylase (PHD)2 in the presence of O_2, Fe^{2+} and 2-OG. This hydroxylated complex is recognized by the von Hippel–Lindau tumor suppressor protein (pVHL) — a tumor suppressor gene that causes polyubiquitination and finally proteasomal degradation of HIF-1α. By contrast, hypoxia causes stabilization of HIF-1α, which, after dimerization with the HIF-1β subunit, translocated to the nucleus. Translocation of the dimerized complex causes activation of numerous genes, which enhances the metabolism of glucose, fatty acids, angiogenesis, metastasis and invasiveness. (b) The relation between HIF-1α and PHDs. HIF-1α and PHDs are expressed equally in normal cells. HIF-1α, being a basic helix-loop-helix protein, possesses 402 and 564 proline residues on its oxygen-dependent degradation

(pHe) and intracellular pH (pHi), downstream regulation of immune response and resistance to chemotherapy (Fig. 1a) [7]. For instance, under the influence of HIF-1α, cancer cells express more glycolytic enzymes, which peculiarly decrease the pH in the extracellular region. Therefore overexpression of fatty acid synthase (FASN) and other enzymes involved in fatty acid biosynthesis is essentially needed to meet the lipid requirement of the rapidly proliferating cells [8].

This pH-induced overexpression of FASN in rapidly dividing cancer cells can be reverted through the modulation of prolyl hydroxylase 2 (PHD2) activities. The PHD enzymes belong to the family of iron- and 2-oxoglutarate (2-OG)-dependent dioxygenases causing hydroxylation and eventually proteasomal degradation of HIF-1α. A downregulation or upregulation of PHD2 activity can modify the activity of HIF-1α downstream or upstream. Inhibition of PHD2 activity increases the HIF-1α stability and this mechanism can be beneficial in disease conditions like myocardial infarction and anemia. Some compounds like 1-(6-(2,6-dimethylphenoxy)-7-fluoro-4oxo-3,4-dihyroquinazolin-2-yl)-H-pyrazole-4-carboxylic acid (JNJ-42905343) have already been developed and tested preclinically for management of myocardial infarction and anemia [9]. By contrast, upregulation of PHD2 activity could curtail HIF-1α expression and therefore PHD2 could be exploited therapeutically to combat cancer progression. The present review summarizes the role of HIF-1α and pHe on upregulation of enzymes involved in glucose and lipid metabolism. We also attempt to summarize the role of PHD2 in the modulation of HIF-1α and to explore the possibilities of PHD2 being a target for cancer research.

HIF-1α–oxygen-sensing mechanism

Rapid growth and division is generally observed in tumor cells and those near to the blood vessel can easily take up oxygen and nutrients from there [10]. As the tumor size increases, the cells located at the periphery become deficient in oxygen and nutrients [11]. This condition is termed hypoxia. Generally, normal cells undergo apoptosis, so-called programmed cell death; however, during hypoxia, tumor cells fail to enter apoptosis. Development of tumor hypoxia is recognized as the main cause of stabilization of the cytoplasmic protein known as HIF-1α.

HIF-1α consists of a basic helix-loop-helix Per-ARNT Sim (PAS) domain that undergoes heterodimerization at two subunits present at the amino terminal. Half of each subunit forms a DNA-binding complex, which is translocated to the nucleus and enhances the expression of several genes. In normoxia, PHD2 causes hydroxylation of HIF-1α at proline residue 402 or 564 and an interface is created as a result of this modification where the von Hippel–Lindau tumor suppressor protein (pVHL) can bind to carry out polyubiquitination of HIF-1α after recruiting an E3 ubiquitin ligase and eventually target it for proteasomal degradation (Fig. 1b) [12]. It is evident from numerous studies that PHD2 plays an important part in the proteasomal degradation of HIF-1α [13]. Activation and inhibition of PHD2 can affect the stability of HIF-1α which in turn can speed up or slow down the proliferation of tumor cells through multiple pathways [14].

During hypoxic conditions, HIF-1α becomes more stable and its binding affinity with another constitutively expressed unit, HIF-1β, transiently increases, and this complex transits to the nucleus where it causes activation of several genes. HIF-1α, being a central transcription factor, modulates the expression of many genes involved in cell metabolism, angiogenesis, invasiveness and proliferation. For instance, it enhances the expression of genes encoding erythropoietin and enzymes involved in glucose metabolism, lipid metabolism and transport [15]. HIF-1α promotes metastasis of tumor cells to distant organs, transforming benign tumors to malignant tumors [16].

PHDs

PHDs are the oxygen-dependent family of enzymes causing proteasomal degradation of HIF-1α in normoxic cells. Molecular oxygen is required for the hydroxylation activity on HIF-1α which is why these enzymes are regarded as oxygen sensor cells [17]. To date, three isoforms of PHD (i.e., PHD1, PHD2 and PHD3) have been discovered that are known to have a role in oxygen sensing. The decreasing order of in vitro hydroxylation potential of all the PHDs toward HIF-1α is: PHD2 > PHD3 > PHD1. PHDs add hydroxyl (OH^-) groups at the proline residue of HIFs but differ in their substrate specificity and distribution. It was reported that PHD2 more-efficiently hydroxylates HIF-1α compared with HIF-2α and HIF-3α, whereas HIF-2α is more-efficiently hydroxylated by PHD1 and PHD3. PHD2 is specifically expressed in the adipose tissue, PHD1 is expressed in testis cells whereas PHD3 is expressed in cardiac cells [18]. PHD2 remains localized to the cytoplasmic region of the cell, PHD3 is found in the nuclear region and PHD1 can be present in cytoplasmic as well as in nuclear regions.

PHDs: a negative regulator of HIF-1α

A direct relationship between hypoxia and PHDs has been confirmed by various studies [19]. Decreased expression of PHD2 has been observed in hypoxic tumor cells in numerous studies. It is inferred that PHD2 controls degradation of HIF-1α in the presence of oxygen. Although oxygen is the prime factor involved in the hydroxylation of HIF-1α, other factors like Fe(II), ascorbate and 2-OG also play important role in HIF-1α degradation.

In normoxic conditions, oxygen is abundant in cells and enhances the hydroxylation activity of PHDs [20]. Activated PHDs build up hydroxyl groups at the Pro402 and Pro502 residues of the C terminus of HIF-1α. Hydroxylation involves the splitting of dioxygen into two oxygen atoms transferring one oxygen to a proline residue to form a hydroxyl group and another to the 2-OG to generate succinate and CO_2 [21]. Fe^{2+} at the active site of the PHDs remains loosely bound by two histidine residues and one aspartic acid forming a 2-histidine-1-carboxylase coordination motif. Ascorbate helps to maintain Fe in the ferrous (Fe^{2+}) state and is important in maintaining and achieving the full activity of the PHDs [22].

Once HIF-1α is hydroxylated at the proline residues by PHD2, it is further captured by pVHL. X-ray crystallographic studies of the pVHL–HIF-1α complex have revealed that pVHL has a surface

domains. PHDs carry out hydroxylation of HIF-1α at Pro402 and Pro564 residues. Like PHD2, factor inhibiting HIF-1α (FIH) also catalyzes hydroxylation of HIF-1α at the aspartic residue to reduce HIF-1α-mediated transcription. The hydroxylated HIF-1α undergoes proteosomal degradation. Abbreviations: HRE, hypoxia response element; 2-OG, 2-oxoglutarate; PCBP, poly (C) binding protein 1,2.

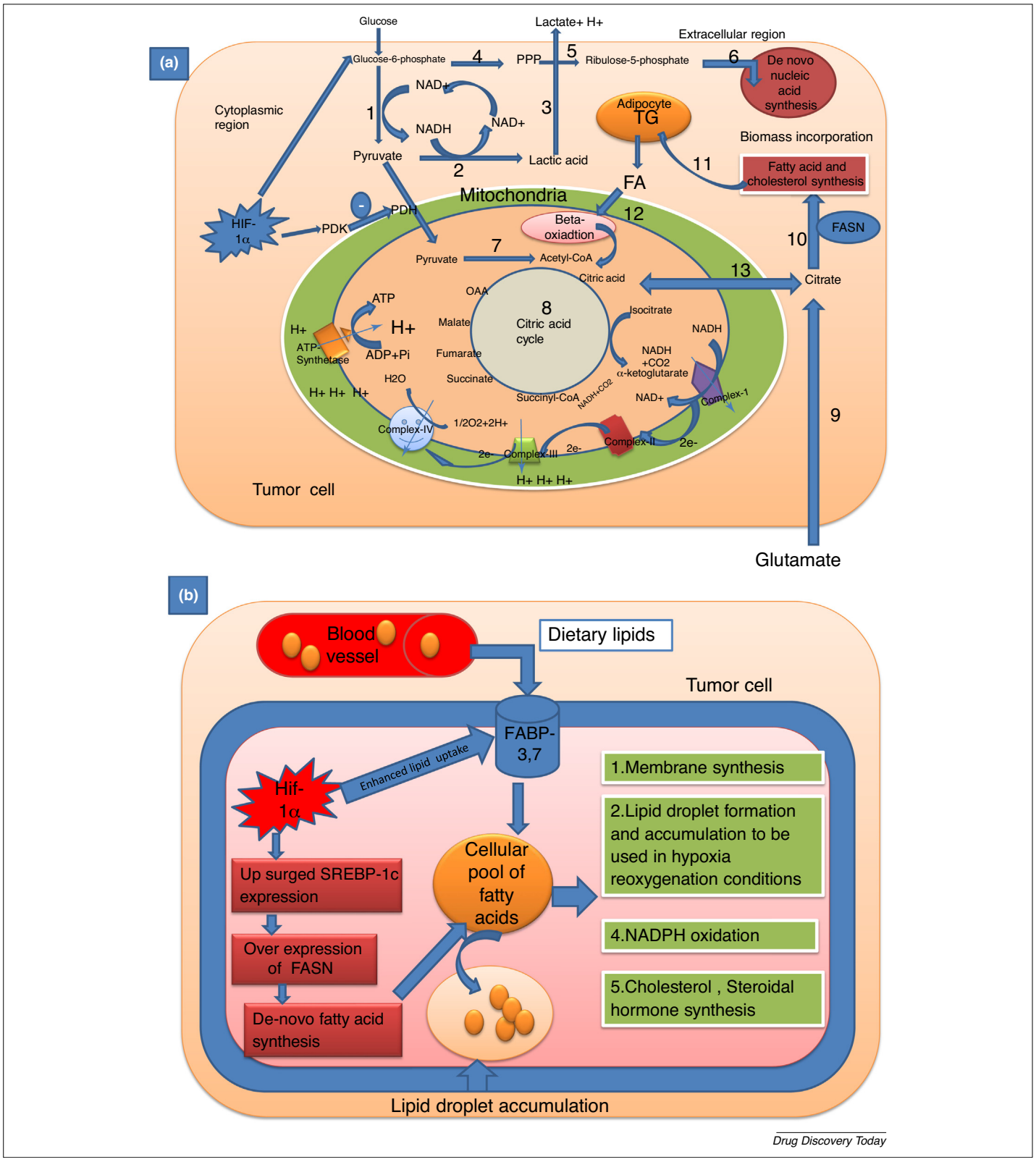

FIGURE 2

(a) Effect of HIF-1α on cellular respiration and energy production. HIF-1α enhances the uptake and utilization of glucose in tumor cells. (1) Oxidation of glucose in tumor cells mainly occurs through the glycolysis pathway and yields 2 moles of pyruvate as the end-product. (2,3) Pyruvate is converted to lactic acid which is exported outside. (4,5,6) Glucose is also metabolized through PPP to yield five carbon sugars like ribulose-5-phosphate to be used in de novo nucleic acid synthesis. (7,8) Further oxidation of pyruvate in mitochondria is inhibited by PDK. (9,10) Circulating glutamine serves as a major bioenergetic substrate and nitrogen donor for proliferating cells, providing citrate to be utilized in cholesterol and fatty acid synthesis. (13) Citrate is also provided from the TCA cycle. (11,12) Excess fatty acids are stored in adipocytes and used when energy is required through β-oxidation. (b) Effect of HIF-1α on fatty acid metabolism. HIF-1α

pocket into which the hydroxylated proline residue of HIF-1α fits accurately and the overall binding is highly specific. After this, proteins (elongin C, elongin B, cullin and Rbx1) bind with the pVHL–HIF-1α complex to form another complex named VCB-Cul2E3 ligase. Binding of HIF-1α to this complex E3 causes poly-ubiquitination of HIF-1α and ultimately targets its proteosomal degradation [23]. Like PHD2, HIF-1α is also hydroxylated by an another cytoplasmic protein known as factor inhibiting HIF-1α (FIH) at the aspartic residue of HIF-1α which further enhances degradation of HIF-1α and thereby reduces its transcriptional activation in tumor cells [24].

Effect of HIF-1α on cellular physiology

The normal cellular physiology of a tumor cell is considerably affected by HIF-1α because the enzymatic machinery of glucose and fatty acid metabolism is tightly regulated at the genetic level. Alongside expression of genes for glucose and fatty acid metabolism, HIF-1α also gives the tumor cell an invasive and metastasis character, which further increases the complications.

Effect of HIF-1α on cellular respiration and energy production

Altered metabolism is the hallmark of tumor cells. The most commonly observed metabolic alteration in tumor cells is enhanced glucose uptake and oxidation of glucose through glycolysis (termed the Warburg effect) [25]. It is well defined that oxidation of glucose in normal cells occurs first by glycolysis in the cytoplasmic region and then by the citric acid cycle in mitochondria. Glucose taken inside the cell undergoes oxidation and reduction reactions to yield 2 moles of pyruvate as an end-product [26]. Pyruvate is further translocated to the mitochondria where it is oxidized to acetyl CoA. Acetyl CoA, thus formed, enters into the citric acid cycle and energy-rich compounds in the form of GTP, NADP and $FADH_2$ are obtained [27]. Further oxidation of the above compounds through oxidative phosphorylation yields 36 ATPs that serve as fuel for various biological processes occurring in a cell (Fig. 2a). To extract such a large amount of energy from a single glucose molecule, oxygen is vital for normal cells as well as for tumor cells. Tumor and normal cells remain dependent upon glucose for all their energy requirements. The blood vessels in the nearby tissue ensure a constant supply of oxygen and other essential nutrients required for proper growth and development [28]. As the tumor mass increases beyond limits, nourishing blood vessels become inefficient and in this way tumor cells at the periphery of the tumor mass do not get oxygen and nutrients. Generally, normal cells stop dividing when oxygen is scarce but this is not true for tumor cells because they keep on dividing even in the absence of oxygen [29].

How tumor cells manage to survive in the absence of oxygen and what fuel they use has been a long-standing question for researchers. Finally, Warburg and colleagues discovered that tumor cells have a high rate of glucose uptake and perform glucose metabolism mainly through glycolysis with the formation of lactic acid [8]. The Warburg effect is crucial for rapidly dividing cells because it enables the tumor cells to generate more building blocks, which are important for cell proliferation [30].

Also, under this oxygen tension, tumor cells stabilize HIF-1α which plays a pivotal part in tumor progression as discussed in earlier sections [31]. In the context of metabolism, enzymes for glucose and fatty acid metabolism are regulated by HIF-1α [32]. HIF-1α is the main cause of the shift in the metabolism of glucose from highly efficient oxidative phosphorylation to the less efficient glycolytic pathway to maintain energy needs in the hypoxic environment. This again raises the question: why would proliferating cells (including tumor cells) choose a pathway that produces fewer ATP molecules? A possible reply to this question is that a cell requires other molecules in addition to ATP to divide. Macromolecules such as amino acids, nucleotides and fatty acids are needed for cellular replication. Consequently, a pathway that supports the synthesis of these biomolecules is preferentially selected [33]. More and more glucose is consumed to meet the energy needs and other requirements. This effect is mediated by HIF-1α, which enhances the transactivation of glucose transporters (GLUTs) and enzymes of the glycolytic pathway that increase glucose intake and utilization by tumor cells. Glucose inside tumor cells is rapidly metabolized through glycolysis to yield pyruvate as the end-product. Further oxidation of glucose in mitochondria is interrupted and lactic acid as an end-product of this pathway is exported outside the tumor microenvironment [34]. In tumor cells, conversion of pyruvate to lactic acid is an adaptive mechanism that keeps the rate of the glycolysis pathway unusually high. In normal conditions, NAD+ is recycled through oxidative phosphorylation. However, in anoxic conditions NAD+ is regenerated only when pyruvate is converted into lactic acid by lactate dehydrogenase (LDH) [35]. In these circumstances, tumor cells oxidize glucose only through the glycolytic pathway and finally through the lactic acid pathway. Lactate, thus formed, is transported outside the cell which is responsible for decreasing the pH in the tumor microenvironment [36].

Effect of HIF-1α on cellular pH

Owing to aberrant metabolism guided by HIF-1α, a tumor cell produces more lactic acid than a normal cell, disturbing the pHi and pHe in the tumor microenvironment. These changes affect the molecular processes such as the cell cycle, cell proliferation, differentiation, metastasis, cell metabolism and angiogenesis. Disturbed pHi and pHe in tumor cells accomplishes three objectives: (i) intracellular alkaline pH stimulates proliferation; (ii) extracellular acidity is a necessary feature for the activation of degrading enzymes like cathepsin, heparanase and metalloprotease — this matrix degradation is necessary for migration, invasion and eventually metastasis; (iii) extracellular acidity blocks immunogenic attacks against malignant cells and decreases tumor access for certain chemotherapeutics [37]. All in all, hypoxia and acidic pHe contribute to tumor progression in the manner of Darwinian selection of resistant cells that can survive in this harsh environment.

increases fatty acid synthesis and uptake. The FABPs are overexpressed and translocated to the cell membrane where they enhance the uptake of dietary fatty acids. SREBP-1c causes overexpression of FASN which further enhances lipid biosynthesis. Excess lipids are accumulated as lipid droplets. Abbreviations: FABP 3–7, fatty acid binding proteins 3–7; FASN, fatty acid synthase; HIF-1α, hypoxia-inducible factor-1α; PDH, pyruvate dehydrogenase; PDK, pyruvate dehydrogenase kinase; PPP, pentose phosphate pathway; SREBP-1c, sterol regulatory element binding protein 1c; TCA, tricarboxylic acid cycle.

An increase in pHe together with a decrease in pHi is accompanied by production and venting of metabolic acid resulting from aerobic glycolysis, fatty acid oxidation and oxidative phosphorylation [38]. The resulting amendment in the aforesaid metabolic pathway is essential to attain a glycolytic phenotype [39]. Tumor cells have two main objectives behind the adoption of the glycolytic pathway as the main source of energy despite the low energy efficacy of this pathway. First, this decreases reactive oxygen species (ROS) production which is much higher under oxidative phosphorylation; second, it is essential for the production of the biological building blocks that are used in other anabolic processes occurring elsewhere in tumor cells. Despite several beneficial effects of the glycolytic phenotype, it has some disadvantages too. The main disadvantage of the glycolytic phenotype is the production of excess protons responsible for decreasing pHi. Lactic acid produced as a result of enhanced glycolysis, ATPs generated through oxidative phosphorylation and carbonic acid produced as a result of hydration of carbon dioxide are the responsible factors for reduction of pHi. Tumor cells also develop special regulatory proteins like vacuolar H+-ATPases (V-ATPases), Na+/H+ exchanger (NHE), bicarbonate transporter, monocarboxylate transporters (MCTs) and carbonic anhydrase on their membrane to get rid of this excessive intracellular acidity [37,40]. These pH-regulatory proteins tightly control the disturbed pH homeostasis in tumor cells.

V-ATPases are ATP-driven proton pumps that function in a wide array of normal physiological process coupled with energy released from ATP hydrolysis to transport protons out of the cytosol [41]. V-ATPase is highly expressed in tumor cell membranes to promote invasions and migration, which is essential for activation of extracellular proteases like cathepsins that facilitate invasion. The activity of cathepsins depends on pH. Lower pHe facilitates activation and lower pHi facilitates inactivation of cathepsins [42]. So, V-ATPases enhance extracellular acidity by extruding metabolically generated protons on glucose metabolism.

Although tumor cells have developed numerous cellular mechanisms to get rid of excessive pHi, activated NHE1 plays pivotal part in cumulation of extracellular acidity and presents a direct benefit to the tumor cells by regulating their motility and invasion via activation of epidermal growth factor receptor (EGFR). NHE1, being an integral membrane protein, regulates the pHi by interchanging the cytosolic proton (H+) with an extracellular sodium ion (Na+) [43]. The role and overactivation of NHE1 in tumor cells have been documented in various studies [44].

Lactate is transported through MCTs. MCTs are generally found in the plasma membrane of erythrocytes, neutrophils and tumor cells. To date, MCT isoforms 1–4 have been isolated and identified. Generally, most of the tissue cells express MCT-1 on their surface but at very low levels. The occurrence of MCT-2 and MCT-3 is limited only to certain tissues: liver, kidney and neurons express MCT-2, whereas retinal pigmented epithelium and the choroid plexus express MCT-3 transporter. MCT-4 is mainly expressed by testicular, lung and placental tissue [45]. HIF-1α also enhances the expression of MCTs on the plasma membrane of tumor cells to pump out protons generated from lactic acid hydrolysis (Fig. 3) [46]. Tumor cells maintain pHi at normal or slightly alkaline levels, whereas pHe in the tumor microenvironment becomes slightly acidic and hence a pH gradient is quickly established [47].

Effect of HIF-1α on fatty acid metabolism

Lipids, like cholesterols, isoprenoids, acylglycerols and phospholipids, constitute a major part of the biological membranes of every cell. They are used for energy metabolism and storage, and have an important role in cell signaling [48]. For instance, lipids like diacylglycerol (DAG) and phosphatidylinositol-3,4,5-triphosphate (PIP_3) are two important cell-signaling molecules that are formed in response to extracellular stimuli [49]. Similarly, stored lipids in the liver and adipocytes are broken down by β-oxidation to release energy when needed. In fact, lipids are the most essential nutrients for normal and tumor cells, because they are being constantly used for generating the membrane constituents necessary for proliferating cells and also for biophysical and signaling pathways that drive diverse aspects of tumorigenesis [50]. Earlier, it was presumed that only altered metabolism of glucose was the characteristic feature of tumor cells. Recent work has however delineated that aberrant lipid metabolism is another metabolic perturbation [51].

Previously, it was published that fatty acids are required in a much larger amount in rapidly proliferating cells [52], and tumor cells must adopt an alternative pathway to uptake and synthesize fatty acids for their membrane synthesis and energy needs. Hypoxia plays a crucial part in adopting this alternative pathway. A study on breast cancer cells reported that genes induced by hypoxia are involved in lipid synthesis, storage and uptake (Fig. 2b). In hypoxic tumor cells, HIF-1α enhances the expression and translocation of fatty-acid-binding proteins (i.e., FABP-3 and FABP-7), which significantly increases the accumulation of lipid droplets (LD). The study also suggested that, during hypoxia reoxygenation, β-oxidation of fatty acid or glycogen degradation can increase ROS toxicity which in turn strongly impairs tumorigenesis [53]. Another study conducted by Roy and colleagues confirmed a relationship between HIF-1α and FASN. In fact, exogenous lipid supplementation curtailed the HIF-1α-induced fatty acid synthesis in experimental animals [54]. Further, a direct relationship between FASN gene and hypoxia was established by Menedez and colleagues. They observed that endogenous fatty acid synthesis was blocked by inhibition of FASN and silencing of FASN resulted in overexpression of vascular endothelial growth factor (VEGF) in response to activation of HIF-1α [55].

Although hypoxia and HIF-1α regulate glycolysis, glutaminolysis and lipid synthesis in tumor cells, suppression of β-oxidation of long-chain polyunsaturated fatty acids (PUFAs) has been reported as well — PUFAs are crucial for cell membrane synthesis [56]. Hypoxia enhances the expression of long-chain acyl-CoA dehydrogenase (LCAD) and medium-chain acyl-CoA dehydrogenase (MCAD), which inhibit the first step of β-oxidation in mitochondria. This results in accumulation of PUFAs and a decrease in expression of tumor suppressor phosphatase and tensin homolog gene (PTEN) which promotes cell proliferation [57]. Another study confirmed that expression of sterol regulatory element binding protein 1c (SREBP-1c), a major transcriptional regulator of FASN, is significantly upregulated in response to hypoxia. To examine the effect hypoxia has on the expression of FASN, the breast tumor cell lines MX1, MCF-7 and MDA-MB157 were cultured in hypoxic and normoxic conditions. SREBP is a membrane-bound basic helix-loop-helix leucine zipper (bHLHZ) transcription factor that plays a crucial part in fatty acid metabolism by controlling the synthesis of fatty acids, triglycerides and cholesterol [58]. Since its discovery,

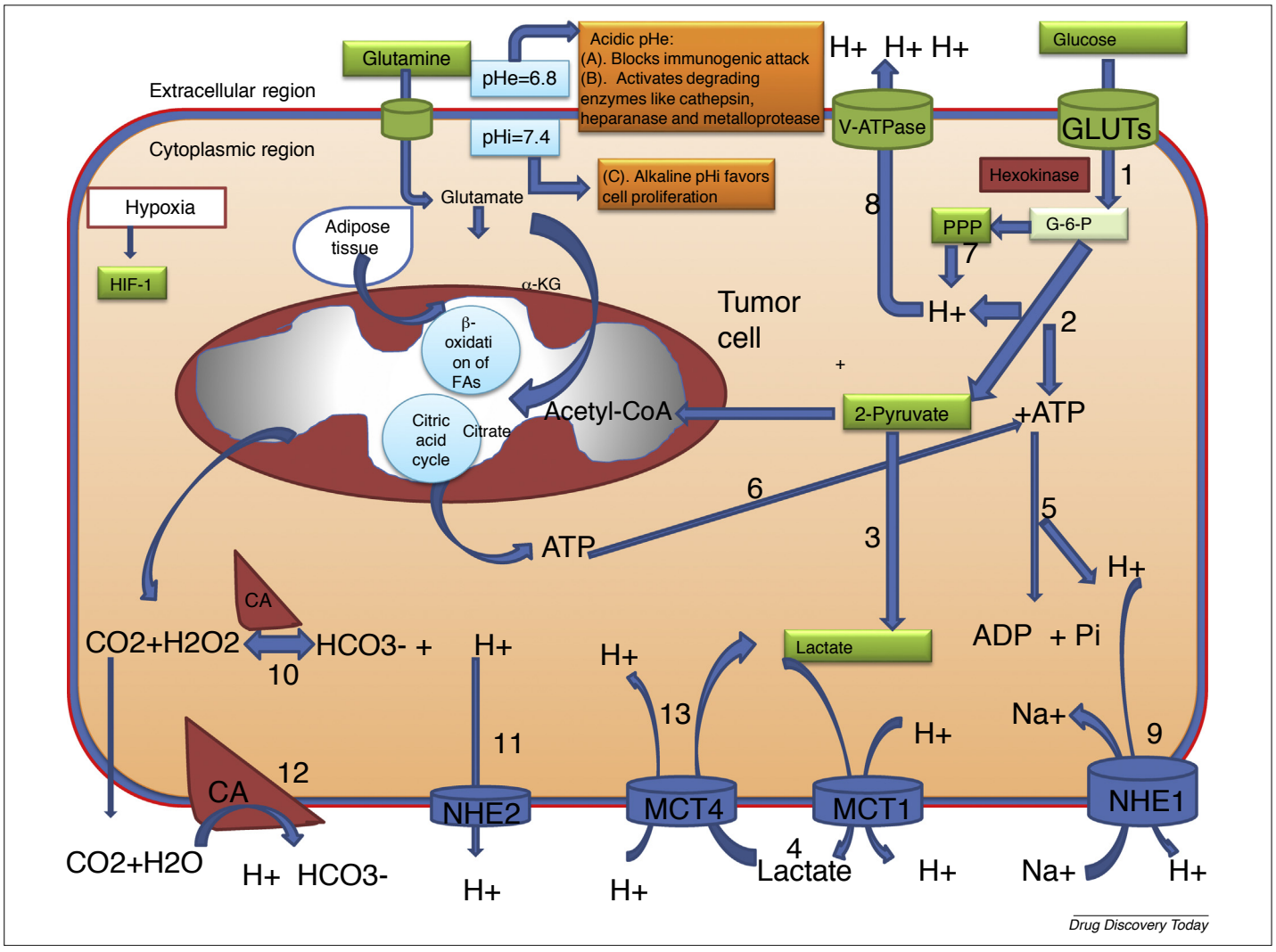

FIGURE 3

HIF-1α role in regulation of pHi and pHe in tumor cells. HIF-1α enhances the expression of various proton transporters to regulate the pHi and pHe in tumor cells. Protons generated from glycolysis and PPP are extruded by V-ATPase (1,2,7,8). NHE1 transport protons are generated from hydrolysis of ATP (2,5,6 and 9). Lactic acid accumulated as a consequence of inhibition of the TCA cycle is first hydrolyzed to lactate and H+ ions which are transported outside through MCT1 (2,3,4). Acidity raised by carbonic acid formed by the activity of C.A is reduced by extruding protons through NHE2 (10,11). Owing to its high partition coefficient, CO_2 is passively diffused out through the plasma membrane and extracellularly again converted to carbonic acid (12). Lactate from the extracellular side is also pumped back into tumor cells through MCT4. Owing to continuous production and venting of protons through these transporters the tumor microenvironment becomes acidic (pHe = 6.8). Reduced pHe and increased pHi in tumor cells is essential to fulfill the objectives A, B and C. Abbreviations: HIF-1α, hypoxia-inducible factor-1α; V-ATPase, vacuolar-ATPase; NHE1–2, sodium hydrogen exchanger 1–2; C.A, carbonic anhydrase; MCT1–4, monocarboxylate transporters 1–4; PPP, pentose phosphate pathway.

three isoforms of mammalian SREBPs (SREBP-1a, SREBP-1c and SREBP-2) have been identified and characterized with distinct but overlapping transcriptional roles in lipogenic programs. SREBP-1a activates fatty acid and cholesterol synthesis, SREBP-1c regulates fatty acid synthesis and SREBP-2 guides cholesterol synthesis and uptake. Previous studies have established the role of SREBPs in lipid homeostasis and regulation of cholesterol and its oxysterol derivatives. These findings altogether suggest that hypoxia itself and hypoxia-induced pH in the tumor microenvironment play pivotal parts in fatty acid synthesis and uptake in tumor cells.

The interplay between HIF-1α, pH, SREBP-1c and FASN

HIF-1α-induced aberrant metabolism of glucose in tumor cells results in formation of lactic acid, which, when transported to the tumor microenvironment, causes reduction in pHe. Protons generated from hydrolysis of ATPs, formation of carbonic acid and the pentose phosphate pathway (PPP) further augment the pHe in the tumor microenvironment. As a result of continuous production and venting of protons in hypoxic tumor cells, pHe in the tumor microenvironment becomes acidic (pHe 6.8), whereas pHi becomes alkaline (pHi 7.8). Reduced pHe rewards the tumor cells in several ways [59]. It has been proved by Kondo *et al.* that a difference in pHe and pHi in tumor cells causes destabilization of an endoplasmic protein SREBP-1c, which further enhances the overexpression of enzymes involved in fatty acid biosynthesis and cholesterol biosynthesis after binding with a sterile responding element (SRE) (Fig. 4a) [60]. Recently, Weiszenstein *et al.* reported mild hypoxia, but not a severe increase in adipogenesis, lipogenesis and lipolysis, in 3T3-L1 cells

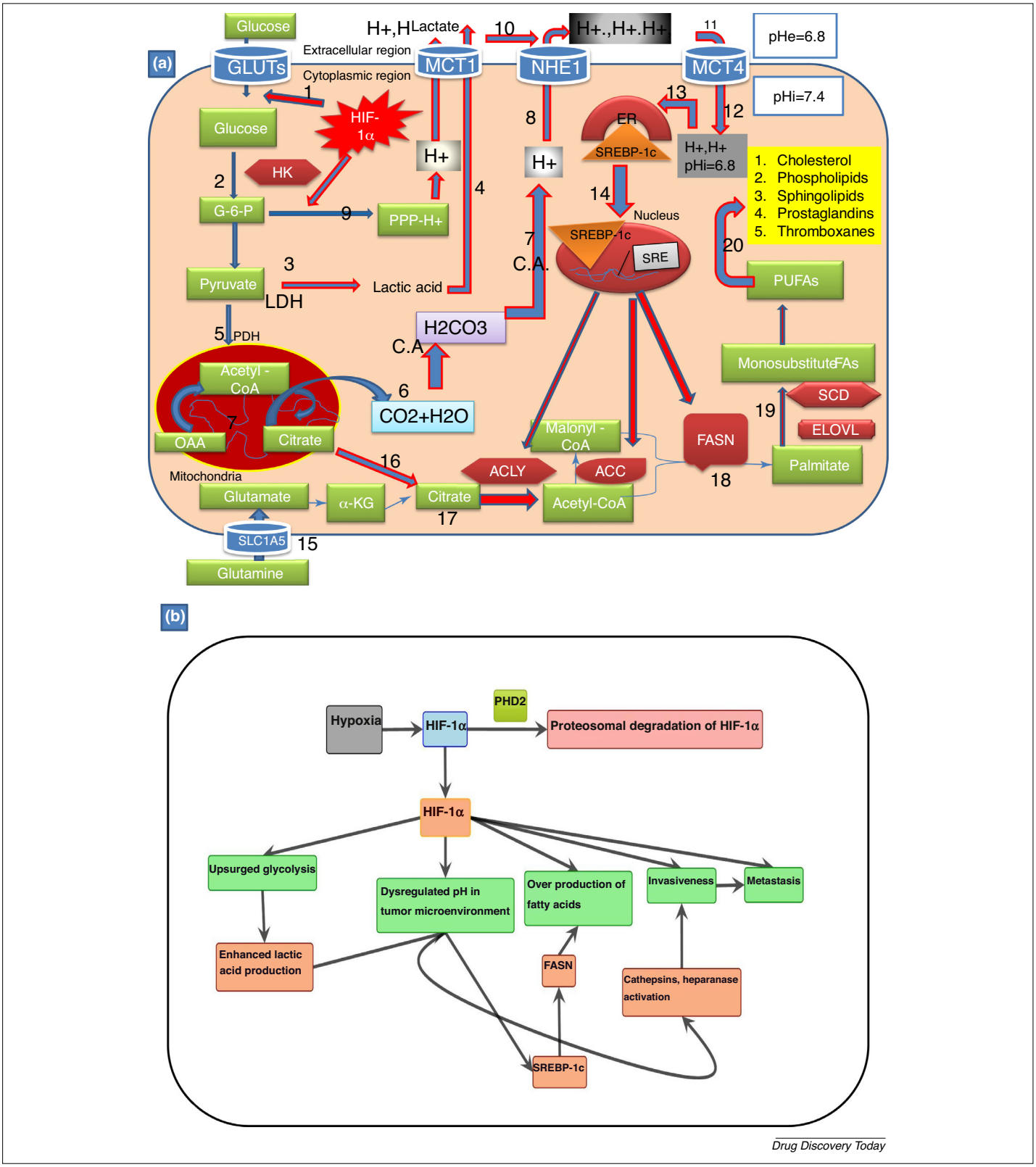

FIGURE 4

(a) The interplay between HIF-1α, pH, SREBP-1c and FASN. HIF-1α is a master regulator of interplay between pH, SREBP-1c and FASN. Glucose metabolism through the glycolytic pathway results in accumulation of lactic acid which is pumped out through the MCT1 (1,2,3,4). Carbonic acid produced through metabolic conversion of CO_2 and H_2O by C.A is transported out through NHE1 (6,7,8). Protons are also generated through glycolysis and PPP and are forced out (9). pHe in the tumor microenvironment becomes acidic and, thus, a proton gradient develops across the plasma membrane (10). Owing to the proton gradient protons from the extracellular region move back through the MCT4 transporter and pHi again becomes acidic (11,12). Acidic pHi activates SREBP-1c located in the ER which is translocated in the nucleus where it causes activation of genes of enzymes involved in fatty acid synthesis like FASN, ACC and ACALY (13,14). Deamination of circulating glutamine to glutamate provides citrate which is used in fatty acid synthesis (15,16). Citrate is also provided from the TCA cycle to be

[61]. Various studies reported the overexpression of SREBP-1c and FASN in response to mild hypoxia. From the above discussion, it can be stated that there is a strong interplay between HIF-1α, pH, SREBP-1c and FASN.

Hypothesis

From this review, it can be hypothesized that activation of PHD2 can regulate the interplay between HIF-1α, pH, SREBP-1c and FASN. Hypoxia-activated HIF-1α is the central regulatory pathway that works in a very smart way and alters the metabolism of glucose. HIF-1α limits the metabolism of glucose through glycolysis and, consequently, pHe is reduced. A pH gradient is developed across the plasma membrane of tumor cells that activates the endoplasmic protein SREBP-1c. Activated SREBP-1c translocates to the nucleus and leads to overexpression of FASN and other enzymes involved in lipid metabolism. HIF-1α is the master regulator of glycolysis, pH, SREBP-1c and FASN. Most of the solid tumors transform into malignant tumors owing to the aforementioned effects of HIF-1α and then therapy becomes even more difficult. It is well understood that PHD2 is a negative regulator of HIF-1α (Fig. 4b), which causes its hydroxylation, followed by polyubiquitination and eventually its proteasomal degradation. So, chemical activation of PHD2 can downregulate all effects of HIF-1α and stops the propagation of cancer to the other organs. Exogenous activation of PHD2 could be a novel strategy to control the tumor microenvironment.

Concluding remarks

Tumor cells rely on fatty acids as cellular building blocks for membrane formation, energy storage and the production of signaling molecules. Therefore, a constant supply of fatty acids is necessary for the tumor cells and hypoxia plays a pivotal part in this adaptation. Hypoxia-induced HIF-1α causes an increase in extracellular acidity in the tumor cell microenvironment through various metabolic processes. The intracellular acidic environment in hypoxic tumor cells activates an endoplasmic protein SREBP-1c, which regulates the expression of enzymes for fatty acid biosynthesis. We conclude that HIF-1α regulates fatty acid biosynthesis in tumor cells indirectly by regulating the interplay between pH, SREBP-1c and FASN. This interplay can be exploited therapeutically in various ways to block the growth of tumor cells. Being a master regulator of interplay between the aforementioned factors, stability of the whole process considerably depends upon the stability of HIF-1α. So, inhibition of HIF-1α itself seems to be one of the best targets in the fight against cancer. However, cellular proliferation is difficult to stop after the activation of HIF-1α; therefore, therapeutic inhibition of HIF-1α at this stage becomes worthless and is thus gaining less importance these days.

Today's fascinating target is PHD2. In the presence of oxygen, PHD2 causes proteolytic degradation of HIF-1α. Therefore, it can be exploited therapeutically to stop cellular proliferation. Chemically induced activation of PHD2 alone can switch off all the effects of HIF-1α. Here, it would be pertinent to mention that activation of PHD2 can prevent transformation of a benign tumor to a malignant tumor because PHD2 acts in an early step of tumor development. Therefore, PHD2-targeted therapy would be a boon for the patients with newly diagnosed tumors. At the same time, better management would be possible in patients with malignant tumors because PHD2-induced degradation of HIF-1α would not be available to cause metastasis, invasiveness and angiogenesis. If anyone wants to target metabolic pathways like glycolysis and fatty acid biosynthesis to control cellular proliferation, the best way is to activate PHD2. So, inhibition of fatty acid biosynthesis to combat tumors of the mammary gland via downregulation of HIF-1α through the activation of PHD2 looks to be a promising intervention.

Conflicts of interest

The authors have no conflicts of interest to declare.

References

1 Al-Dujaili, Z. *et al.* (2017) Skin cancer concerns particular to women. *Int. J. Women Dermatol.* 3, S49–S51
2 Becker, A. *et al.* (2016) Extracellular vesicles in cancer: cell-to-cell mediators of metastasis. *Cancer Cell* 30, 836–848
3 Torre, L.A. *et al.* (2015) Global cancer statistics, 2012. *CA: Cancer J. Clin.* 65, 87–108
4 Muz, B. *et al.* (2015) The role of hypoxia in cancer progression, angiogenesis, metastasis, and resistance to therapy. *Hypoxia* 3, 83
5 Fan, L. *et al.* (2014) The hypoxia-inducible factor pathway, prolyl hydroxylase domain protein inhibitors, and their roles in bone repair and regeneration. *BioMed Res. Int.* 2014, 239356
6 Sadri, N. and Zhang, P.J. (2013) Hypoxia-inducible factors: mediators of cancer progression; prognostic and therapeutic targets in soft tissue sarcomas. *Cancers* 5, 320–333
7 Tanimoto, K. (2017) Genetics of the hypoxia-inducible factors in human cancers. *Exp. Cell Res.* 356, 166–172
8 Park, J.S. *et al.* (2015) Hypoxia-induced IL-32β increases glycolysis in breast cancer cells. *Cancer Lett.* 356, 800–808
9 Barrett, T.D. *et al.* (2015) Prolyl hydroxylase inhibition corrects functional iron deficiency and inflammation-induced anaemia in rats. *Br. J. Pharmacol.* 172, 4078–4088
10 Lowry, M.C. and O'Driscoll, L. (2018) Can hi-jacking hypoxia inhibit extracellular vesicles in cancer? *Drug Discov. Today* 22 S1359-6446(17)30325-2
11 Armitage, E.G. *et al.* (2014) Cancer hypoxia and the tumour microenvironment as effectors of cancer metabolism, In *Correlation-based Network Analysis of Cancer Metabolism*, VI, Chapter 2, ISBN:978-1-4939-0614-7, Springer Briefs in Systems Biology. pp. 7–13

used in fatty acid synthesis (17). Finally, citrate is converted to palmitate which is further utilized to form long-chain PUFAs like cholesterol, sphingolipid and thromboxane (18,19,20). (b) Hypothesis: PHD2 regulates the interplay between HIF-1α, pH, SREBP-1c and FASN. Hypoxia-activated HIF-1α enhances the expression of GLUT-1 and GLUT-4 receptors to enhance glycolysis. Glucose is finally oxidized to the pyruvate lactate pathway and thus reduces pHe in the tumor microenvironment. Reduced pHe activates SREBP-1c protein which in turn enhances the expression of FASN and thus fatty acid synthesis. The acidic tumor microenvironment also activates enzymes like cathepsins. Heparanase enhances invasiveness. Lower pHe also enhances the process of angiogenesis and metastasis in tumor cells. PHD2 is a negative regular of HIF-1α and can downregulate a series of its effects. Abbreviations: FASN, fatty acid synthesis; SREBP-1c, sterol regulatory element binding protein 1c; ACC, acetyl-CoA carboxylase; ACLY, ATP citrate lyase; SCD, stearoyl-CoA desaturase-1; ELOVL-1, elongation of very long chain fatty acids-1; PUFA, polyunsaturated fatty acids; C.A, carbonic anhydrase; pHe, extracellular pH; pHi, intracellular pH; GLUTs, glucose transporters; NHE1, Na^+H^+ exchanger-1; PPP, pentose phosphate pathway; HIF-1α, hypoxia-inducible factor-1α.

12 Nagy, M. (2011) HIF-1 is the commander of gateways to cancer. *J. Cancer Sci. Ther.* 3, 35–40
13 Niecknig, H. *et al.* (2012) Role of reactive oxygen species in the regulation of HIF-1 by prolyl hydroxylase 2 under mild hypoxia. *Free Radic. Res.* 46, 705–717
14 Kant, R. *et al.* (2013) Prolyl 4 hydroxylase: a critical target in the pathophysiology of diseases. *Korean J. Physiol. Pharmacol.* 17, 111–120
15 Dumas, J.-F. *et al.* (2017) Metabolic reprogramming in cancer cells, consequences on pH and tumour progression: integrated therapeutic perspectives with dietary lipids as adjuvant to anticancer treatment. *Semin. Cancer Biol.* 43, 90–110
16 Kollmann, K. *et al.* (2013) A kinase-independent function of CDK6 links the cell cycle to tumor angiogenesis. *Cancer Cell* 24, 167–181
17 Thompson, C.B. (2016) Into thin air: how we sense and respond to hypoxia. *Cell* 167, 9–11
18 Wong, B.W. *et al.* (2013) Emerging novel functions of the oxygen-sensing prolyl hydroxylase domain enzymes. *Trends Biochem. Sci.* 38, 3–11
19 Na, Y.-R. *et al.* (2016) Pyrithione Zn selectively inhibits hypoxia-inducible factor prolyl hydroxylase PHD3. *Biochem. Biophys. Res. Commun.* 472, 313–318
20 Nguyen, L.K. *et al.* (2015) A dynamic model of the hypoxia-inducible factor 1a (HIF-1a) network. *J. Cell Sci.* 128, 422
21 Meneses, A.M. and Wielockx, B. (2016) PHD2: from hypoxia regulation to disease progression. *Hypoxia* 4, 53
22 Nandal, A. *et al.* (2011) Activation of the HIF prolyl hydroxylase by the iron chaperones PCBP1 and PCBP2. *Cell Metab.* 14, 647–657
23 Badawi, Y. and Shi, H. (2017) Relative contribution of prolyl hydroxylase-dependent and-independent degradation of HIF-1alpha by proteasomal pathways in cerebral ischemia. *Front. Neurosci.* 11, 239
24 Tarhonskaya, H. *et al.* (2015) Kinetic investigations of the role of factor inhibiting hypoxia-inducible factor (FIH) as an oxygen sensor. *J. Biol. Chem.* 290, 19726–19742
25 Tekade, R.K. and Sun, X. (2017) The Warburg effect and glucose-derived cancer theranostics. *Drug Discov. Today* 22, 1637–1653
26 Forgan, L.G. (2009) Influence of oxygen supply on metabolism and energetics in fish muscles. Available at: https://ir.canterbury.ac.nz/bitstream/handle/10092/4295/Thesis_fulltext.pdf;sequence=2
27 Lyssiotis, C.A. and Kimmelman, A.C. (2017) Metabolic interactions in the tumor microenvironment. *Trends Cell Biol.* 27, 863–875
28 Vaupel, P. *et al.* (1989) Blood flow, oxygen and nutrient supply, and metabolic microenvironment of human tumors: a review. *Cancer Res.* 49, 6449–6465
29 Jose, C. *et al.* (2011) Choosing between glycolysis and oxidative phosphorylation: a tumor's dilemma? *Biochim. Biophys. Acta Bioenerg.* 1807, 552–561
30 Gottfried, E. *et al.* (2012) Tumor metabolism as modulator of immune response and tumor progression. *Semin. Cancer Biol.* 22, 335–341
31 Zeng, W. *et al.* (2015) Hypoxia and hypoxia inducible factors in tumor metabolism. *Cancer Lett.* 356, 263–267
32 Quaegebeur, A. *et al.* (2016) Deletion or inhibition of the oxygen sensor PHD1 protects against ischemic stroke via reprogramming of neuronal metabolism. *Cell Metab.* 23, 280–291
33 Masson, N. and Ratcliffe, P.J. (2014) Hypoxia signaling pathways in cancer metabolism: the importance of co-selecting interconnected physiological pathways. *Cancer Metab.* 2, 3
34 Solaini, G. *et al.* (2010) Hypoxia and mitochondrial oxidative metabolism. *Biochim. Biophys. Acta Bioenerg.* 1797, 1171–1177
35 Palazon, A. *et al.* (2017) An HIF-1α/VEGF-A axis in cytotoxic T cells regulates tumor progression. *Cancer Cell* 32 669–683.e665
36 Justus, C.R. *et al.* (2015) Molecular connections between cancer cell metabolism and the tumor microenvironment. *Int. J. Mol. Sci.* 16, 11055–11086
37 Xu, J. *et al.* (2016) Na^+/H^+ exchanger 1, Na^+/Ca^{2+} exchanger 1 and calmodulin complex regulates interleukin 6-mediated cellular behavior of human hepatocellular carcinoma. *Carcinogenesis* 37, 290–300
38 Eales, K. *et al.* (2016) Hypoxia and metabolic adaptation of cancer cells. *Oncogenesis* 5, e190
39 DeBerardinis, R.J. and Chandel, N.S. (2016) Fundamentals of cancer metabolism. *Sci. Adv.* 2, e1600200
40 Yang, K. *et al.* (2015) Intracellular pH-triggered, targeted drug delivery to cancer cells by multifunctional envelope-type mesoporous silica nanocontainers. *ACS Appl. Mater. Interface* 7, 17399–17407
41 Stransky, L. *et al.* (2016) The function of V-ATPases in cancer. *Physiol. Rev.* 96, 1071–1091
42 Cotter, K. *et al.* (2015) Activity of plasma membrane V-ATPases is critical for the invasion of MDA-MB231 breast cancer cells. *J. Biol. Chem.* 290, 3680–3692
43 Spugnini, E.P. *et al.* (2015) Proton channels and exchangers in cancer. *Biochim. Biophys. Acta Biomembr.* 1848, 2715–2726
44 Cardone, R.A. *et al.* (2015) A novel NHE1-centered signaling cassette drives epidermal growth factor receptor-dependent pancreatic tumor metastasis and is a target for combination therapy. *Neoplasia* 17, 155–166
45 Romero-Garcia, S. *et al.* (2016) Lactate contribution to the tumor microenvironment: mechanisms, effects on immune cells and therapeutic relevance. *Front. Immunol.* 7, 52
46 Draoui, N. and Feron, O. (2011) Lactate shuttles at a glance: from physiological paradigms to anti-cancer treatments. *Dis. Models Mech.* 4, 727–732
47 Abaza, M. and Luqmani, Y.A. (2013) The influence of pH and hypoxia on tumor metastasis. *Exp. Rev. Anticancer Ther.* 13, 1229–1242
48 Flaveny, C.A. *et al.* (2015) Broad anti-tumor activity of a small molecule that selectively targets the Warburg effect and lipogenesis. *Cancer Cell* 28, 42–56
49 Zechner, R. (2015) FAT FLUX: enzymes, regulators, and pathophysiology of intracellular lipolysis. *EMBO Mol. Med.* 7, 359–362
50 Nomura, D.K. and Cravatt, B.F., eds (2013) *Lipid Metabolism in Cancer*, Elsevier
51 Harjes, U. *et al.* (2016) Targeting fatty acid metabolism in cancer and endothelial cells. *Crit. Rev. Oncol. Hematol.* 97, 15–21
52 Luo, X. *et al.* (2017) Emerging roles of lipid metabolism in cancer metastasis. *Mol. Cancer* 16, 76
53 Bensaad, K. *et al.* (2014) Fatty acid uptake and lipid storage induced by HIF-1α contribute to cell growth and survival after hypoxia-reoxygenation. *Cell Rep.* 9, 349–365
54 Roy, S. *et al.* (2017) Alpha-linolenic acid stabilizes HIF-1α and downregulates FASN to promote mitochondrial apoptosis for mammary gland chemoprevention. *Oncotarget* 8, 70049
55 Menendez, J.A. and Lupu, R. (2017) Fatty acid synthase regulates estrogen receptor-α signaling in breast cancer cells. *Oncogenesis* 6, e299
56 Lau, B.Y. *et al.* (2013) Investigating the role of polyunsaturated fatty acids in bone development using animal models. *Molecules* 18, 14203–14227
57 Huang, D. *et al.* (2014) HIF-1-mediated suppression of acyl-CoA dehydrogenases and fatty acid oxidation is critical for cancer progression. *Cell Rep.* 8, 1930–1942
58 Kuzu, O.F. *et al.* (2016) The role of cholesterol in cancer. *Cancer Res.* 76, 2063–2070
59 Sau, S. *et al.* (2018) A tumor multicomponent targeting chemoimmune drug delivery system for reprograming the tumor microenvironment and personalized cancer therapy. *Drug Discov. Today*. http://dx.doi.org/10.1016/j.drudis.2018.03.003
60 Kondo, A. *et al.* (2017) Extracellular acidic pH activates the sterol regulatory element-binding protein 2 to promote tumor progression. *Cell Rep.* 18, 2228–2242
61 Weiszenstein, M. *et al.* (2016) Adipogenesis, lipogenesis and lipolysis is stimulated by mild but not severe hypoxia in 3T3-L1 cells. *Biochem. Biophys. Res. Commun.* 478, 727–732

www.impactjournals.com/oncotarget/ Oncotarget, 2017, Vol. 8, (No. 41), pp: 70049-70071

Research Paper

Alpha-linolenic acid stabilizes HIF-1 α and downregulates FASN to promote mitochondrial apoptosis for mammary gland chemoprevention

Subhadeep Roy[1], Atul Kumar Rawat[2], Shreesh Raj Sammi[3], Uma Devi[4], Manjari Singh[1], Swetlana Gautam[1], Rajnish Kumar Yadav[1], Jitendra Kumar Rawat[1], Lakhveer Singh[1], Mohd. Nazam Ansari[5], Abdulaziz S. Saeedan[5], Rakesh Pandey[3], Dinesh Kumar[2] and Gaurav Kaithwas[1]

[1]Department of Pharmaceutical Sciences, Babasaheb Bhimrao Ambedkar University, Lucknow (UP), India

[2]Central for Biomedical Research, Sanjay Gandhi Post Graduate Institute of Medical Sciences Campus, Lucknow (UP), India

[3]Department of Microbial Technology and Nematology, CSIR-Central Institute of Medicinal and Aromatic Plants, Lucknow (UP), India

[4]Department of Pharmaceutical Sciences, Faculty of Health and Medical Sciences, Sam Higginbottom Institute of Agricultural Sciences and Technology, Allahabad (UP), India

[5]Department of Pharmacology, College of Pharmacy, Prince Sattam Bin Abdulaziz University, Al-Kharj, KSA

Correspondence to: *Gaurav Kaithwas,* ***email:*** *gauravpharm@hotmail.com*

Keywords: *alpha linolenic acid, apoptosis, polyunsaturated fatty acid, hypoxia, fatty acid synthase*

Received: *February 06, 2017* ***Accepted:*** *June 12, 2017* ***Published:*** *July 25, 2017*

ABSTRACT

Alpha linolenic acid is an essential polyunsaturated fatty acid and is reported to have the anti-cancer potential with no defined hypothesis or mechanism/s. Henceforth present study was in-quested to validate the effect of alpha linolenic acid on mitochondrial apoptosis, hypoxic microenvironment and de novo fatty acid synthesis using *in-vitro* and *in-vivo* studies. The IC_{50} value of alpha linolenic acid was recorded to be 17.55μM against ER+MCF-7 cells. Treatment with alpha linolenic acid was evident for the presence of early and late apoptotic signals along with mitochondrial depolarization, when studied through acridine orange/ethidium bromide and JC-1 staining. Alpha linolenic acid arrested the cell cycle in G2/M phase. Subsequently, the *in-vivo* efficacy was examined against 7, 12-dimethylbenz anthracene induced carcinogenesis. Treatment with alpha linolenic acid demarcated significant effect upon the cellular proliferation as evidenced through decreased in alveolar bud count, restoration of the histopathological architecture and loss of tumor micro vessels. Alpha linolenic acid restored the metabolic changes to normal when scrutinized through ^{1}H NMR studies. The immunoblotting and qRT-PCR studies revealed participation of mitochondrial mediated death apoptosis pathway and curtailment of hypoxic microenvironment after treatment with alpha linolenic acid. With all above, it was concluded that alpha linolenic acid mediates mitochondrial apoptosis, curtails hypoxic microenvironment along with inhibition of de novo fatty acid synthesis to impart anticancer effects.

INTRODUCTION

α-Linolenic acid (ALA) (18: 3, ω-3) is an essential polyunsaturated fatty acid (PUFA). ALA (18: 3, ω-3) cannot be synthesized by the human body and needs to be obtained from dietary sources [1]. ALA is the major plant-based PUFA and is found in walnuts, flaxseeds, hemp seeds and their oils. ALA is also found in rapeseed (canola) oil; and

frontiers in Pharmacology

ORIGINAL RESEARCH
published: 06 April 2018
doi: 10.3389/fphar.2018.00314

DuCLOX-2/5 Inhibition Attenuates Inflammatory Response and Induces Mitochondrial Apoptosis for Mammary Gland Chemoprevention

*Swetlana Gautam[1], Atul K. Rawat[2], Shreesh R. Sammi[3], Subhadeep Roy[1], Manjari Singh[1], Uma Devi[4], Rajnish K. Yadav[1], Lakhveer Singh[1], Jitendra K. Rawat[1], Mohd N. Ansari[5], Abdulaziz S. Saeedan[5], Dinesh Kumar[3], Rakesh Pandey[3] and Gaurav Kaithwas[1]**

[1] Department of Pharmaceutical Sciences, School of Biosciences and Biotechnology, Babasaheb Bhimrao Ambedkar University (A Central University), Lucknow, India, [2] Center for Biomedical Research, Sanjay Gandhi Post Graduate Institute of Medical Sciences Campus, Lucknow, India, [3] Department of Microbial Technology and Nematology, CSIR-Central Institute of Medicinal and Aromatic Plants, Lucknow, India, [4] Department of Pharmaceutical Sciences, Faculty of Health and Medical Sciences, Sam Higginbottom Institute of Agricultural Sciences and Technology, Allahabad, India, [5] Department of Pharmacology, College of Pharmacy, Prince Sattam Bin Abdulaziz University, Al-Kharj, Saudi Arabia

OPEN ACCESS

Edited by:
Anna Rita Migliaccio, Icahn School of Medicine at Mount Sinai, United States

Reviewed by:
Harikumar K.B., Rajiv Gandhi Centre for Biotechnology, India
Fabrizio Martelli, Istituto Superiore di Sanità, Italy

***Correspondence:**
Gaurav Kaithwas
gauravpharm@hotmail.com

Specialty section:
This article was submitted to Cancer Molecular Targets and Therapeutics, a section of the journal Frontiers in Pharmacology

Received: *05 December 2017*
Accepted: *19 March 2018*
Published: *06 April 2018*

Citation:
Gautam S, Rawat AK, Sammi SR, Roy S, Singh M, Devi U, Yadav RK, Singh L, Rawat JK, Ansari MN, Saeedan AS, Kumar D, Pandey R and Kaithwas G (2018) DuCLOX-2/5 Inhibition Attenuates Inflammatory Response and Induces Mitochondrial Apoptosis for Mammary Gland Chemoprevention. Front. Pharmacol. 9:314. doi: 10.3389/fphar.2018.00314

The present study is a pursuit to define implications of dual cyclooxygenase-2 (COX-2) and 5-lipoxygenase (5-LOX) (DuCLOX-2/5) inhibition on various aspects of cancer augmentation and chemoprevention. The monotherapy and combination therapy of zaltoprofen (COX-2 inhibitor) and zileuton (5-LOX inhibitor) were validated for their effect against methyl nitrosourea (MNU) induced mammary gland carcinoma in albino wistar rats. The combination therapy demarcated significant effect upon the cellular proliferation as evidenced through decreased in alveolar bud count and restoration of the histopathological architecture when compared to toxic control. DuCLOX-2/5 inhibition also upregulated levels of caspase-3 and caspase-8, and restored oxidative stress markers (GSH, TBARs, protein carbonyl, SOD and catalase). The immunoblotting and qRT-PCR studies revealed the participation of the mitochondrial mediated death apoptosis pathway along with favorable regulation of COX-2, 5-LOX. Aforementioned combination restored the metabolic changes to normal when scrutinized through ^{1}H NMR studies. Henceforth, the DuCLOX-2/5 inhibition was recorded to import significant anticancer effects in comparison to either of the individual treatments.

Keywords: DuCLOX-2/5 inhibition, angiogenesis, apoptosis, cyclooxygenase, lipoxygenase, NMR, Zaltoprofen, Zileuton

INTRODUCTION

Accruing numbers of factors involved in tumorigenesis, mounting evidence indicates that the inflammatory microenvironment accounts for the tumor development. Arachidonic acid (AA) and its metabolites involve the presumed convincing role in cancer biology (Hammamieh et al., 2007; Greene et al., 2011). Prolonged treatment with the non-steroidal anti-inflammatory drugs (NSAIDs) was well proved evidence to be associated with a lower risk of the several cancers, including mammary gland cancer (Dubois, 2000; Jänne and Mayer, 2000; Joyce and Pollard, 2009; Qian and Pollard, 2010).

J. Dairy Sci. 103
https://doi.org/10.3168/jds.2019-16239

Short communication: Evaluation of α-linolenic acid–based intramammary nanosuspension for treatment of subclinical mastitis*

Rajnish K. Yadav,[1] Manjari Singh,[1] Subhadeep Roy,[1] Swetlana Gautam,[1] Jitendra K. Rawat,[1] Lakhveer Singh,[1] Mohd Nazam Ansari,[2] Abdulaziz S. Saeedan,[2] and Gaurav Kaithwas[1]†
[1]Department of Pharmaceutical Sciences, School of Biosciences and Biotechnology, Babasaheb Bhimrao Ambedkar University (A Central University), Lucknow 226 025, India
[2]Department of Pharmacology, College of Pharmacy, Prince Sattam Bin Abdulaziz University, Al-Kharj 16278, Saudi Arabia

ABSTRACT

The current study investigates the therapeutic efficacy of an α-linolenic acid (ALA, 18:3n-3)–based intramammary nanosuspension (ALA-NS) for treatment of subclinical mastitis. After confirmation of mastitis with the help of field-based testing, a total of 9 mixed-breed cows (23 udder quarter samples) were divided into 3 groups and treated with ALA-NS and cefoperazone intramammary suspension for 10 d. Subclinical mastitis on d 1 was confirmed through field-based tests such as pH, California Mastitis Test (CMT), Whiteside test (WST), and bromothymol blue test (BBT) scores. Treatment with ALA-NS (F1 and F2) exhibited significant effects on field-based parameters, along with curtailment of total microbial count [28 ± 3.16 (mean ± standard deviation) and 25 ± 4.24 cfu/50 μL] and somatic cell count (SCC; 3.9 and 2.8 log SCC cells/mL), respectively for ALA-NS F1 and F2, after 10-d treatment. The efficacy of ALA-NS was further affirmed using more stringent markers for inflammation (nuclear factor kappa-light-chain-enhancer of activated B cells, NFκB-p65), milk quality (sterol response element-binding protein-1c, SREBP-1c), and bacterial resistance (ubiquitin carboxyl-terminal hydrolase-1, UCHL-1) in milk samples. Treatment with ALA-NS (at 2 concentrations of ALA, F1 and F2) significantly decreased expression of NFκB-p65, SREBP-1c, and UCHL-1 after d 10 of treatment. Apparently, anti-inflammatory, antibacterial, peripheral analgesic properties of ALA could account for the therapeutic efficacy of the proposed regimen.

Key words: bovine mastitis, α-linolenic acid, inflammation, NFκBp65, UCHL-1

Short Communication

Bovine mastitis is an inflammatory condition of the mammary glands of lactating animals, characterized by pain, edema, swelling, and polymorphic neutrophil infiltration. Mastitis is a curse for the dairy industry, as it decreases the productivity and quality of milk and increases the cost of herd management. Currently, antibiotics, either alone or in combination with nonsteroidal anti-inflammatory agents (NSAID) are most commonly prescribed for clinical management of bovine mastitis. However, long-term use of antibiotics causes bacterial resistance and has negative effects on consumer health (Li et al., 2013). Therefore, alternative, safer drugs with universal effectiveness, lasting benefits, and fewer side effects are requisite in the area of mastitis management.

Omega-3 (n-3) fatty acids may be among the best examples of how diet may affect inflammation. These fats exert a remarkable variety of biological responses, including inflammation and related clinical conditions (Yadav et al., 2018). α-Linolenic acid (**ALA**; 18:3n-3) is an n-3 PUFA and is transformed to class-3 and class-5 eicosanoids through sequences of desaturation and elongation processes. Previous study has affirmed the relationship between ALA (18:3n-3) supplementation and anti-inflammatory effects (Anand and Kaithwas, 2014). It is interesting to note that *Linum usitatissimum* fixed oil, containing 57.38% ALA (18:3n-3), has been found to display anti-inflammatory, antimicrobial activity and efficacy against subclinical cases of bovine mastitis (Kaithwas et al., 2011a,b). The present study was designed to explore ALA (18:3n-3) as a complimentary therapeutic agent, with efforts to provide a ready-to-use intramammary formulation (pre-filled syringes) of ALA (18:3n-3) and cefotaxime nanosuspension. For this purpose, ALA (18:3n-3) was taken as oil phase, with Tween-80 as surfactant and polyethylene glycol-400 (PEG-400) as co-surfactant. The formulations were optimized and evaluated for particle size, size distribution, and stability parameters. Before proceeding

Received January 2, 2019.
Accepted November 1, 2019.
*This study has applied for Indian Patent No. 201911032651, dated Aug. 13, 2019.
†Corresponding author: gauravpharm@hotmail.com

J. Dairy Sci. 103
https://doi.org/10.3168/jds.2019-16239

Short communication: Evaluation of α-linolenic acid–based intramammary nanosuspension for treatment of subclinical mastitis*

Rajnish K. Yadav,[1] Manjari Singh,[1] Subhadeep Roy,[1] Swetlana Gautam,[1] Jitendra K. Rawat,[1] Lakhveer Singh,[1] Mohd Nazam Ansari,[2] Abdulaziz S. Saeedan,[2] and Gaurav Kaithwas[1]†
[1]Department of Pharmaceutical Sciences, School of Biosciences and Biotechnology, Babasaheb Bhimrao Ambedkar University (A Central University), Lucknow 226 025, India
[2]Department of Pharmacology, College of Pharmacy, Prince Sattam Bin Abdulaziz University, Al-Kharj 16278, Saudi Arabia

ABSTRACT

The current study investigates the therapeutic efficacy of an α-linolenic acid (ALA, 18:3n-3)–based intramammary nanosuspension (ALA-NS) for treatment of subclinical mastitis. After confirmation of mastitis with the help of field-based testing, a total of 9 mixed-breed cows (23 udder quarter samples) were divided into 3 groups and treated with ALA-NS and cefoperazone intramammary suspension for 10 d. Subclinical mastitis on d 1 was confirmed through field-based tests such as pH, California Mastitis Test (CMT), Whiteside test (WST), and bromothymol blue test (BBT) scores. Treatment with ALA-NS (F1 and F2) exhibited significant effects on field-based parameters, along with curtailment of total microbial count [28 ± 3.16 (mean ± standard deviation) and 25 ± 4.24 cfu/50 μL] and somatic cell count (SCC; 3.9 and 2.8 log SCC cells/mL), respectively for ALA-NS F1 and F2, after 10-d treatment. The efficacy of ALA-NS was further affirmed using more stringent markers for inflammation (nuclear factor kappa-light-chain-enhancer of activated B cells, NFκB-p65), milk quality (sterol response element-binding protein-1c, SREBP-1c), and bacterial resistance (ubiquitin carboxyl-terminal hydrolase-1, UCHL-1) in milk samples. Treatment with ALA-NS (at 2 concentrations of ALA, F1 and F2) significantly decreased expression of NFκB-p65, SREBP-1c, and UCHL-1 after d 10 of treatment. Apparently, anti-inflammatory, antibacterial, peripheral analgesic properties of ALA could account for the therapeutic efficacy of the proposed regimen.

Key words: bovine mastitis, α-linolenic acid, inflammation, NFκBp65, UCHL-1

Short Communication

Bovine mastitis is an inflammatory condition of the mammary glands of lactating animals, characterized by pain, edema, swelling, and polymorphic neutrophil infiltration. Mastitis is a curse for the dairy industry, as it decreases the productivity and quality of milk and increases the cost of herd management. Currently, antibiotics, either alone or in combination with nonsteroidal anti-inflammatory agents (NSAID) are most commonly prescribed for clinical management of bovine mastitis. However, long-term use of antibiotics causes bacterial resistance and has negative effects on consumer health (Li et al., 2013). Therefore, alternative, safer drugs with universal effectiveness, lasting benefits, and fewer side effects are requisite in the area of mastitis management.

Omega-3 (n-3) fatty acids may be among the best examples of how diet may affect inflammation. These fats exert a remarkable variety of biological responses, including inflammation and related clinical conditions (Yadav et al., 2018). α-Linolenic acid (**ALA**; 18:3n-3) is an n-3 PUFA and is transformed to class-3 and class-5 eicosanoids through sequences of desaturation and elongation processes. Previous study has affirmed the relationship between ALA (18:3n-3) supplementation and anti-inflammatory effects (Anand and Kaithwas, 2014). It is interesting to note that *Linum usitatissimum* fixed oil, containing 57.38% ALA (18:3n-3), has been found to display anti-inflammatory, antimicrobial activity and efficacy against subclinical cases of bovine mastitis (Kaithwas et al., 2011a,b). The present study was designed to explore ALA (18:3n-3) as a complimentary therapeutic agent, with efforts to provide a ready-to-use intramammary formulation (pre-filled syringes) of ALA (18:3n-3) and cefotaxime nanosuspension. For this purpose, ALA (18:3n-3) was taken as oil phase, with Tween-80 as surfactant and polyethylene glycol-400 (PEG-400) as co-surfactant. The formulations were optimized and evaluated for particle size, size distribution, and stability parameters. Before proceeding

Received January 2, 2019.
Accepted November 1, 2019.
*This study has applied for Indian Patent No. 201911032651, dated Aug. 13, 2019.
†Corresponding author: gauravpharm@hotmail.com

International Conference on Updates in Cancer Prevention and Research (ICUCPR-2017)

&

Satellite Conference on Translational Pharmaceutical Research: Trends and Implications

14th - 16th & 20th February 2017

Certificate

This is to certify that Prof /Dr./Mr./Ms Lakhveer Singh

has chaired the session/presented an invited lecture/oral presentation/poster presentation/participated

entitled HIF: A master gene in cancer progression

in IPCBBAU-2017 organised by Department of Pharmaceutical Sciences at Babasahib Bhimrao Ambedkar University, Lucknow, Uttar Pradesh.

Anand Prakash
Convener ICUCPR-2017

Sudipta Saha
Convener IPCBBAU-2017

Shahbaaz A. Sayed
Organizing Secretary
IPCBBAU-2017

R.C. Sobti
Vice Chancellor
Patron

ANNEXURE-IV

DRUG APPROVAL

National Cancer Institute
Drug Synthesis and Chemistry Branch
Chemotherapeutic Agents Repository
Operated By:
Fisher BioServices
20301 Century Boulevard
Building 6, Suite 800
Germantown, Maryland 20874

CUSTOMS INVOICE

DATE OF EXPORT: **FEBRUARY 06, 2019**	FEDEX TRACKING#: **7743 8995 0047**	EXPORT REFERENCES: CONTROL# **0205013425**

SHIPPER/EXPORTER:	**CONSIGNEE:**
NATIONAL CANCER INSTITUTE	MR. LAKHVEER SINGH
DCTD / DTP / DSCB	BABASAHEB BHIMRAO AMBEDKAR UNIVERSITY
ROOM 4W638	DEPARTMENT OF PHARMACEUTICAL SCIENCES
9609 MEDICAL CENTER DRIVE	SBBT BUILDING, ROOM NO. 17
ROCKVILLE, MD 20850-9734	SHAHEED PATH, RAIBARELI ROAD
USA	LUCKNOW, UTTAR PRADESH 226025
TEL: (240) 276-5941	INDIA
c/o FISHER BIOSERVICES	TEL: 9453764961 EMAIL: lakhveer.singh52@gmail.com

COUNTRY OF EXPORT:	COUNTRY OF ULTIMATE DESTINATION:	IMPORTER (OTHER THAN CONSIGNEE):
USA	**INDIA (IN)**	

NUMBER OF PAGES:	CONTAINER TYPE / QTY:	DIMENSIONS:	TOTAL WEIGHT:
2	**ONE CARTON**	**12 x 10 x 8 IN**	**1 LB**

COMPLETE DESCRIPTION OF GOODS	TOTAL QUANTITY	VALUE (USD)
CHEMICALS, NON-HAZARDOUS 1 compound weighing 50 mg, detailed on page 2. THIS SHIPMENT HAS BEEN PREPARED ACCORDING TO ICAO/IATA REGULATIONS. RUSH. URGENTLY NEEDED FOR RESEARCH. FOR INVESTIGATIONAL USE ONLY. MATERIAL IS BEING PROVIDED FREE OF CHARGE AND IS NOT FOR RESALE. VALUE FOR CUSTOMS PURPOSES ONLY. MAY GO PASSENGER OR CARGO AIRCRAFT.	**50 mg**	**$ 585.00** **$ 585.00** **TOTAL DECLARED VALUE**

These items are controlled by the U.S. Government and authorized for export only to the country of ultimate destination for use by the ultimate consignee or end-user(s) herein identified. They may not be resold, transferred, or otherwise disposed of, to any other country or to any person other than the authorized ultimate consignee or end-user(s), either in their original form or after being incorporated into other items, without first obtaining approval from the U.S. government or as otherwise authorized by U.S. law and regulations.

I DECLARE THAT ALL INFORMATION CONTAINED IN THE INVOICE TO BE TRUE AND CORRECT.

SIGNATURE OF SHIPPER FOR AND ON BEHALF OF DR. STEPHEN WHITE:

DATE:

06 FEBRUARY 2019

ALEXANDER MARTINKOSKY, ASSISTANT PROJECT DIRECTOR, NATIONAL CANCER INSTITUTE – CHEMOTHERAPEUTIC AGENTS REPOSITORY

MR. ALEXANDER MARTINKOSKY
ASSISTANT PROJECT DIRECTOR
FISHER BIOSERVICES
(240) 686-4720
martinkoskya@mail.nih.gov

DR. STEPHEN WHITE
PROJECT OFFICER
NATIONAL CANCER INSTITUTE - DSCB
(240) 276-5941

Fisher BioServices
20301 Century Boulevard
Building 6, Suite 800
Germantown, MD 20874

NCI Chemotherapeutic Agents Repository

Phone: 240.686.4720
Fax: 301.515.4297

Waybill number: 7743 8995 0047
Export references: Control# 0205013425

Date of exportation: February 06, 2019

Compound Information

NSC: 82591

CAS#: 3371-85-5

Chemical name: Ibogamine-18-carboxylic acid, 12-methoxy-13-[(3.alpha.)-17-methoxy-17-oxovobasan-3-yl]-, methyl ester (9CI)